BIOLOGICALLY ACTIVE COMPOUNDS FROM PACIFIC TUNICATES

by

David Francis Sesin

A dissertation submitted to the faculty of
The University of Utah
in partial fulfillment of the requirements for the degree of

Doctor of Philosophy

Department of Medicinal Chemistry
The University of Utah

December 1986

THE UNIVERSITY OF UTAH GRADUATE SCHOOL

SUPERVISORY COMMITTEE APPROVAL

of a dissertation submitted by

DAVID FRANCIS SESIN

This dissertation has been read by each member of the following supervisory committee and by majority vote has been found to be satisfactory.

September 16, 1986 — M. Ph.D.

September 16, 1986 — Arthur D. Broom, Ph.D.

ark E. Sanders, Ph.D.

Martin P.

September 16, 1986 — David M. Grant, Ph.D.

THE UNIVERSITY OF UTAH GRADUATE SCHOOL

FINAL READING APPROVAL

To the Graduate Council of The University of Utah:

I have read the dissertation of David Francis [redacted] in its final form and have found that (1) its format, citations, and bibliographic style are consistent and acceptable; (2) its illustrative materials including figures, tables, and charts are in place; and (3) the final manuscript is satisfactory to the Supervisory Committee and is ready for submission to the Graduate School.

[redacted]
Date

[redacted]
Chris M. Ireland, Ph.D.
Chairperson, Supervisory Committee

Approved for the Major Department

[redacted]
Arthur D. Broom, Ph.D.
Chairman / Dean

Approved for the Graduate Council

[redacted]
Dean of The Graduate School

ABSTRACT

Tunicates have proven to be a rich source of structurally-diverse metabolites covering a broad spectrum of biological activities. Initial testing of the methanolic extract from three Pacific didemnid tunicates indicated the presence of cytotoxic metabolites. The active compounds were isolated by various chromatographic procedures and their structures elucidated by spectroscopic techniques (UV, MS, IR, NMR). In addition, derivatization, chemical conversion and total synthesis were performed to secure the assigned structures.

TABLE OF CONTENTS

LIST OF TABLES

LIST OF FIGURES

LIST OF DEFINITIONS AND ABBREVIATIONS

sessile	permanently attached
pelagic	free-swimming; oceanic
benthic	oceanic bottom
COSY	correlation spectroscopy
SECSY	spin echo correlation spectroscopy
NOESY	nuclear Overhauser enhancement spectroscopy
EIMS	electron impact mass spectrometry
FABMS	fast atom bombardment mass spectrometry
L1210	murine leukemia cell line
CEM 360	human T-cell tumor line
TMP	isooctane

ACKNOWLEDGEMENTS

To my wife Melani and my two children Danny and Lindsey my sincerest gratitude for the love, patience, understanding and moral support that you showed me. To my mom and dad for an upbringing that taught me the value of hard work. To Chris for your support and guidance in my development as a scientist. I understand why you pushed me so hard and I will be forever grateful for the scientific knowledge that you taught me. A special thanks to Joe for being an understanding and caring friend. I will always remember the good times that we shared. To Dr. Broom for allowing me to bend your ear when I needed someone to talk to. To Diana for sharing with me the good times and the bad. I will always treasure the friendship that we developed in the short time that we were together. To Jay for helping in my development as an NMR spectroscopist. To Raissa, Paula and Betty for keeping me in line. To Debbie, Mark, Tawnya, John and all my friends at the U; thank you for being my friend.

BIOLOGY OF TUNICATES

The phylum Chordata represents a diverse group of vertebrate animals. However, within the chordate hierarchy is a subphylum, Tunicata, (= Urochordata), whose members do not possess vertebrae. Their eggs develop tiny, free swimming "tadpole larvae" possessing a notochord which acts as a dorsal supporting structure and a dorsal hollow nerve cord, both of which are missing in some adult forms, and pharyngeal slits. These three characteristics allow placement of tunicates into the chordate family, (Table 1).[1] Many scientists feel that tunicates represent the anatomical organization from which the earliest vertebrates originated at the beginning of the Paleozoic era.

Due to their evolutionary position as probable vertebrate ancestors the biology of tunicates has been thoroughly investigated. Most tunicates are soft-bodied organisms. Therefore, there are few known fossils that have been uncovered. They are exclusively marine and are found all over the world from coastal tide pools to a hundred miles out to sea on the continental shelves.

Most tunicates, (2000 species), are sessile animals remaining permanently attached to coral reefs, seaweeds or shells. About 100 species have become secondarily modified

Table 1

Taxonomy of Tunicates

Phylum	Chordata
Subphylum	Tunicata
Class	Thaliacea (scalps)
	Larvacea (appendicularians)
	Ascidiacea (sea squirts)

for a pelagic life; however, these modifications enabling their oceanic existence have drastically altered their structural features from the normal. Both sessile and pelagic tunicates exist in two different forms - simple and compound (colonial). The simple tunicates are solitary individuals of relatively uniform proportion. The general shape of colonial tunicates is much less uniform. They can exist as massive colonies of brilliantly colored individuals, sometimes connected by a common creeping stolon, or as thin encrusting species on marine plants and shells.

The subphylum Tunicata is divided into three classes, Ascidiacea, Thaliacea, and Larvacea. Thaliacea, (i.e., Salpa, Doliolum, Pyrosoma, Cyclosalpa), are pelagic tunicates living in warm waters (Figure 1). They have circular bands of muscles enabling the animal to shoot

through the water by jet propulsion. The mouth and atriopore are at opposite ends of the body. The tunic is thin and, like the rest of the body, transparent. Salps have the ability to swim forward or backwards but their outstanding characteristic is the powerful luminescent light that shines when the animal is stimulated. Scientists believe that the flashes of light protect the salps against enemies. This is based on laboratory observations that show dying colonies of Pyrosoma that do not light up being eaten by fish whereas those that light up when seized are subsequently dropped. Larvacea, (i.e., Appendicularia, Oikopleura), are small pelagic tunicates that retain some larval or immature characteristics in adulthood (Figure 2). Hence the name Larvacea given to this class. They represent a very common and important component of the planktonic community. Interestingly, instead of a tunic, each individual builds a house by secretion from a special part of the skin, the "oikoplastic epithelium." Tail movements cause a current of water to pass through an elaborate filtering apparatus in the house. Nanoplankton are trapped by filter pipes and surface in front of the mouth. At frequent intervals the tail movements stop and the food particles are sucked back into the mouth. After a few hours the filtering system becomes clogged. The house is then abandoned and a new one secreted. An important modification that has enabled appendicularians to adapt to their pelagic

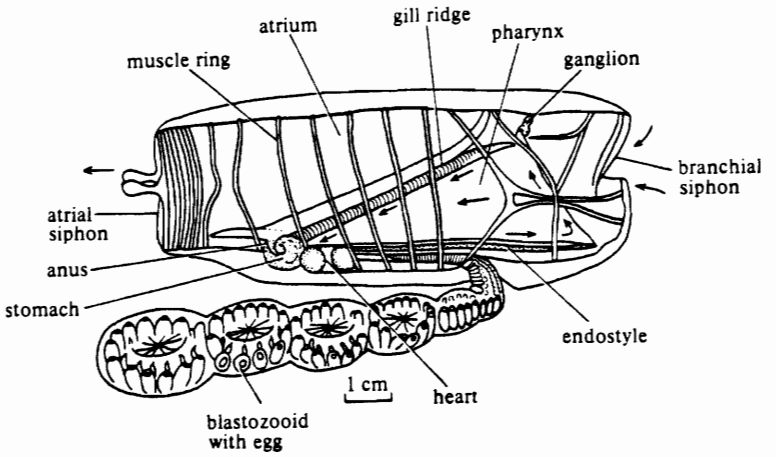

Figure 1. Structure of Thaliacea[15]

Reprinted by permission

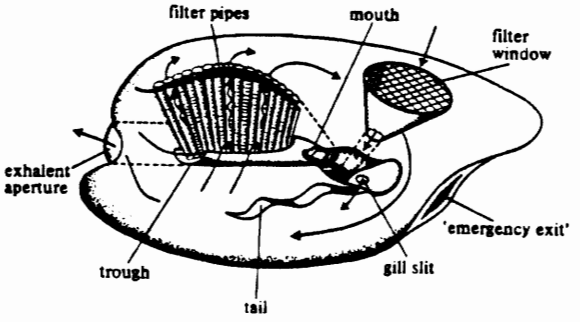

Figure 2. Structure of Larvacea[15]

Reprinted by permission

existence is the development of the tail into a highly specialized organ that supplies locomotion, nutrition and aids in the building of the house. (The larval tail of Thaliacea and Ascidiacea species is ultimately absorbed.)

In contrast to Thaliacea, (salps), and Larvacea, (appendicularians), which exist in a pelagic environment, members of the class Ascidiacea, (i.e., Ciona, Ascidia, Eudistoma, Didemnum, Lissoclinum), are usually benthic in their adult stage. For this reason Ascidiacea, (ascidians or sea squirts), are collected much more easily and therefore have been studied in much greater detail. The remainder of this thesis will concentrate on members of this class.

Ascidians are mainly sessile organisms that can be found living on the sea floor or attached to marine plants and shells. They occur as solitary organisms or as colonies of individuals. The former state is possibly the primitive condition for the group. These sac-like creatures, (Figure 3), obtain their food by ciliary action. The entire body is covered by a tough barrel-shaped covering or tunic in which there are only two siphon openings, an incurrent (oral) opening and a dorsal excurrent (atrial) opening. The tunic lends protection and support to the animal. It is a living tissue supplied by blood vessels and composed largely of fibers of a carbohydrate tunicin, (closely related to cellulose), embedded in a ground substance of acid

mucopolysaccharide with some protein. The tunic is lined by a mantle covered by a single-layered epidermis. The mantle contains longitudinal muscle fibers which draw the animal together and in the process expel a jet of water from the animal, hence the name sea squirt. Most of the body is comprised of an immense pharynx beginning below the mouth and forming a sac reaching nearly to the base. The pharynx serves as a food-collecting apparatus. Its walls are pierced by rows of gill slits whose muscular cilia set up a food current entering at the mouth and exiting from the atrium. An endostyle runs longitudinally along the outside of the pharynx (Figure 4). It has three rows of secretory cells separated by rows of cilia cells with a single median set of cells with very long cilia. The inner rows of secretory cells secrete protein, the outer row secretes iodinated tyrosine. The iodine is supplied by iodine-uptake cells (Figure 4)[2]. The resulting substance, iodinated protein, is spread over the inside of the pharynx. Food particles are caught in this layer and the entire curtain is digested.

Autoradiographs made from tunicates that had been provided with isotopes of iodine indicated that the major compounds formed were 3-iodotyrosine (1) and 3,5-diiodotyrosine (2).[3] These compounds show a close structural resemblance to thyroxin (3) and triiodothyronine (4), two characteristic hormones secreted by the mammalian

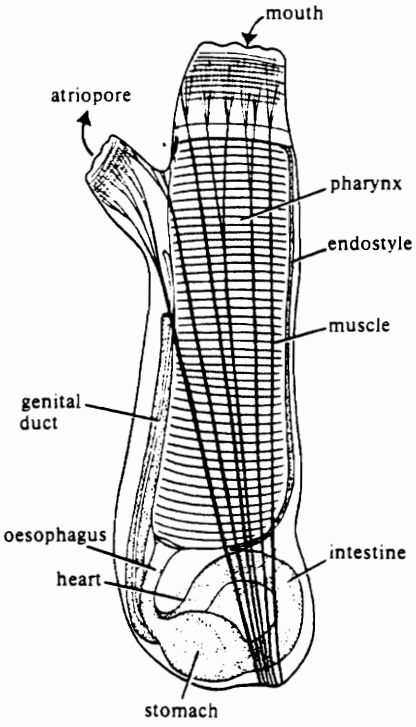

Figure 3. Structure of Ascidiacea[15]

Reprinted by permission

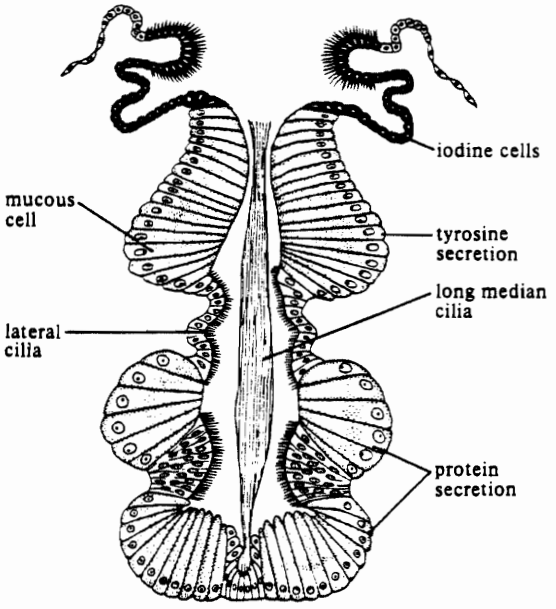

Figure 4. The structure of an endostyle[15]

Reprinted by permission

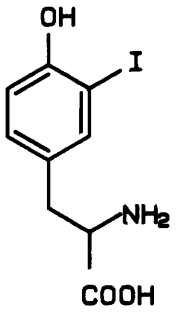

1

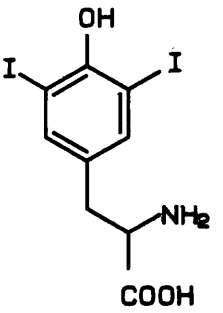

2

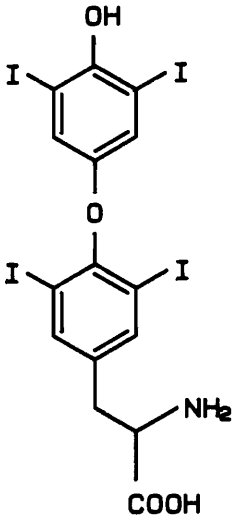

3

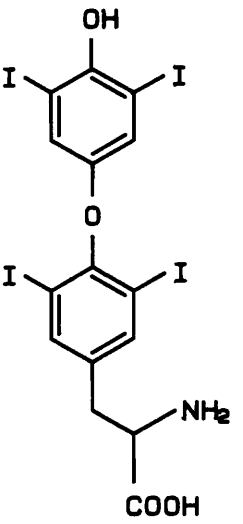

4

thyroid gland. This new information sparked interest in the search for a prototype of the thyroid gland. Salvatore confirmed the presence of the necessary machinery for the biosynthesis of thyroxin in certain tunicate species. His elegant experiments suggested that the major site for the synthetic process was the tunic and not the endosytle which had been assumed to be a homologous organ of the thyroid gland.[4] In a similar set of experiments Suzuki also demonstrated that 90% of the incorporated ^{131}I was found in the tunic proteins.[3] However, Suzuki felt that the tunic was, from an embryological or evolutionary viewpoint, a very unlikely prototype for the thyroid gland and thought it more reasonable to study those organs of the tunicate that could serve as the functional prototype. His previous studies had revealed a higher incorporation of ^{131}I into the iodo-amino acids of branchial sac (pharynx) proteins rather than into those of the endostyle proteins or other tissue proteins.[5] The branchial elements in vertebrates are embryologically related to the thyroid.[6] Therefore, Suzuki proposed that the branchial sac of tunicates functionally resembled the thyroid gland of vertebrates based on the presence of large molecules with iodo-amino acid residues in their peptides. (These molecules also appeared to have a subunit structure similar to thyroglobulin). He also hypothesized that part of the biosynthetic machinery for producing hormones had already appeared in the branchial sac of tunicates.

Returning now to the morphology of tunicates, the oesophagus leads to a large stomach with a folded wall containing gland cells that produce mucus and digestive enzymes. The enzymes present include amylase, invertase, lipase, and a weak protease. The organ is therefore unlike the stomach of a vertebrate- it contains no cellulase. A short intestine extends from the stomach and leads upwards to open by a rectum near the atrium. The intestine is the absorptive region of the gut and is lined by mucus-secreting and absorptive cells. The curtain of iodinated protein is formed into a food cord by the cilia of the oesophagus before being "softened" by the enzymes in the stomach. Digestion is extracellular and there is no evidence of uptake of solid particles.

The heart, lying below the pharynx, is a sac surrounded by a pericardium. Blood circulation is similar to that in vertebrates but there are no capillaries and no valves. The blood circulates in a closed system of spaces pumped by peristaltic contractions passing from one end of the heart to the other, first in one direction for 2-3 minutes and then the other. The periodic reversal may be connected with the need to supply blood to the tunic as well as to the brachial sac and viscera. The blood system distributes digested food materials, oxygen and a store of inorganic ions. The blood plasma is colorless but contains several types of compounds. The blood cells contain pigments which

complex trace metals such as vanadium, iron, titanium, tantalum or niobium.[7-9] Kustin demonstrated the extraction of vanadium from sea water[10] and Dingley showed that this occurs via a specific anion transport system[11] housed in the branchial epithelium. Vanadium, whose concentration may be a million times greater in the ascidian than in the sea, is then transported to other parts of the tunicate via the blood cells. The heavy metal chromogens of these morula cells act as powerful reducing agents being held in their reduced state by sulfuric acid. They break up in the tunic and assist in the conversion of simple carbohydrates to polysaccharides.

The blood is isotonic with sea water but has little sulfate. Since tunicates are exclusively marine organisms it is not surprising that they have no power in regulating their osmotic pressure. As a result they are unable to colonize brackish waters or those of low salinity. An explanation for this uncommon vertebrate trait is the need to expose a large surface area to the water. Also, tunicates do not possess tubular excretory organs that could maintain an osmotic gradient. As a result, 95% of the nitrogenous waste products are excreted as ammonia.

Ascidians possess a central nervous system consisting of a round solid ganglion lying above the front end of the pharynx. The ganglion is unlike the nerve cord of vertebrates in that it has a surrounding layer of cells and

a central mass of neuropil. From the ganglion, nerves proceed to the siphons, mantle, muscle, and viscera.

Movement consists mainly of contraction and closure of the apertures. The amount of closure is proportional to the strength of the stimulus. Interestingly, when the interior of one of the siphons is aggravated the other siphon closes first, followed by the one stimulated and finally contraction of the body occurs, causing a jet of water to be expelled out the stimulated siphon.

The surface of the body is sensitive to changes in light intensity. Local or total contractions are observable with the highest sensitivity being in the region of the ganglion.

The neuromuscular system serves as a reflex apparatus for producing protective movements in response to certain stimuli. Although most ascidians are sessile organisms, the nervous system is not activated merely by external stimuli. Some experiments suggest that "rhythmical" activities are initiated from within, one example being a hunger contraction in the absence of food. The food-collecting operation is regulated by cilia found along the pharyngeal wall. In the absence of food a "hunger contraction" occurs causing more water to pass through the machinery than by the ciliary current alone.

The neural gland is a sac lying beneath the ganglion and opening by a ciliated funnel on the roof of the pharynx.

It originates from the ectoderm of the larval nervous system. It has been compared with the infundibulum and hypophysis of vertebrates. It also displays similarities with the pituitary in that it controls the release of gametes. The position of the gland suggests a connection with the feeding mechanism and there is a daily cycle of secretion, the product of which may be mixed with the food cord. It is possible that this pharyngal mucus-secreting organ stimulated by the environment has evolved into a glycoprotein-secreting endocrine gland controlled by substances reaching it in the blood.[12]

Tunicates are hermaphrodites. The ovaries and testis are sacs lying close to the intestine that open by ducts near the atrium. Solitary ascidians pass their eggs directly into the sea water where they develop into fish-like larvae. In colonial ascidians the eggs are fertilized at the upper end of the oviducts and develop in the atrial cavity to the tadpole stage. The tadpole larva (Figure 5, left) is distinctive, possessing an eyespot, four rows of gill slits and a tail containing a fine dorsal nerve cord and a thicker rod or notochord. The mouth of the larvae remains undeveloped. Therefore the ascidian never feeds during development. The larvae swims a few minutes to an hour, then becomes attached to a suitable benthic surface at the front end. The tail is rapidly reabsorbed, a large pharynx develops, and the two siphons break through. The

entire development process takes one to two days. The whole development process is so strikingly like that of chordates that it establishes the affinities of the tunicates far more clearly than the vague indications of a chordate plan of organization seen in the adult.

Tunicates also undergo vegetative budding of the parent individual (Figure 5, right). In certain species this second form of reproduction may occur coincidentally with sexual reproduction. A long branching stolon appears from under each zooid. At irregular intervals a portion of the stolon thickens and buds form. Each bud develops into a parent without passing through the larval stage. In some species the zooids form a branching colony interconnected by the stolon through which the communal blood system flows. In others, the zooids separate from the parent and become solitary individuals. Many simple ascidian species are incapable of vegetative budding.

The life span of a typical ascidian species is approximately one year. However, this is sufficient to allow distribution and continuation of the species.[13-16]

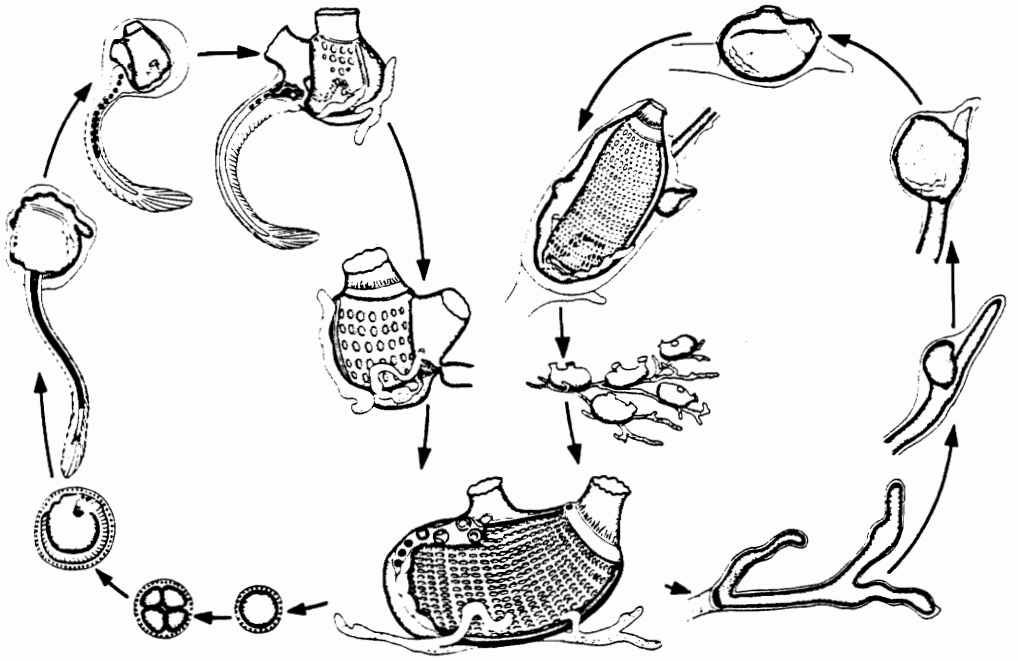

Figure 5. Reproduction in tunicates[14]

Reprinted by permission

SYMBIOSIS IN DIDEMNID TUNICATES

A phenomenon that has intrigued scientists for many years is the symbiotic association between certain marine ascidians and unicellular algae. The algae are found living on the surface or within the cloacal cavities of certain didemnid ascidians (i.e., Didemnum voeltzkowi, Lissoclinum patella, Tridemnum cyclops). This association represents the highest life form that uses symbionts to contribute to its nutrition. The literature describing the taxonomy of the symbiont has demonstrated a general confusion concerning its phylogenetic position. The microscopic algae, once thought to be a zooxanthellae[17] and later defined as zoochlorellae[18] synthesizes chlorophylls a & b (i.e., eukaryotes) but no phycobilin pigments and has a prokaryotic cellular organization. This necessitated that the algae be placed in a new plant division, the Prochlorophyta,[19] in the new genus Prochloron.[20] The literature investigating the nutritive role of the symbiont is equally rich in conflicting opinions. In 1935 Smith suggested that, even though the augmented concentrations of CO_2 produced by the tunicates were peculiarly suited to the algal physiology which in return provided photosynthetically-evolved oxygen, the algae did not contribute significantly to the nutrition of the host.[17] Twenty years later, however, the elegant

work of Sargent and Austin[21] and of Odum and Odum[22] suggested that the abundant presence in coral reef communities of photosynthetic algae was crucial to growth and maintenance of the entire reef biotope. Recently, Akazawa[23] and Pardy and Lewin,[24] using $^{14}CO_2$, corroborated the nutritive role of the algae by demonstrating the photosynthetic capacity of the algal symbiont to supply the host with O_2 and low molecular weight molecules.

In the past eight years tunicates have proven to be a rich source of biologically active compounds. Several nitrogen containing compounds have been isolated from didemnid species harboring algal symbionts. The ability of certain algal species to fix nitrogen[25] prompted scientists to speculate a biosynthetic role for the unicellular algae. The contribution from the tunicate and its host in the biosynthesis of these compounds remains an intriguing question. Complex molecules have been isolated from several ascidian species devoid of algal symbionts (i.e., Ascidia nigra)[26] suggesting that they possess the necessary biosynthetic machinery. Evidence also exists suggesting that some sponge metabolites are derived from their symbiotic microorganisms.[27]

The biosynthetic origin of these compounds will remain a mystery until the host and the symbiont are cultured separately and the compounds produced by each organism are isolated. Bancroft successfully cultured colonies of

Botryllus and Botrylloides, both encrusting ascidians in their natural habitat, easily obtaining vigorous growth and sexual reproduction.[28] Culturing the algal symbionts is dependent on the ability to free them from their host. Lewin demonstrated the ability to free Prochloron from the didemnids.[29] Unfortunately, all attempts at culturing Prochloron failed until Patterson and Withers determined that cell division occurs under acidic conditions (pH 5.5) in the presence of tryptophan.[30] The culturing of the aposymbiont[31] involves culturing the symbiont-containing tunicate in the dark thereby causing the tunicate to expel the symbiont. This has yet to be demonstrated successfully.

THE CHEMISTRY OF TUNICATES

Rinehart[32] and Weinheimer[33] demonstrated that crude extracts from several tunicate species possessed significant biological activity. This prompted several research groups working independently to isolate and identify the active compounds. The potent metabolites covered a broad spectrum of activities (i.e., cytotoxic, antibiotic, antiviral, antimicrobial). In some cases the novelty of these compounds was more interesting than their biological activity. Many of these compounds have become target molecules for synthetic research groups. Biosynthetically, the metabolites can be divided into two major groups: those derived from acetyl CoA and those derived from amino acids. The latter group includes the majority of the metabolites, a fact that is not surprising since tunicates have demonstrated the ability to absorb amino acids from sea water.[15]

An example of amino acid derived metabolites are polyandrocarpidine I (5) and II (6), derived from a red encrusting Polyandrocarpa sp. collected in the Gulf of California.[34] A mixture of the two compounds inhibits Bacillus subtilus (100μg. 16mm zone), Staphylococcus aureus (100 g, 15mm), Streptococcus pyogenes (100μg, 244mm), and Mycobacterium avium (100μg, 15mm); was cytotoxic towards L1210 cells (ID_{50} 4.8μg/ml) and monkey kidney tissue culture

L1210 cells (ID_{50} 4.8μg/ml) and monkey kidney tissue culture (CV-1 cells, 200μg, 14mm); and exhibited slight antiviral activity against Herpes simplex virus, type 1. The structure elucidation was performed by spectroscopic analysis and chemical modifications. The assigned structures were remarkably similar to the acarnidines (7-9), natural products isolated from a sponge (Phylum-Porifera).[35] In 1972 Faulkner had reported that crude extracts of the same Polyandrocarpa sp. exhibited potent antimicrobial activity. However, Faulkner's ^1H NMR data did not corroborate Rinehart's published structures for the polyandrocarpidines.[36] Faulkner revised the structures of polyandrocarpidine I and II to contain the γ-methylene-γ-lactam ring system as represented by (10) and (11), respectively. He also reported geometric isomers (12) and (13) for each homolog. Soon thereafter, Rinehart synthesized and published the revised structures of hexahydropolyandrocarpidine I (14) and II (15) which were in complete agreement with Faulkner's revised structures.[37]

Halocynthia roretzi was investigated by two different Japanese groups. Kobayashi and co-workers isolated five mycosporine-like amino acids (16-20) from the ascidian.[38] The water soluble substances were characterized by a UV-absorption maximum in the range of 310-360 nm. Spectroscopic and amino acid analysis of the hydrolysis products were instrumental in assigning the final

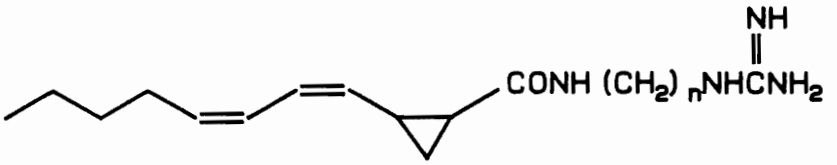

5. n = 4
6. n = 5

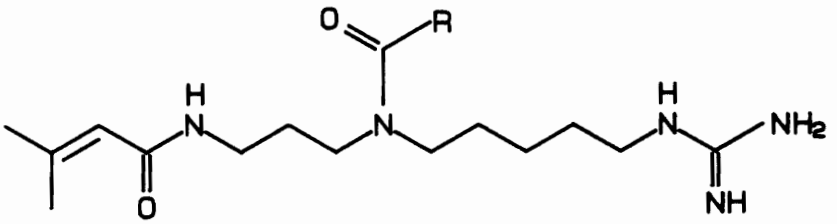

7. R = $(CH_2)_{10}CH_3$
8. R = $(CH_2)_3CH{=}CH(CH_2)_5CH_3$ [Z]
9. R = $(CH_2)_3(CH{=}CHCH_2)_3CH_3$ [all Z]

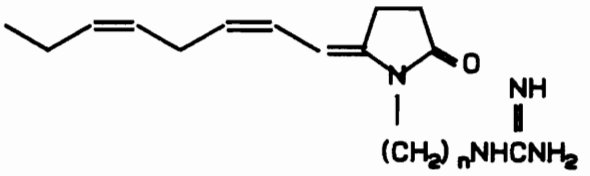

10. n = 4

11. n = 5

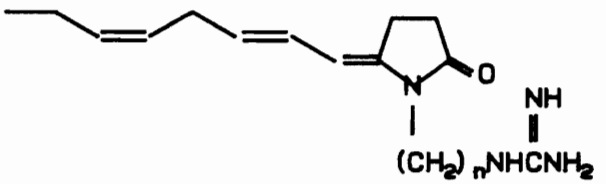

12. n = 4

13. n = 5

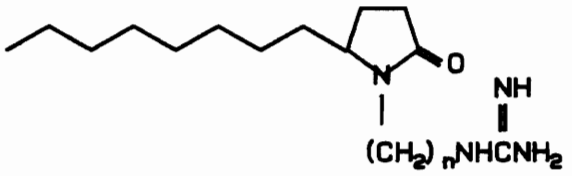

14. n = 4

15. n = 5

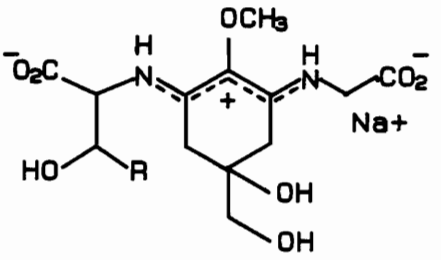

16. R = H

17. R = CH_3

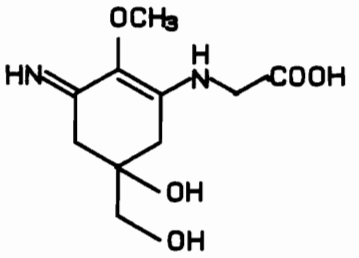

18

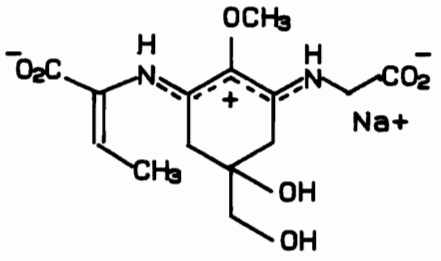

19

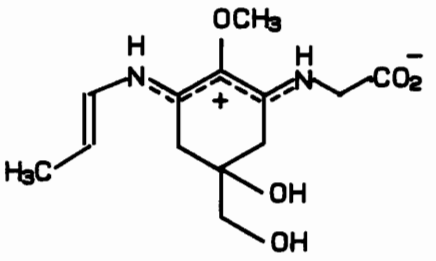

20

structures. Their biological role *in vivo* is still unknown. Watanabe isolated a novel lysine-derived betaine from the muscle of *H. roretzi*.[39] The structure was determined to be (R)-2-hydroxy-6-trimethyl ammoniohexanoate (*21*). Its gross structure was assigned based on FDMS, FABMS, ^{1}H and ^{13}C NMR data. The positioning of the substituents was based on a comparison of the ^{13}C NMR values of halocynine with those of laminine (*22*), an analogous betaine occasionally found in algal extracts or in some proteins.[40] To verify their proposed structure, L-lysine was exhaustively methylated and treated with $NaNO_2$ in 0.1 M pyridine-acetic acid buffer (pH 3.75). The spectral data of the synthetic product and the spectral data of the natural product were found to be identical. The biological role of halocynine is also unknown.

Nakanishi successfully isolated and identified a bright yellow blood pigment, tunichrome B-1(TB-1, *23*) from the tunicate *Ascidia nigra*.[26] The black tunicate accumulates vanadium in its pentavalent state, concentrates its 10^{6}-fold and stores the metal as a complex in its reduced V(III) or V(IV) states.[41] V(IV) is unstable in aqueous media above pH 2.5 prompting Nakanishi to propose a reducing nature of tunichrome B-1 based on its pyrogallol moiety which is known to reduce V(V) to V(IV) and form complexes.[42] Tunichrome B-1, derived from three (3,4,5-trihydroxyphenyl) alanine units, represents the first member of a group of novel blood

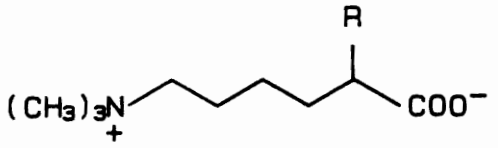

21. R = OH

22. R = NH_3

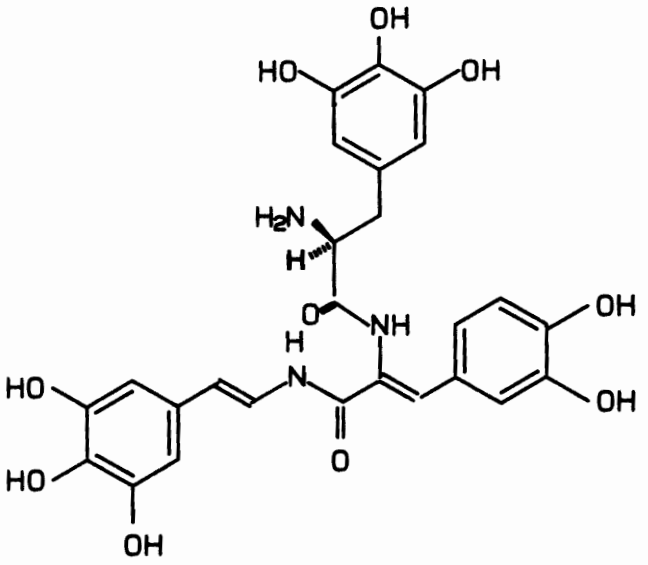

23

reducing pigments. Due to the instability of TB-1, the isolation procedure was performed in a dry O_2-free Ar atmosphere and most of the spectral data were obtained using the diacetate. Tunichrome B-1 may prove instrumental in deducing the biochemical role of vanadium and other trace metals in marine ascidians.

Several indole-derived metabolites have been isolated from three ascidian species. Guyot isolated a unique 1,2,4-thiadiazole from the dark red clustering tunicate Dendrodoa grossularia.[43] X-ray analysis and interpretation of the spectral data for the parent compound and the monoacetate derivative established the structure as 5-[(3-N-dimethyl-amino)-1,2,4-thiadiazolyl]-3-indanyl methanone (24) to which the name dendrodoine was given. The metabolite inhibited DNA synthesis when tested in vitro against the L1210 murine leukemia cell line. As is often the case with novel cytotoxic natural products, dendrodoine became the target molecule for a synthetic laboratory in the UK. Hogan and Sainsbury synthesized dendrodoine by a 1,3-dipolar addition reaction between indolyl-3-carbonyl nitrile (25) and N,N-dimethylaminonitrile sulphide (26) generated in situ.[44] Following chromatographic purification, the synthetic product and the natural product exhibited identical spectral data. In 1984, Guyot published the structure of a novel derivative, Grossularine (27) from the same tunicate.[45] The final structure was based solely on interpretation of the ^1H

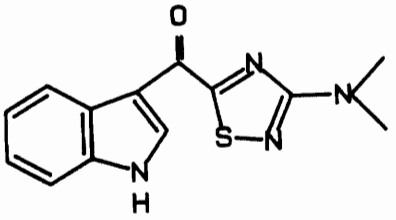

24

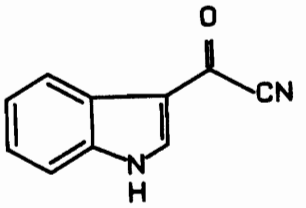

25

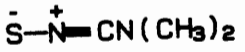

26

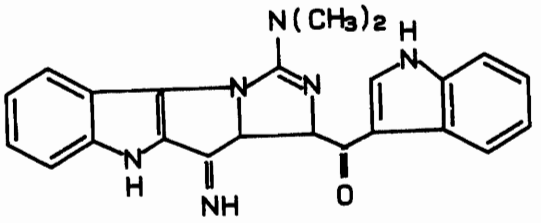

27

NMR, ^{13}C NMR and mass spectral data. No biological activity was reported.

Rinehart isolated fifteen indole-derived metabolites (28-42) all containing the β-carboline ring system from the colonial tunicate Eudistoma olivaceum.[46,47] Eudistomins C,E,K and L (28-31) contain the novel oxathiazepine ring system and exhibited potent antiviral activities against Herpes simplex virus, type 1 (K, 250ng/disk; L, 100ng/disk).[46] Their biosynthesis involves the condensation of tryptophan (N-2 - C-9a) and cysteine (C-1,C-10,C-11,S-12). In a separate communication[47] Rinehart reported the isolation and structure elucidation of Eudistomins A,D,G,H,I,J.M,N,O,P and Q (32-42) assigning the previously unreported 1-pyrrolinyl-ß-carboline ring system to eudistomins G,H,I,P and Q. These eudistomins exhibited modest activity against Herpes simplex virus, type 1 (D,G,H,I,N and O), Saccharomyces cerevisiae, a yeast (H,N,O and P), and Bacillus subtilus, a Gram (+) bacterium (D,I,N,O,P and Q). It should be noted that of the 650 species assayed during Rinehart's 1978 Caribbean Expedition, Eudistoma olivaceum yielded the most potent antiviral compounds.

Recently, Roll and Ireland reported the isolation of a novel bromoindole derivative from the Pacific tunicate Polycitorella mariae.[48] Citorellamine (43) exhibited potent antimicrobial activity against Gram (+) and Gram (-) bacteria, was cytotoxic in the L1210 assay (IC_{50} 3.7 μg/ml)

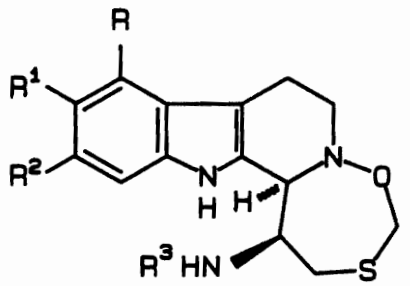

	R	R^1	R^2	R^3
28.	H	OH	Br	H
29.	Br	OH	H	H
30.	H	H	Br	H
31.	H	Br	H	H

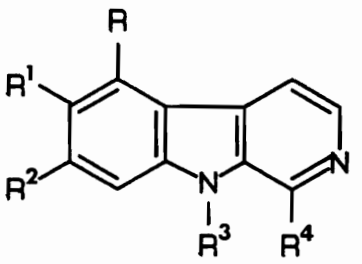

	R	R^1	R^2	R^3	R^4
32.	H	OH	Br	H	b
33.	Br	OH	H	H	H
34.	H	OH	Br	H	H
35.	H	OH	H	H	b
36.	H	Br	H	H	H
37.	H	H	Br	H	H
38.	H	H	Br	H	c
39.	H	Br	H	H	c
40.	H	H	H	H	c
41.	H	OH	Br	H	c
42.	H	OH	H	H	c

[b] 2-pyrrolyl

[c] 1-pyrridin-2-yl

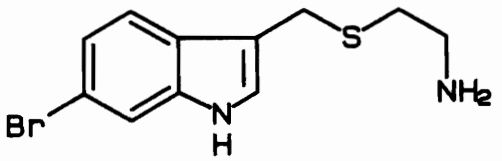

43

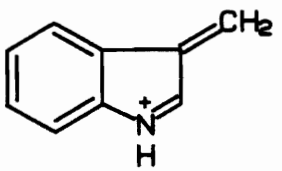

44

and exhibited mild insecticidal activity against the tobacco budworm. Citorellamine can be biosynthesized from a gramine intermediate (44) and one molecule of cysteine.

Sesin and Ireland reported the isolation of 3,5-diiodo-4-methoxyphenethylamine (45) and its urea analog (46) from an unidentified Didemnum sp..[49] The tunicate was found devoid of algal symbionts. This absence calls into question the biosynthetic origin of these nitrogen-containing compounds. However, it is not surprising that compounds of this type were isolated from such a tunicate since tunicates are known to harbor tyrosine-secreting cells and iodine uptake cells (See Figure 5).[15] The phenethylamine derivative (45) proved to be a potent antifungal metabolite and was weakly cytotoxic in the L1210 assay (IC_{50} 20µg/ml). Ireland also published the structure of N,N'- diphenethyl urea (47) from Didemnum ternatanum. It proved to be a weak depressant lacking acute toxicity.[50] Unlike the aforementioned didemnid species, Didemnum ternatanum harbors prokaryotic algae suggesting a symbiotic biosynthesis for this amino acid. N,N^1-diphenethyl urea (47) may also arise from enzymatic manipulation of tyrosine followed by dimerization to form the urea. Ireland confirmed the structure of 47 synthetically from phenethylamine and phosgene.

The final group of amino acid derived metabolites from marine ascidians are the cyclic peptides. Most of the

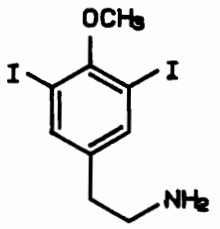

45

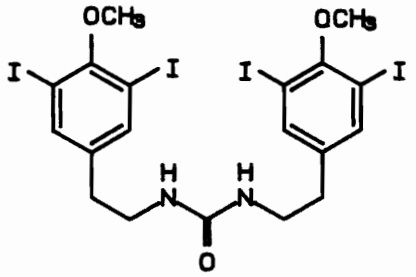

46

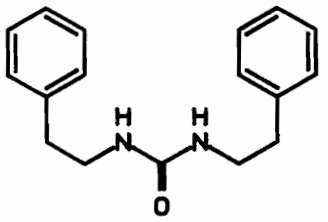

47

metabolites contain normal amide linkages. However, three metabolites, didemnin A-C (48-50), possess ester linkages and are referred to as depsipeptides. These latter cyclic peptides were isolated from a Caribbean tunicate of the family Didemnidae (Tridemnum sp.), hence the trivial name didemnin.[51,52] Acid hydrolysis followed by GC of the N-trifluoroacetyl n-butyl ester derivatives indicated the presence of Leu, Meleu, Pro, Thr, Me_2Tyr (all possessing the L configuration), and the uncommon amino acid statine. Another interesting structural feature was the presence of the hydroxyisovaleryl propionyl group. The amino acids were further identified by FDMS and/or EIMS of the hydrolysates and interpretation of the ^{1}H NMR signals. The didemnins inhibit the growth of both RNA and DNA viruses, are highly cytotoxic to L1210 leukemia cells and protect mice against P388 leukemia and B16 melanoma. Specifically, didemnin B, which is presently in Phase 1 of clinical trials,[53] has an IC_{50} 0.0011μg/ml vs. L1210 leukemia cells, T/C up to 199 vs. P388 leukemia, and T/C = 160 vs. B16 melanoma. Trace amounts of a lower homolog of each didemnin [D-F, (51-53)] were found to contain a previously unreported lower homolog of statine, for which Rinehart proposed the name norstatine.

The larger of the two groups of cyclic peptides are those containing normal amide linkages. Lissoclinum patella is the source of a family of cyclic peptides,(54-64) characterized by the presence of heterocyclic thiazole and

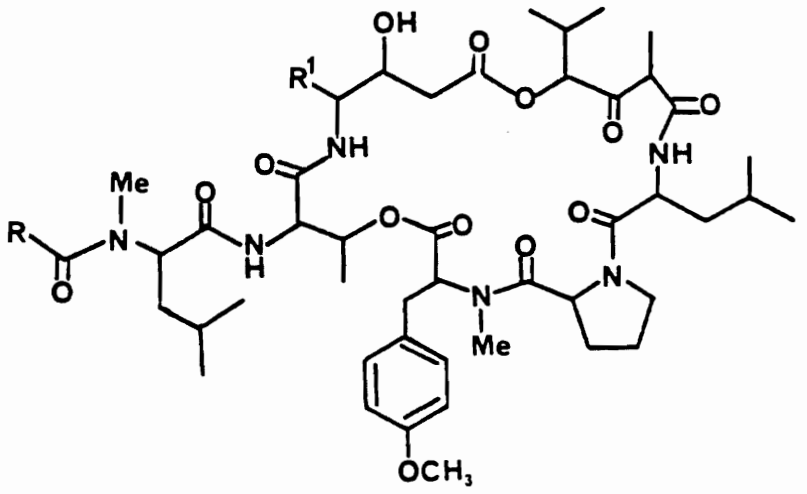

$R^1 = CH_2CH(CH_3)_2$	
48.	R = H
49.	R = Pro-COCH (OH) CH_3
50.	R = $COCHOHCH_3$

$R^1 = CH(CH_3)_2$	
51.	R = H
52.	R = Pro-COCH (OH) CH_3
53.	R = COCH (OH) CH_3

oxazoline amino acids and possessing varying degrees of activity in the L1210 murine leukemia cell assay and the CEM 360 human tumor cell assay (See Table 1). The first report appeared in 1980 when Ireland and Scheuer published the structure of ulicyclamide (54) and ulithiacyclamide (55).[54] This was followed in 1982 with the structures of patellamides 1-3 (56-58).[55] The structural characteristic of the patellamides was a fused oxazoline-thiazole ring system based partly on the FAB mass spectral fragmentation pattern and partly on the lack of homoallylic coupling between the alpha proton of the oxazoline ring and the alpha proton of the amino acid substituent at C-2 of the oxazoline ring. In 1983 Ireland and co-workers published the structures of lissoclinamide 1-3 (59-61) and the revised structure of ulicyclamide (54) based on newly acquired FAB mass spectral fragmentation data.[56] In that same year the Suntory group reported the structure of ascidiacyclamide (68) isolated from an unidentified ascidian species.[57] This symmetrical compound demonstrated a potent lethal effect on PV_4 cultured cells transformed with polyoma virus (T/C 100% at 10μg/ml).

The amino acid composition of the lissoclinum peptides was determined by interpretation of the ^{1}H NMR, ^{13}C NMR, EIMS and FABMS data with the latter two techniques instrumental in assigning the amino acid sequence. The absolute configuration of the amino acids was determined by

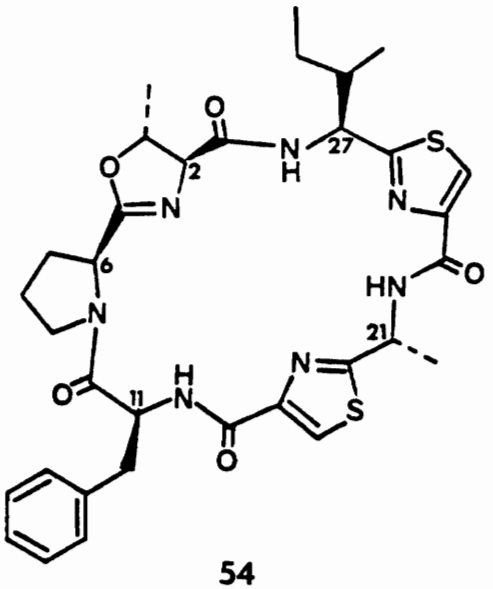

54

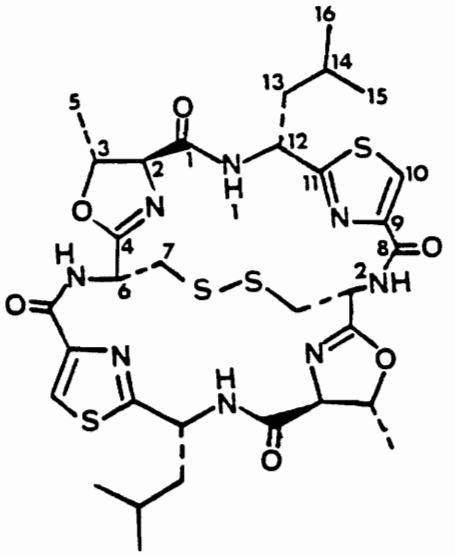

55

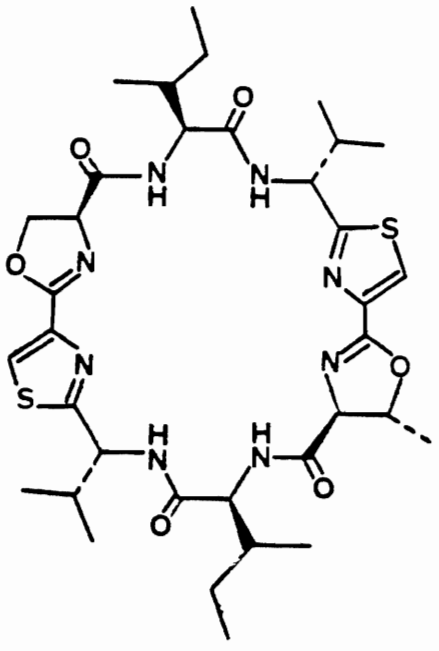

56

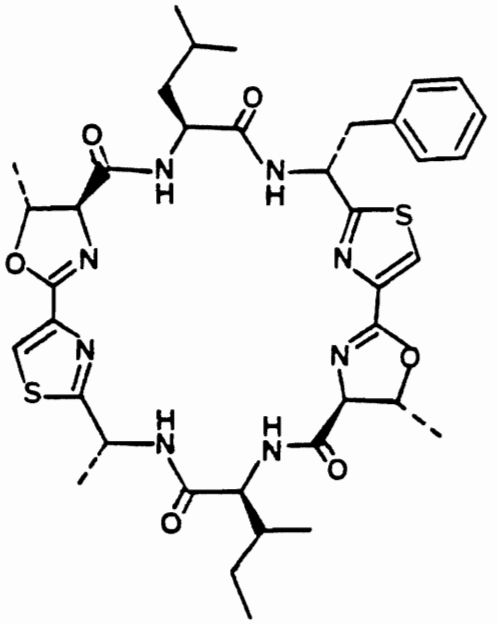

57

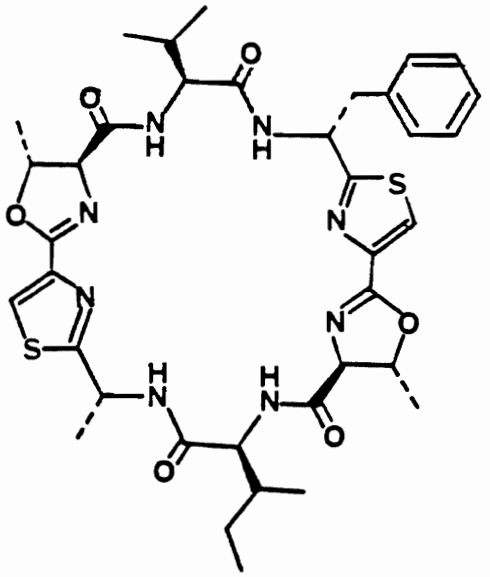

58

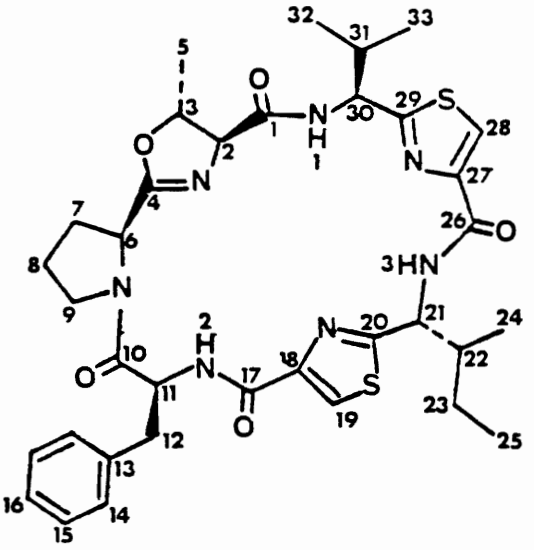

59

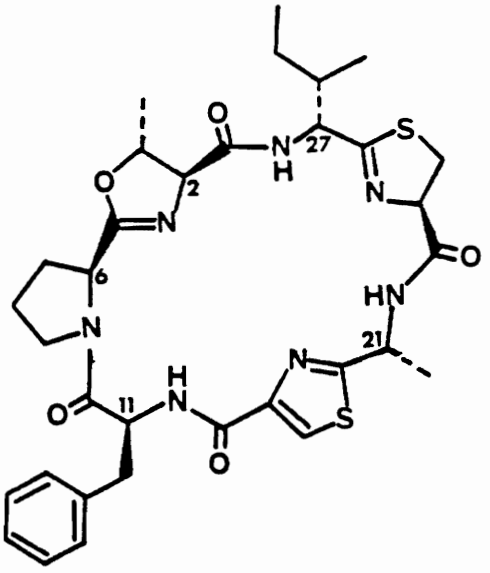

60

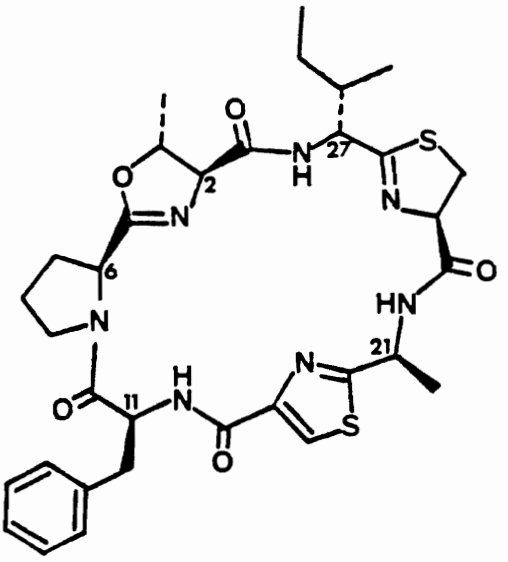

61

comparing the GC retention times of the methyl ester trifluoroacetyl derivatives of the total hydrolysis products with standards. The majority of the amino acids were found to possess the L configuration. Acid hydrolysis caused racemization of the thiazole amino acids. To circumvent this problem Biskupiak and Ireland published a general and mild method for determining the chirality of thiazole amino acids using singlet oxygen ($^1O_2$)[58].

In 1986 Sesin and Ireland published the revised structures of the patellamides A-C (65-67) based on FAB MS/MS daughter ion analysis of a tripeptide obtained from hydrolysis of patellamide B and 2D COSY-45 data.[59] Concurrently, the revised structures were confirmed in an elegant synthesis performed by Professor Shioiri.[60] The COSY 45 technique was also useful in assigning the structures of three new minor Lissoclinum metabolites (62-64), all containing threonine.[59] It is possible that prelissoclinamide 2 (62), prepatellamide-B-formate (63) and preulicyclamide (64) are precursors and that the final step in the biosynthesis of the lissoclinum peptides is formation of the oxazoline ring.

The remaining secondary metabolites isolated from marine tunicates represent four major groups: sterols, terpenes, quinones (all biosynthesized from acetyl CoA) and those of questionable origin. Djerassi reported the isolation of novel coprostanols (5β-stanols, 69), Δ^4-3-keto

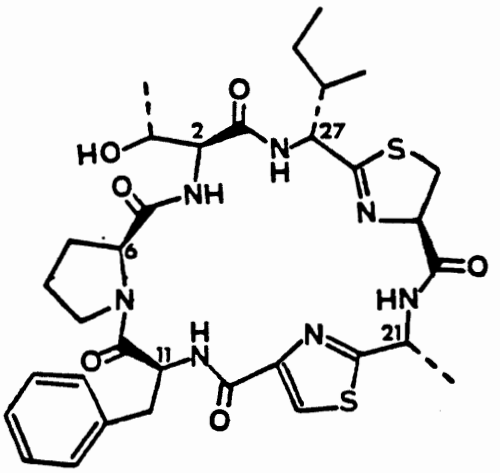

62

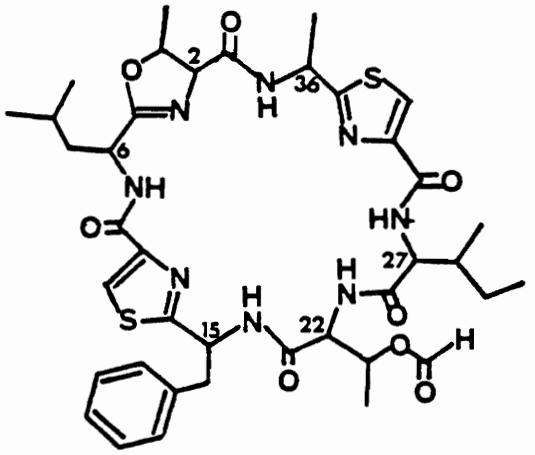

63

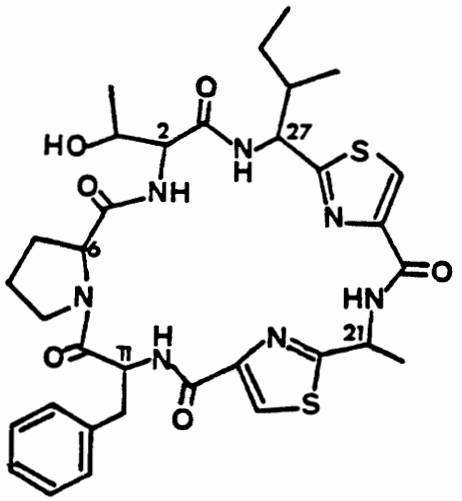

64

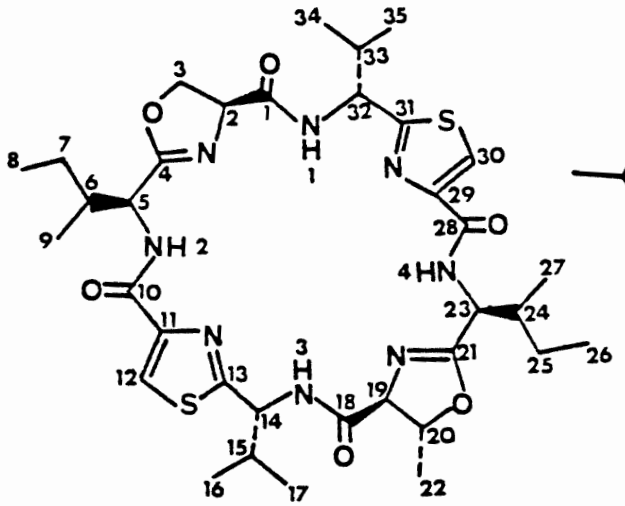

65

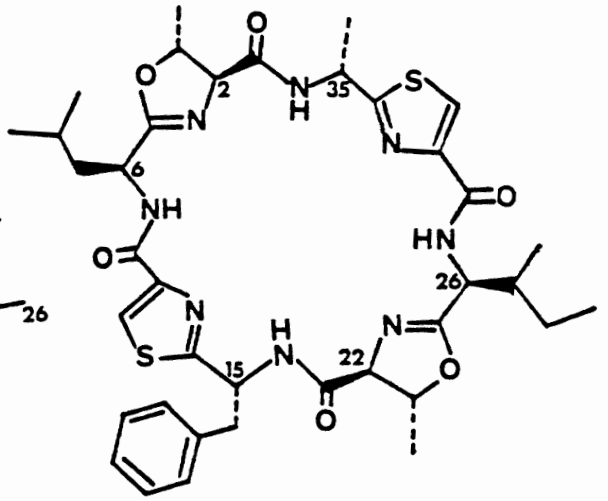

66

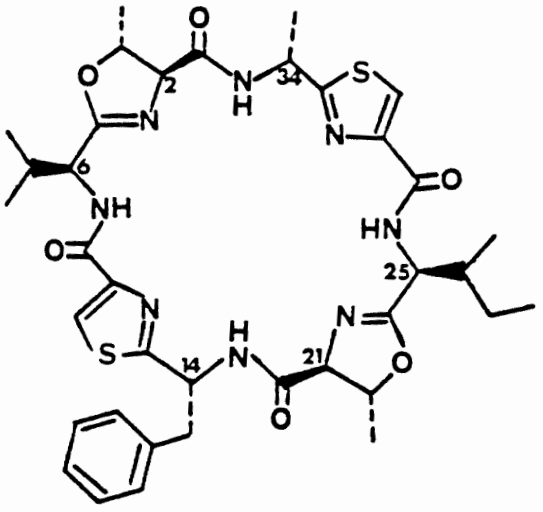

67

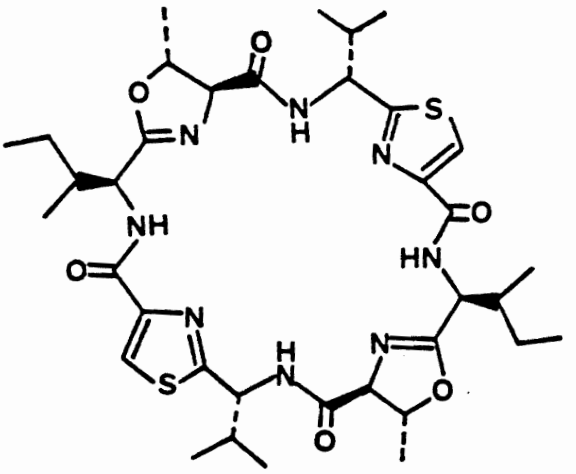

68

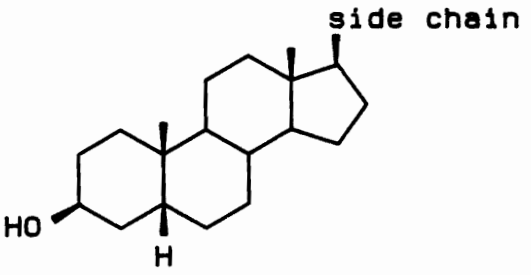

69

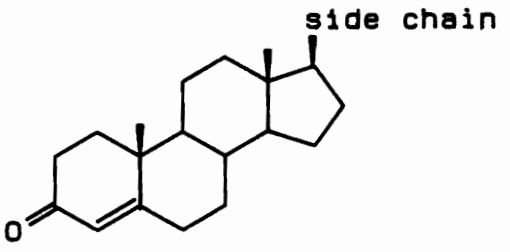

70

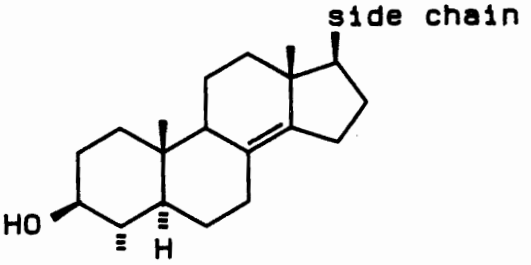

71

steroids (70) and 4 -methyl sterols (71).[61] In all cases structure elucidation was based on a comparison of their spectral data (UV, CD, NMR and mass spectral fragmentation patterns) with that of known compounds. The origin of these uncommon sterols is an intriguing question. Algal symbiosis was impossible because the ascidian, upon careful inspection, was found devoid of all algal symbionts. In the biosynthesis of regular sterols, 4α-methyl sterols (71) are intermediates. The complexity of the mixture of 4α-methyl sterols (71) and the absence of main sterols with a cholesterol side chain suggested that Ascidia nigra is unable to synthesize sterols. Therefore, the 4α-methyl sterols (71) were most likely of planktonic origin. Coprostanol is ubiquitous in the marine environment leading Djerassi to propose a dietary origin for the novel coprostanols (69) with possible chemical modification occurring in the ascidian's digestive tract.

Guyot isolated two different types of sterols from two solitary tunicates collected on the French coast- Phallusia mamillata and Ciona intestinalis. Column chromatography yielded a mixture whose characteristic features were those of sterol peroxides (72-75).[62] All four 9(11)-unsaturated sterol peroxides were obtained from P. mamillata. C. intestinalis yielded only sterol peroxide 72. Structure elucidation was based on spectral data and confirmed by synthesis. These novel sterols probably originate from

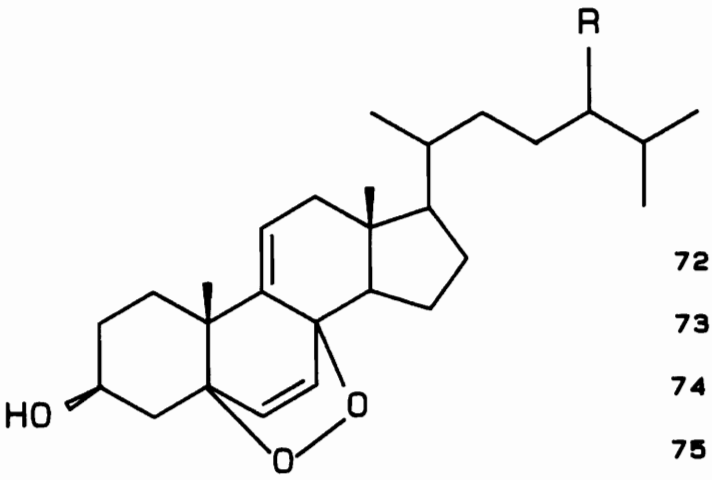

72. R: H
73. R: $=CH_2$
74. R: CH_3
75. R: CH_2CH_3

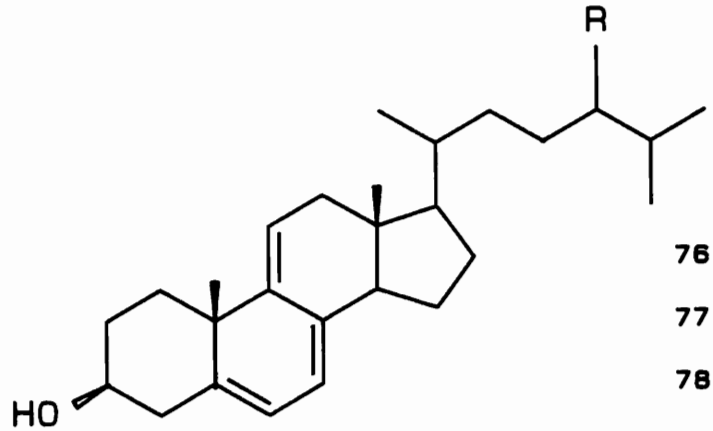

76. R: H
77. R: $=CH_2$
78. R: CH_3
79. R: CH_2CH_3

their corresponding trienes (76-79) and are generated by the 4+2 cyclo-addition of O_2 across the 5,7 diene. To eliminate the possibility that these compounds were artifacts, Guyot performed the extraction procedure in the dark and obtained the same results. The second class of sterols isolated from the same two ascidians (P. mamillata, C. intestinalis) are those possessing hydroperoxides. Guyot isolated 24-hydroperoxy-24-vinyl cholesterol (80) and confirmed the structure by reducing it to the known 24-hydroxy-24-vinyl cholesterol (saringosterol, 81) using $LiAlH_4$.[63] This compound represents 0.004% of the total extract. Therefore, to obtain a sufficient amount of material for testing, fucosterol (82) was oxidized by $^1O_2$ oxidation (O_2, $h\nu$) yielding the derived product in one step.[64] The hydroperoxide exhibited cytotoxic activity against the L1210 murine leukemia cell line (IC_{50} 2μg/ml), spleen lymphocytes without mutagens (IC_{50} 1μg/ml) and spleen lymphocytes with Concanavalin A (IC_{50} 1μg/ml).

The steroidal composition of ascidian membranes is quite unique. Morris and co-workers investigated three tunicate species and found a preponderance of 5α-stanols (83) and their corresponding Δ^5-sterols (84).[65] The saturated ring sterols are considered the intermediate in the conversion of Δ^5-sterols to Δ^7-sterols (85).However, the latter compounds were present in only 1% of the total extract. Based on the observation that some tunicates

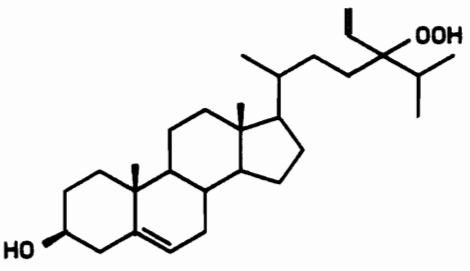

80

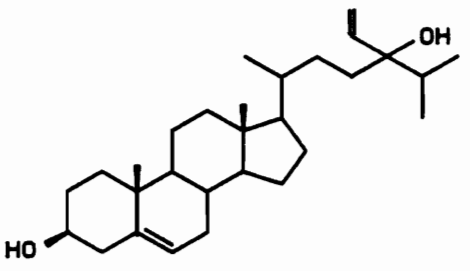

81

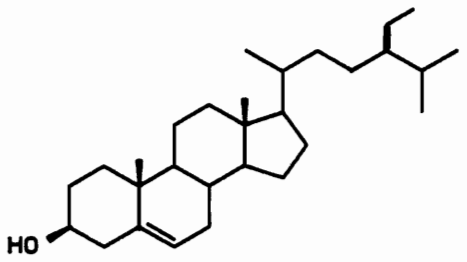

82

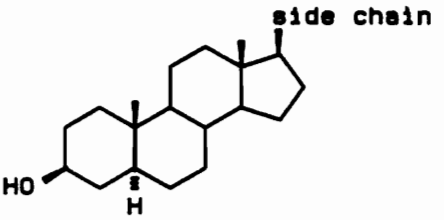

83

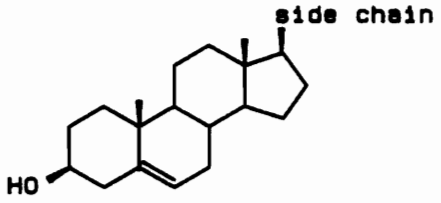

84

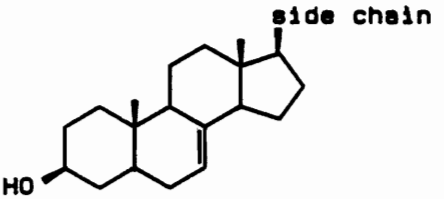

85

selectively concentrate certain metal ions from sea water[66], Morris concluded that the Δ^5-sterols (84) are involved in the specialized properties of membranes.

A series of carotenoids have been isolated from two Japanese tunicate species. Matsuno and Ookubo reported the structure of halocynthiaxanthin (86)[67] and mytiloxanthinone (87)[68] from Halocynthia roretzi. Amarouciaxanthin A (88) + B (89) were isolated from Amaroucium pliciferum.[69] These compounds may represent metabolic products from fucoxanthin (90), a carotenoid found in phytoplankton and sea weeds on which the tunicates feed (See Figure 6).[70] Guyot isolated sidnyaxanthin from the bright orange colonial tunicate Sidnyum argus.[71] Sidnyaxanthin was structurally identical to amarouciaxanthin B (89). All the carotenoids mentioned above were obtained as bright red crystals. Assignment of their final structures was based on spectral interpretation and chemical transformations. They exhibited no biological activity.

Hydroquinone derivatives offer protection against leukemia and tumor development in test animals. Wells isolated geranyl hydroquinone (91), its chromenol (92) and an unidentified ten-membered ring ether derivative from the Australian tunicate Aplidium cavernosa.[72] Following a thorough investigation of another aplidium species (Aplidium californicum), Howard isolated three simple prenylated hydroquinone derivatives: prenylhydroquinone (93), 6-

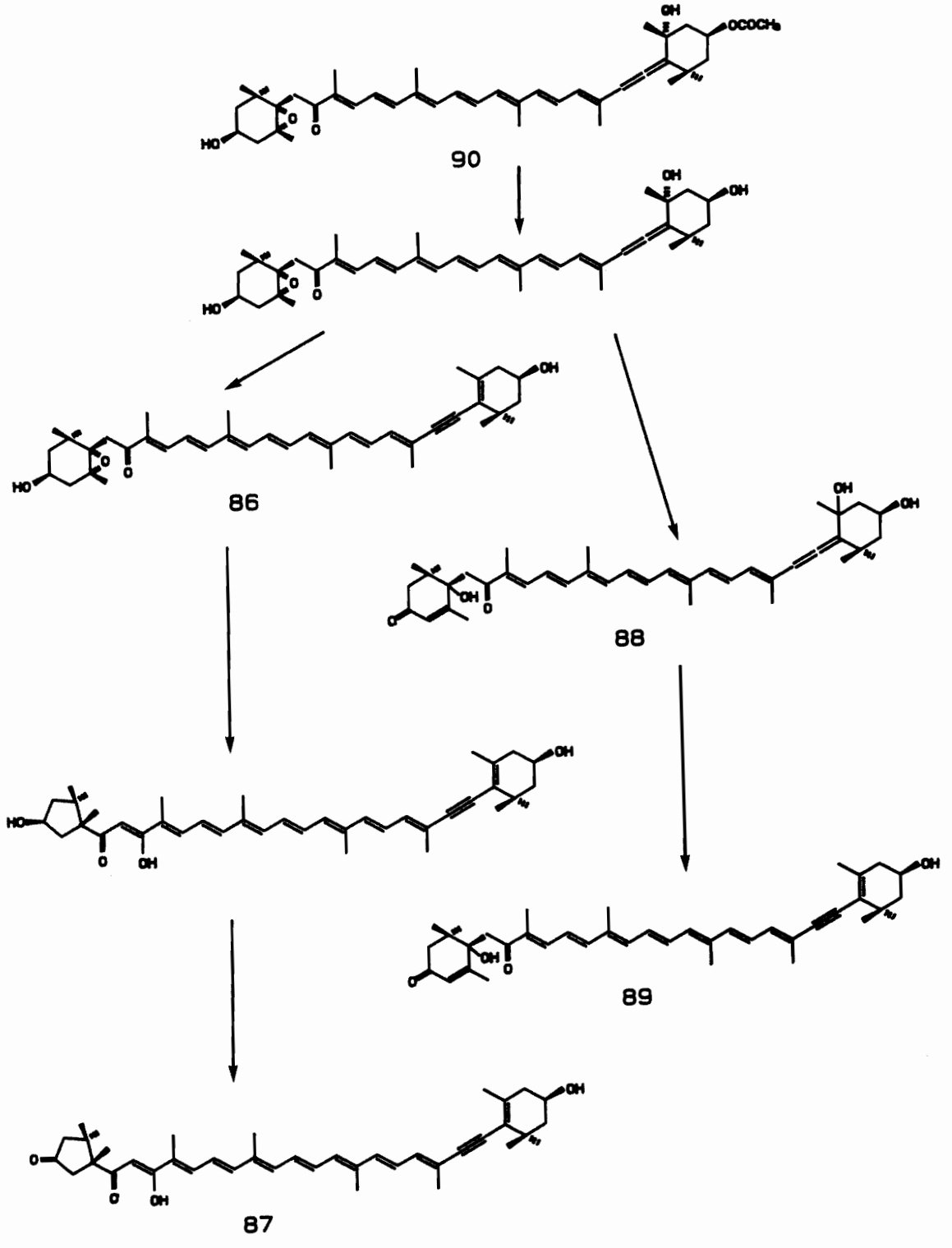

Figure 6. Metabolic pathway of fucoxanthin

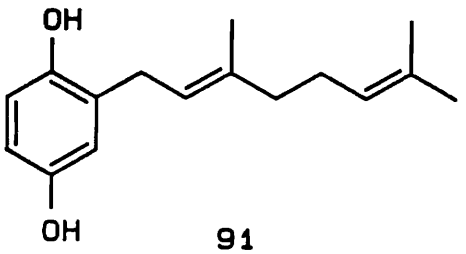

91

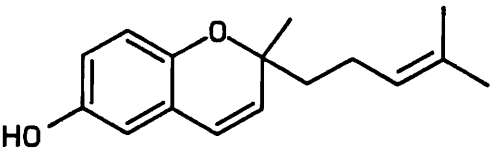

92

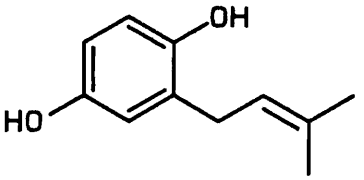

93

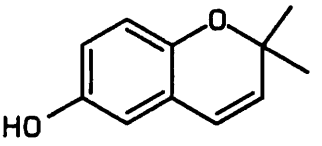

94

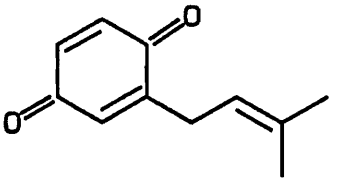

95

hydroxy-2,2-dimethylchromene (94) and prenylquinone (95).[73] The structures of all three compounds were secured by synthesis. Prenylhydroquinone (93) exhibited *in vivo* (mice) activity against P388 lymphocytic leukemia (T/C = 138 at 3.12mg/kg). Furthermore, prenylhydroquinone (93) and its chromenol (94) inhibited the mutagenic effects of benzo(a)pyrene, aflatoxin B, and UV light on *Salmonella typhimurium* (modified Ames Assay). Compounds 93 and 94 also exhibited antioxidant properties.

Sesin and Ireland isolated four novel cytotoxic metabolites (96-99) from the encrusting ascidian *Didemnum voeltzkowi*.[74] Voeltzkowinols A,B,C,D exhibited varying degrees of activity in the L1210 assay (voeltzkowinol A: 3.9 µg/ml; voeltzkowinol B & C: 5.6 µg/ml; voeltzkowinol D: 0.56 µg/ml) and are structurally similar to compound(100) also isolated from a didemnid tunicate.[75]

Rinehart isolated a metabolite from an orange-flecked *Aplidium* sp. which is biosynthesized from an acetyl CoA derivative (diterpene) and an amino acid (serine minus its carboxyl group).[76] The compound, appropriately called aplidiasphingosine (101), was identified by spectral interpretation and chemical modification. Its stereochemistry was deduced based on an asymmetric synthesis in which the key reaction was the Sharpless asymmetric epoxidation and a ^{13}C NMR study of sphingosine relatives.[77] Aplidiasphingosine possessed antimicrobial activity (at 80

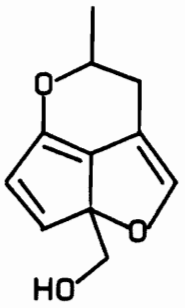

96

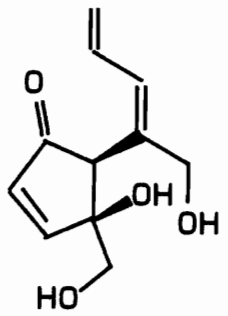

97

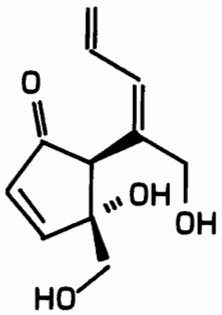

98

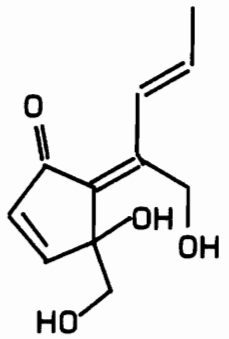

99

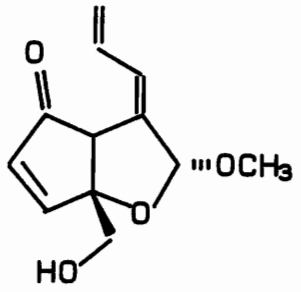

100

µg/12.7mm disc) against Gram (+) bacteria (Bacillus subtilis, 24mm; Sarcina lutea, 20mm), Gram (-) bacteria (Klebsiella pneumoniae, 21mm; Mycobacterium avium, 21mm), and fungi (Candida albicans, slight), and was cytotoxic towards KB (IC_{50} 8.3µg/ml) and L1210 (IC_{50} 1.9µg/ml) tumor cells.

It should also be noted that tunicates possess significant concentrations of riboflavin (102), isoxanthopterin (103) and 2-amino-4 hydroxypteridine (104) suggesting that they serve an important role in the nutritive cycle as a source of vitamins and other trophic factors.[78]

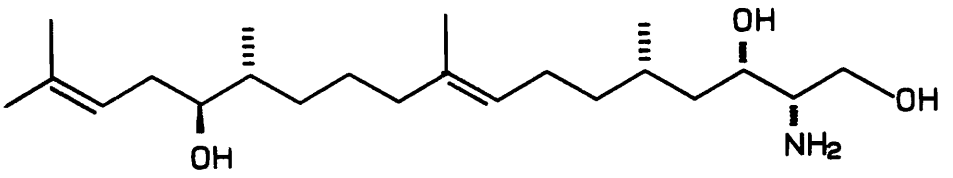

101

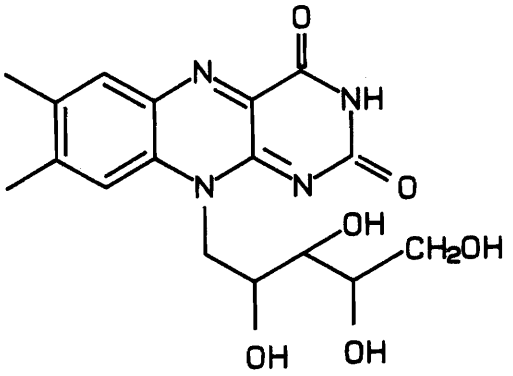

102

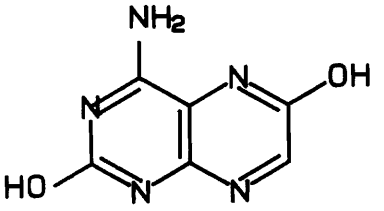

103

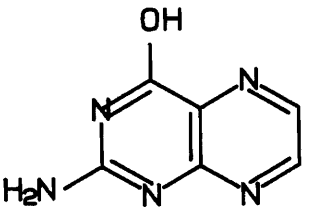

104

THE CHEMISTRY OF SOME PACIFIC TUNICATES

Rinehart[32] and Weinheimer[33] defined marine tunicates as potential sources of biologically-active compounds. This prompted Dr. Ireland to pursue a systematic investigation of Pacific ascidians. During my tenure as a graduate student I have isolated several biologically-active compounds from the following Pacific tunicates: an unidentified didemnid, Didemnum voeltzkowi and Lissoclinum patella. Most of the compounds isolated from these tunicates are biosynthesized from amino acids. These nitrogen-containing metabolites possess varying degrees of cytotoxic activity in the L1210 murine leukemia cell assay and the CEM 360 assay. One of the compounds (3.5-diiodo-4-methoxyphenethylamine, 45) exhibited significant antifungal activity against the yeast Candida albicans. D. voeltzkowi produced four non-nitrogenous prostaglandin-like compounds that also demonstrated good activity in the L1210 assay. The following sections will discuss the isolation and structure elucidation of the active metabolites from each tunicate.

The Chemistry of an Unidentified Tunicate

An unidentified didemnid tunicate[79] was collected from the exposed rocks at the northwest end of Cocos Lagoon, Guam where it was found as an encrusting species. The ascidian

was collected at two different times,(1981, 1982). Both collections produced the same chemistry.

The ascidian was kept frozen until work-up. The first step in the isolation procedure was lyophilization of the frozen tissue. The freeze dried tissue (116g) was placed in a soxhlet extraction apparatus and exhaustively extracted with pet ether, CCl_4 and then $CHCl_3$. The extracted tissue was then placed in a 1 liter flask containing MeOH and allowed to extract overnight. Initial testing of each crude extract in the L1210 assay indicated borderline activity (10 µg/ml) in the $CHCl_3$ extract.

While the $CHCl_3$ extract was cooling at room temperature a brown solid, 3,5-diiodo-4-methoxyphenethylamine (45) (450 mg 0.4% dry weight) precipitated from solution as the HCl salt. Upon refrigeration of the $CHCl_3$ extract a second metabolite, subsequently identified as the urea analog (46), precipitated from solution. Column chromatography of the $CHCl_3$ extract (Silica gel 60, 95:5:0.7 EtOAc/MeOH/NH_4OH) yielded 3 fractions. The more polar fraction appeared as a light red liquid and exhibited good activity in the L1210 assay (3.4 µg/ml). Unfortunately, the sample weight was approximately 1 mg and with the unlikelihood of obtaining more freeze-dried tissue attention was focused on compounds 45 and 46.

The major metabolite (45) was assigned the molecular formula $C_9H_{11}NOI_2$ (HRMS: obs 402.8929, calc. 402.8941)

indicating four degrees of unsaturation. The ^{13}C NMR spectrum contained signals for 6 sp^2 carbons: 157.1 (s), 139.7 (d, 2C), 137.7 (s), 91.5 (s, 2C). The lack of a carbonyl stretch between 1800-1600 cm^{-1}, a UV λmax of 268nm and IR stretches at 1600, 1460, 860 and 710 cm^{-1} suggested the presence of a substituted benzene ring. Present in the ^1H NMR spectrum was an A_2B_2 spin system [3.03 (t, 2H, J = 7 Hz); 2.86 (t, 2H, J = 7 Hz)] assignable to the four methylene protons of a phenethylamine. Signals in the ^1H and ^{13}C NMR spectra defined the following substituents attached to the benzene ring: one methoxyl (^1H: 3.73 ppm; ^{13}C: 157.1 ppm), two iodines [^{13}C: 91.5 (s, 2C)] and two degenerate protons [^1H: 7.76 (s, 2H); ^{13}C: 139.7 (d, 2C)]. Placement of the substituents about the ring was based on the following arguments: the final structure should be symmetrical based on the degeneracy of the aromatic proton signals. The methoxyl and iodine atoms were placed in the para and meta positions,respectively, to mimic the structure of thyroxin (3).

Instrumental in assigning the final structure was complete analysis of the major fragment ions in the EI mass spectrum (Figure 7). Present is the molecular ion at m/z 403 that peak matched to within 3 mmu (or 3 ppm) of its calculated molecular weight. β-cleavage of the side chain results in formation of the base peak at m/z 373. This ion can easily be converted into the highly stable tropyllium

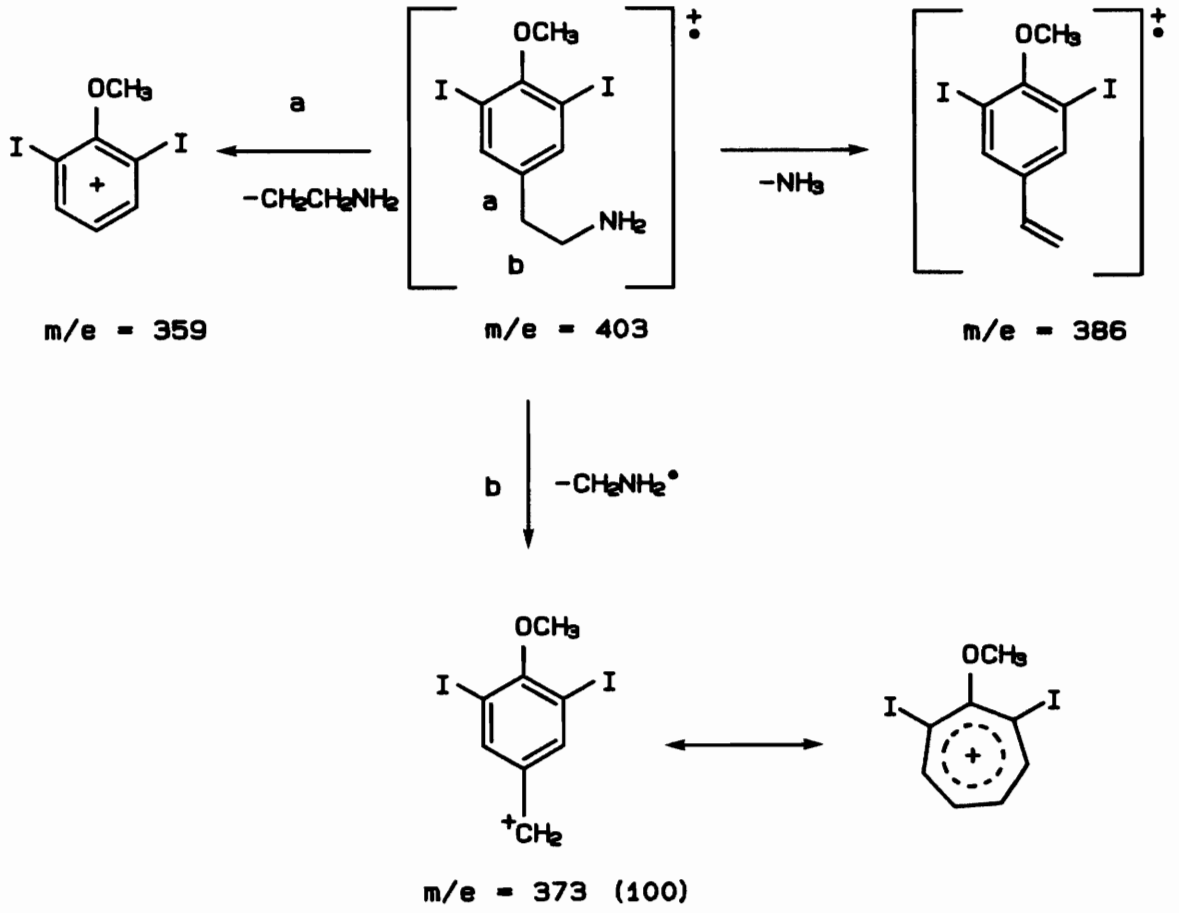

Figure 7. EIMS fragmentation pattern of 45

ion. Para substituted anisoles have been shown to undergo alpha cleavage.[80] This cleavage results in a m/z 359 ion. The ion at m/z 386 results from the expulsion of NH_3 from the parent molecule.

To confirm placement of the substituents about the ring the natural product was synthesized. The first synthetic route involved decarboxylation of 3,5-diiodo-tyrosine followed by methylation of the phenol to yield the desired product (Figure 8). The two methods used to decarboxylate the starting material proved to be exercises in futility. Enzymatic decarboxylation using tyrosine decarboxylase[81] was hampered by poor solubility of the substrate in the acetate buffer. To alleviate this problem the substrate was first dissolved in a 50:50 mixture of acetone and water. The acetone was removed by heating on a steam bath. To maintain solubility 2 drops of concentrated Tween-80 (surfactant) were added immediately. The solution was cooled to room temperature. Pyridoxal 5'-phosphate and tyrosine decarboxylase were added to the flask. The flask was stoppered with a wad of cotton and left to react in an oil bath set at 37°C. High-voltage electrophoresis of the enzymatic reaction mixture indicated the presence of only starting material. Evidently, 3,5-diiodo-tyrosine is not an acceptable substrate for tyrosine decarboxylase. As an alternative method catalytic decarboxylation using $Cu(OAc)_2$ was attempted.[82] The first intermediate formed is a metal

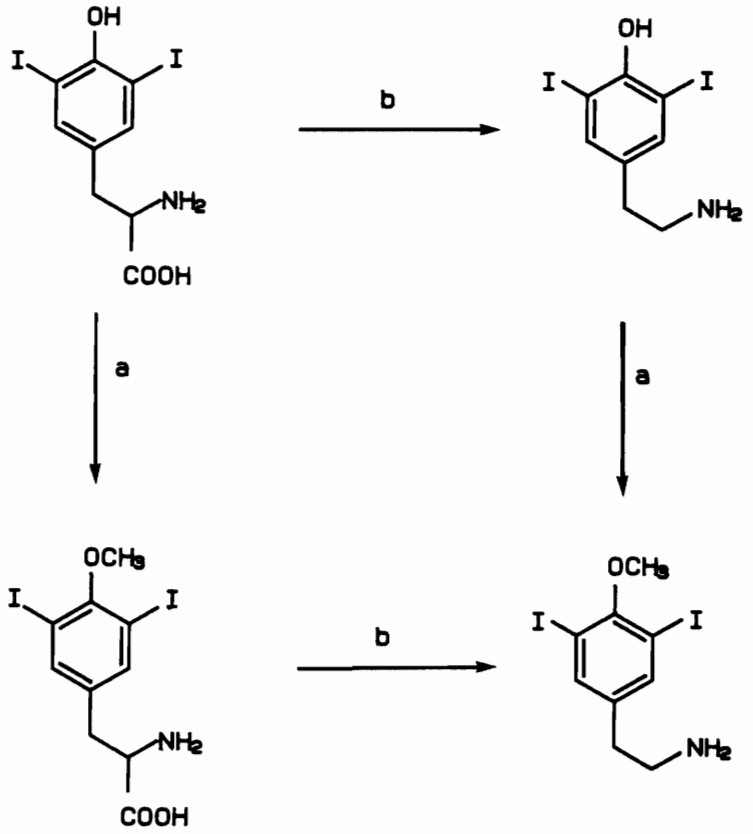

a. CH_2N_2/MeOH

b. tyrosine decarboxylase
or $Cu(OAc)_2$/DMSO

Figure 8. Decarboxylation of tyrosine

complex involving the amine and the carboxyl group. The complex is subsequently degraded by heating in DMSO. All attempts to decarboxylate 3,5-diiodo-tyrosine failed. Several attempts to methylate the phenol (CH_2N_2,MeOH) prior to the decarboxylation step also failed prompting the formulation of an entirely new reaction sequence using tyramine (105) as the starting material. This new reaction sequence involved methylation of the phenol followed by electrophilic attack by I^+. The amine was blocked to prevent N-methylation. This was accomplished by acetylating the nitrogen with acetic anhydride in H_2O. The order of methylation and iodination was very critical. Methylation followed by iodination resulted in the formation of mono-iodinated products. Presumably, the first iodo group directs the methoxyl group such that the methyl sterically hinders approach of the second iodide atom. The successful reaction sequence is shown in Figure 9. Tyramine was first acetylated using Ac_2O/H_2O, affording N-acyl tyramine (106). Compound 106 was then iodinated using ICl and glacial acetic acid[83] forming intermediate 107. The hydroxyl group is a much stronger ortho director than an alkyl group. Therefore electrophilic substitution of compound 106 resulted in the substitution pattern as shown for compound 107. Methylation of the phenol using NaH and dimethyl sulfate yielded 108. Attempts to methylate with CH_2N_2/MeOH were unsuccessful indicating that the phenolic proton was fairly acidic.

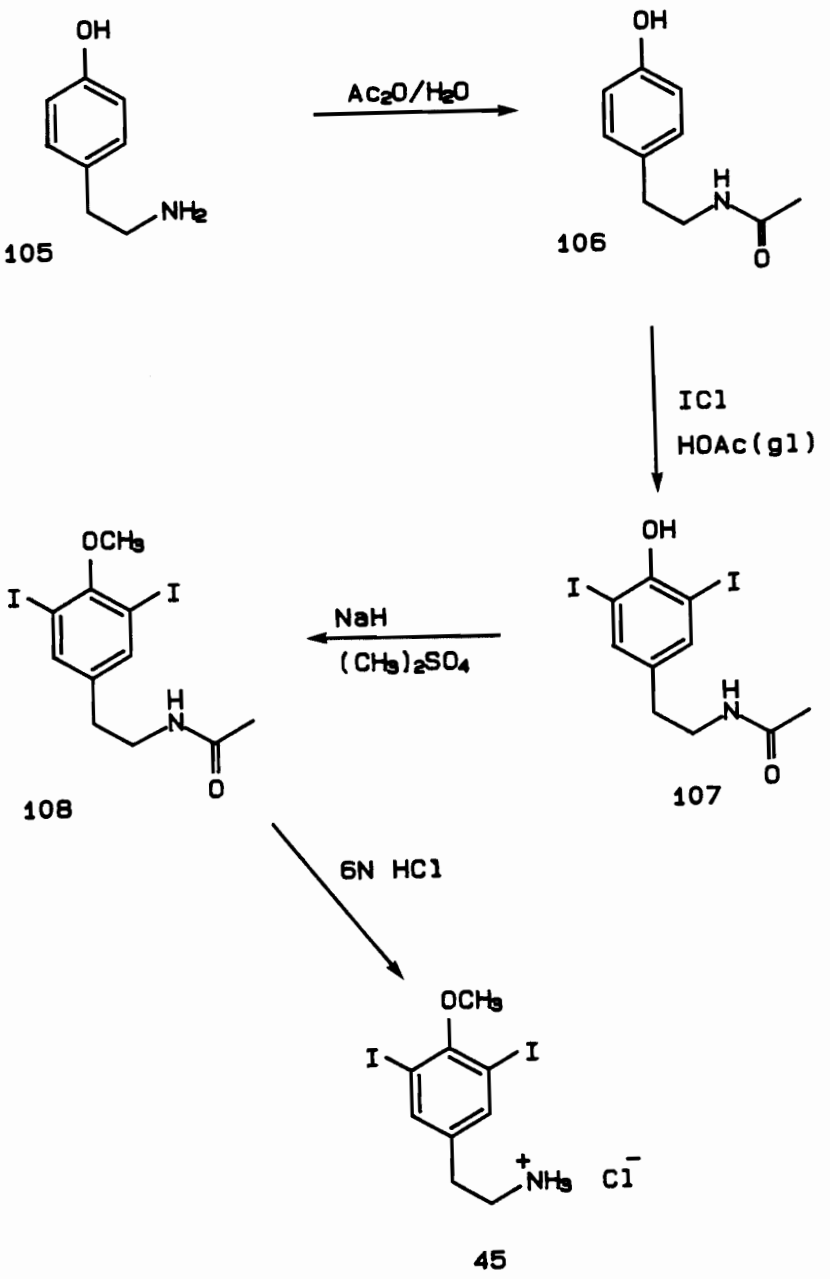

Figure 9. Synthesis of 3,5-diiodo-4-methoxyphenethylamine

Acid hydrolysis of 108 (6N HCl, threaded test tube, 110°C, 12 h) followed by column chromatography (Silica gel, 70:20:10 $CHCl_3$/MeOH/NH_4OH) yielded 3,5-diiodo-4-methoxyphenethylamine (45) as the HCl salt in 80% yield. The spectral data of the synthetic product and the natural product were identical.

The minor metabolite, 3,5 diiodo-4-methoxyphenethylurea (46), represented 0.01% of the total dry weight. It was assigned a molecular formula $C_{19}H_{20}N_2O_3I_4$ (HRMS: obs. 831.7699, calc.831.7675). The ^1H NMR of compound 46 contained signals directly assignable to a phenethylamine unit [δ7.56 (s, 2H); 3.62 (s, 3H); 3.08 (dt, 2H, J = 7, 6 Hz); 2.49 (t, 2H, J = 7 Hz)] and a new signal at 5.78 ppm (t, J = 6 Hz) assigned to the NH proton of the urea. The ^{13}C NMR spectrum contained only 8 signals, seven of which were consistent for the phenethylamine unit (δ157.8 (s), 140.2 (d, 2C), 139.6 (s), 91.0 (s, 2C), 60.1 (q), 40.4 (t), 34.1 (t), and the eighth signal, a singlet at 156.6 ppm, which was assigned to a urea carbonyl. These pieces of data suggested that the urea was symmetrical.

Again, complete analysis of the major fragment ions (Figure 10) in the EI mass spectrum was instrumental in confirming the structure. A molecular ion appeared at m/z 832 which peak matched to within 3 mmu (or 3 ppm) of its calculated molecular weight. Loss of an iodide atom results in the formation of an ion at m/z 705. Baldwin has

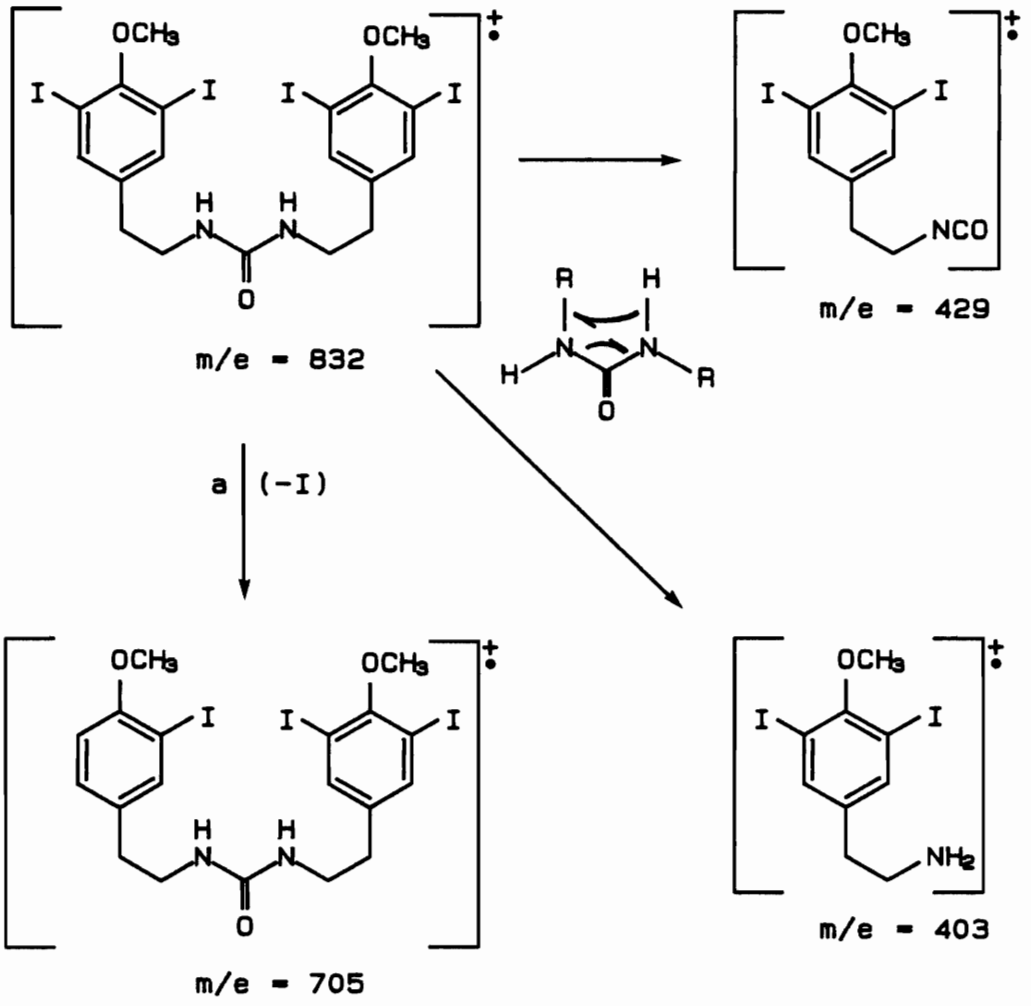

Figure 10. EIMS fragmentation pattern of 46

demonstrated that urea derivatives undergo four major modes of fragmentation as illustrated in Figure 11.[84] Pathways (3) and (4) account for the formation of the radical cations at m/z 429 and 403. Previously, N,N'-diphenethylurea was isolated from a didemnid tunicate[50], suggesting that the urea analog is a natural product and not an artefact.

3,5-Diiodo-4-methoxyphenethylamine (45) exhibited moderate activity in the L1210 murine leukemia cell assay (IC_{50} 20μg/ml). When tested *in vitro* against the yeast *Candida albicans* it proved to be a potent antifungal metabolite. This observation was very rewarding because there are very few marine natural products that successfully eliminate yeast infections. Compound 45 was also mildly active against gram(+) and gram(-) pathogens. In sharp contrast, the urea analog exhibited no biological activity.

These two metabolites are also interesting from a biosynthetic viewpoint. Several nitrogen-containing metabolites, such as the Lissoclinum peptides (54-64)[54-56] and N,N'diphenethylurea (47), have been isolated from didemnid tunicates harboring unicellular prokaryotic algae. As discussed earlier, it is theorized that the symbiotic algae may be responsible for the biosynthesis of these compounds. However, compounds 45 and 46 were isolated from a didemnid species devoid of all algal symbionts. Therefore compounds 45 and 46 are of dietary origin or are biosynthesized by the tunicate. The detection of tyrosine

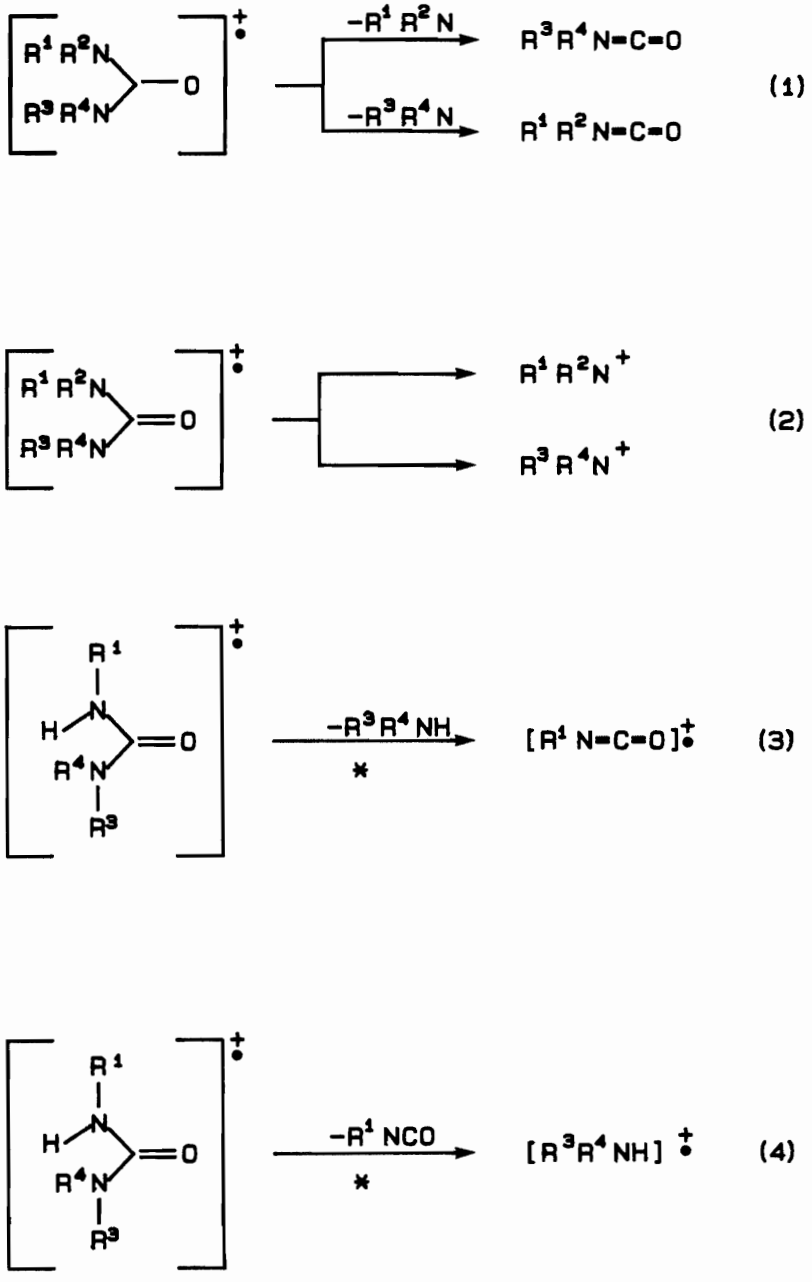

Figure 11. Fragmentation patterns for urea derivatives

secreting cells and iodine uptake cells in the endostyle of ascidians[2] strongly suggests that the tunicate is responsible for their biosynthesis.

The Chemistry of Didemnum voeltzkowi

Didemnum voeltzkowi was collected on the main fringing reef of Suva Harbor, Fiji, where it was found as an encrusting species on coral and coralline algae. The tunicate harbors symbiotic algae as defined by the speckling of green dots seen throughout the test of the organism. Initial testing of a crude methanolic extract in the L1210 assay gave a cytotoxicity value of 5.5μg/ml. This value is indicative of borderline activity; however, for a crude extract in which many of the components are salts and lysed cells it was encouraging.

Isolating the active metabolites proved to be very challenging due to their propensity to decompose. Leaving the extract on the lab bench in a small amount of MeOH for one hour or overnight storage in a refrigerator was sufficient to initiate decomposition of the active compounds. All chromatographic techniques were performed in the dark and once isolated the pure compounds were dissolved in MeOH and stored in a freezer.

The general protocol for initial extraction of freeze-dried tissue was switched from the high-temperature soxhlet extraction procedure, which became unappealing due to its ability to thermally decompose compounds, to the more gentle

but equally effective Kupchan fractionation scheme.[85] A modification of the latter technique proved to be effective in isolating the active components from Didemnum voeltzkowi. The freeze-dried tissue (625 g) was blended with 1.25L of MeOH. The homogenate was divided into three equal portions. Each portion was transferred to a 1L erlenmeyer flask and extracted overnight. The solvent was removed in vacuo. The residue was redissolved in MeOH and partitioned with $CHCl_3$ (3 x 125 ml). Three of the four cytotoxic metabolites were strongly UV-active; the fourth metabolite appeared as a dark yellow spot on the TLC plate. Examination of the $CHCl_3$ and MeOH fractions by TLC (Silica gel, EtOAc/TMP 8:2) indicated that all four compounds were concentrated in the MeOH fraction. A $BuOH/H_2O$ partition of the methanolic fraction isolated the metabolites from the salts and lysed cells. The butanol fraction was chromatographed on a 6 ft. Sephadex column (LH-20, MeOH:$CHCl_3$ 1:1) yielding a light yellow oil that tested at 2.7 μg/ml (L1210 assay). This oil was further purified by HPLC (μ partisil, EtOAc/TMP 8:2) to yield voeltzkowinol A (96, 0.002% dry weight), B (97, 0.007% dry weight), C (98, 0.006% dry weight) and D (99, 0.02% dry weight) in order of increasing polarity.

Voeltzkowinol B (97) was assigned the molecular formula $C_{11}H_{14}O_4$ (HREIMS: obs. 210.0893; calc. 210.0888) indicating 5 degrees of unsaturation. Acetylation of voeltzkowinol B (Ac_2O, pyridine) produced a diacetate [(109), EIMS: m/z =

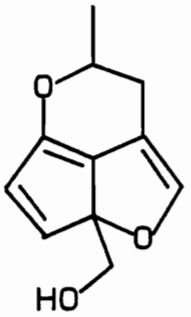

96

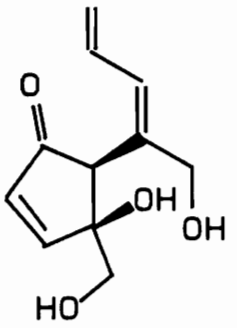

97

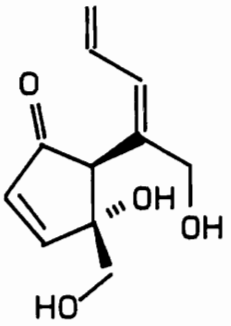

98

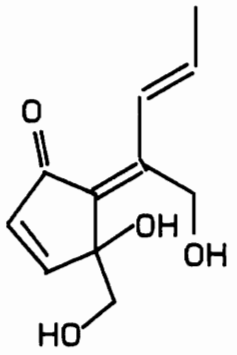

99

294; ^{1}H NMR: δ2.09 (s, 3H), 2.04 (s, 3H)] indicating the presence of two 1° and/or 2° hydroxyls in the molecule. An IR stretch at 1704 cm^{-1} and a UV max of 231 nm suggested the presence of a cyclopentenone ring system. The NMR spectral data of voeltzkowinol B is shown in Figure 12. Present in the ^{1}H NMR spectrum is an isolated AB spin system [δ6.25 (d, 1H, J = 6 Hz), 7.51 (d, 1H, J = 6 Hz)] for the α and β protons of the cyclopentenone and two isolated AB spin systems [δ3.96 (d, 1H, J = 12.6 Hz), 4.24 (d, 1H, J = 12.6 Hz); 3.59 (d, 1H, J = 10.5 Hz), 3.69 (d, 1H, J = 10.5 Hz)] for two primary alcohols. Also present are four olefinic signals [δ6.38 (d, 1H, J = 11.2 Hz), 6.65 (ddd, 1H, J = 10.6, 11.2, 16.5 Hz), 5.31 (d, 1H, J = 16.5 Hz), 5.21 (d, 1H, J = 10.6 Hz)] defining a conjugated 1,1 disubstituted diene. The multiplicities of the olefinic carbon signals [δ136.1 (t), 133.7 (d), 133.5 (d), 119.8 (s)] corroborated this assignment. Placement of substituents about the cyclopentenone ring system was based on the multiplicities and chemical shifts of the remaining signals in the ^{1}H and ^{13}C NMR spectra. Present in the ^{13}C NMR spectrum is a singlet at 82.2 ppm and a doublet at 53.0 ppm indicating that there is only one additional proton attached to the cyclopentenone ring. This proton appears as a sharp singlet at 3.88 ppm necessitating that it be placed adjacent to the carbonyl.

Assignments have been made for all nuclei except an

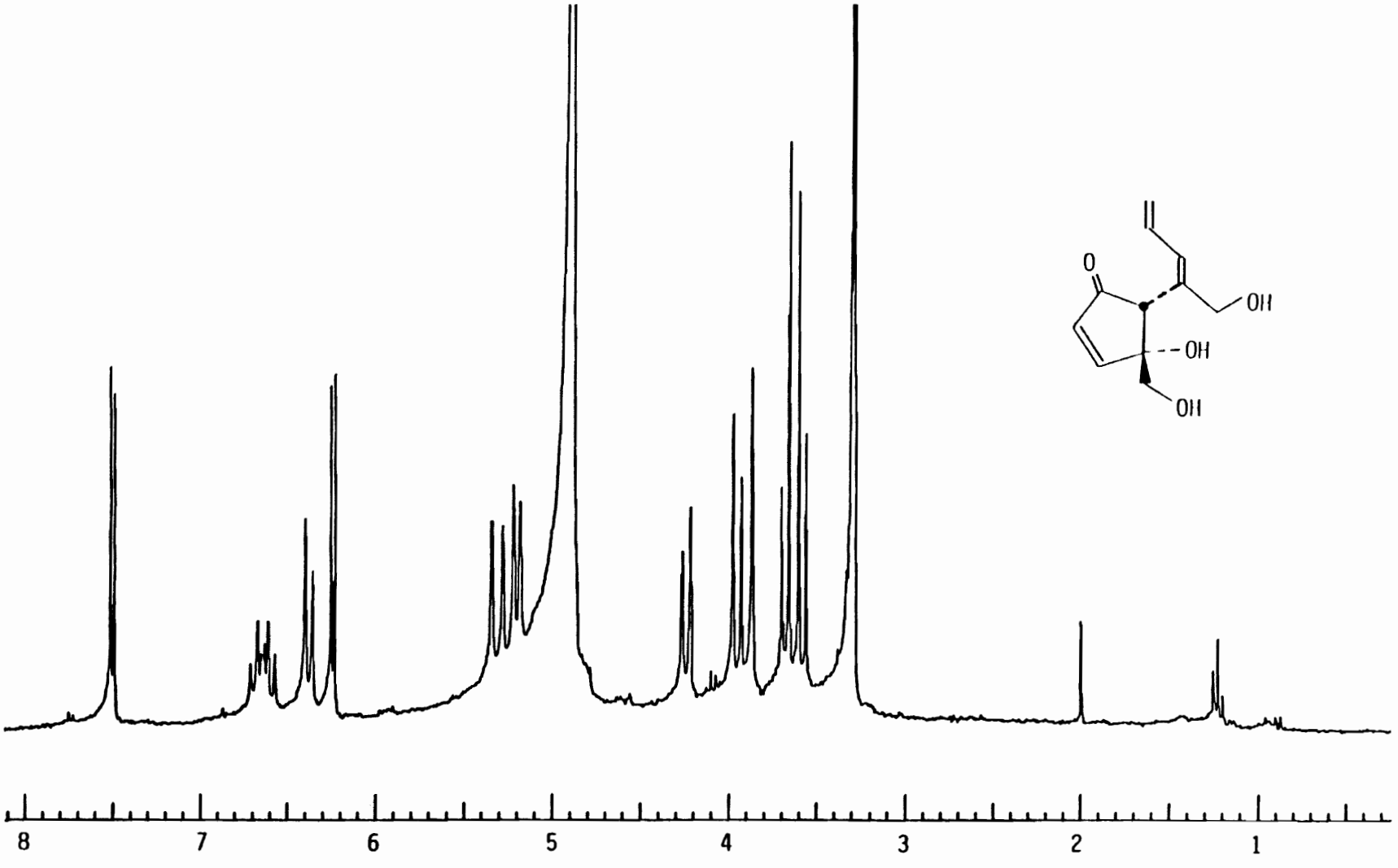

Figure 12. ^{1}H NMR of voeltzkowinol B

oxygen and a proton. The IR spectrum was transparent in the region defining a C-O stretch for an ether (1300-1000 cm^{-1}) implying the presence of an additional hydroxyl group. Recalling that acetylation of voeltzkowinol B produced a diacetate suggested that the third hydroxyl was tertiary. The diene carbon signals showed no appreciable polarization due to the attachment of a heteroatom indicating that one of the diene substituents must be a primary alcohol and not the tertiary alcohol. Therefore the tertiary alcohol had to be placed on the ring carbon adjacent to the methine.

There are two possible ways of constructing voeltzkowinol B as shown in Figure 13. Structure B was chosen based on the multiplicity of the methinyl proton at C-5 [δ3.88 (s)] and the well-defined AB system assigned to the nonallylic primary alcohol [δ3.69 (d, 1H, J = 10.5 Hz, 3.59 (d, 1H, J = 10.5 Hz]. If structure A was correct the methinyl proton should appear as a triplet and the well-defined AB signal for the nonallylic hydroxyl methylene protons should appear as a doublet of quartets. Additional evidence confirming the assignment of voeltzkowinol B was obtained from chemical modifications as described below.

Voeltzkowinol C (98) was isomeric with voeltzkowinol B (97) and exhibited virtually identical spectral data. Acetylation of voeltzkowinol C gave a diacetate (110) indicating the presence of two primary alcohols. The ^1H NMR spectrum of 98 is shown in Figure 14. Present are peaks for

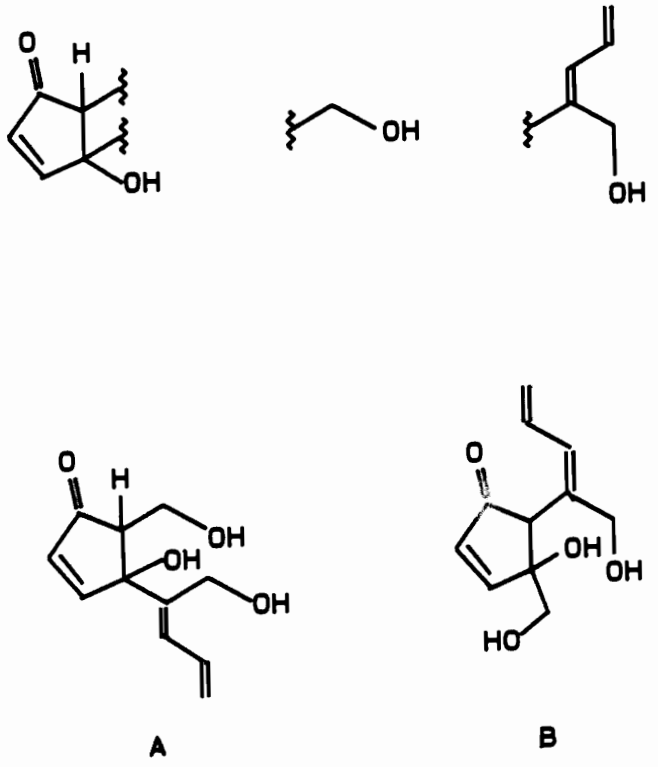

Figure 13. Partial structures and possible structures A and B for voeltzkowinol B

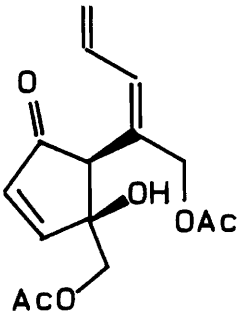

109

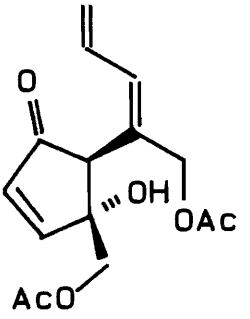

110

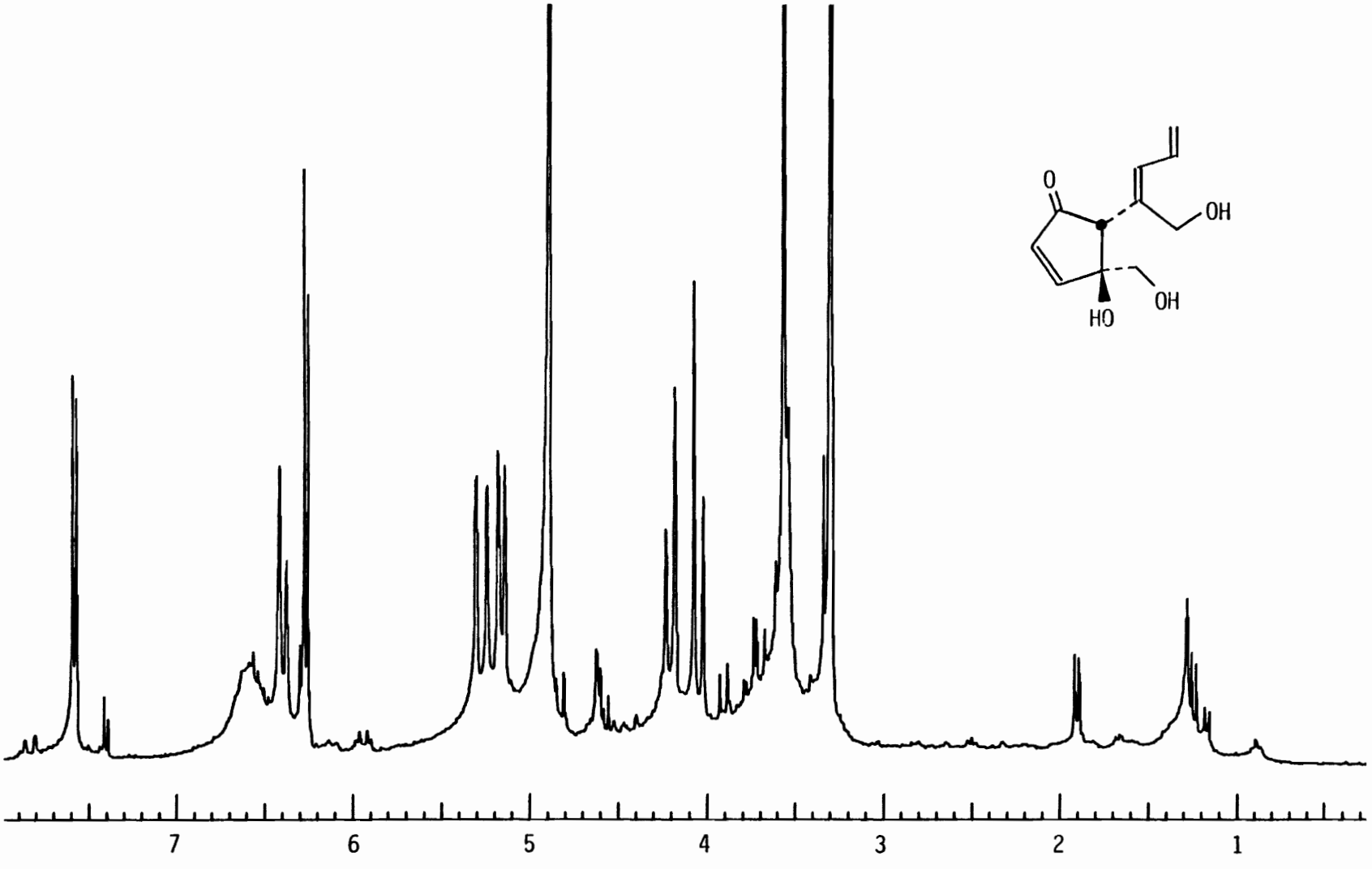

Figure 14. ^{1}H NMR of voeltzkowinol C

the cyclopentenone ring [δ7.58 (d, 1H, J = 6 Hz), 6.15 (d, 1H, J = 6 Hz)] and the diene side chain [δ6.41 (m, 1H, J = 16.4, 16, 10 Hz), 6.26 (d, 1H, J = 16 Hz), 5.27 (d, 1H, J = 16.4 Hz), 5.16 (d, 1H, J = 10 Hz)]. The ^{1}H NMR spectrum differed from that of voeltzkowinol B in the region between 3.5-4.5 ppm (Figure 15). This region contains the signals for the two primary alcohols and the methine proton at C-5. Due to the allylic nature of the primary alcohol at C-6 it was assigned to the downfield spin system centered at 4.1 ppm. Present in the ^{1}H NMR of voeltzkowinol C is the AB spin system for the allylic primary alcohol. Missing is the AB spin system for the primary alcohol at C-4. Instead one finds a broad singlet at 3.5 ppm that integrates for three protons. This signal was assigned to the methinyl proton at C-5 and the two primary alcohol protons at C-4 suggesting that voeltzkowinol B and voeltzkowinol C were epimeric at C-4 or C-5.

The stereochemical relationship between the diene side chain and the hydroxyl substituents at C-4 was solved by the following chemical analysis. Allylic oxidation of voeltzkowinol B and C should yield the five or six-membered ring lactone depending on which alcohol attached at C-4 is cis to the diene side chain. The results of the chemical study are shown in Figure 16. Allylic oxidation of voeltzkowinol B with MnO_2 in CH_2Cl_2 afforded the gamma lactone (111) as the only product in good yield. The first

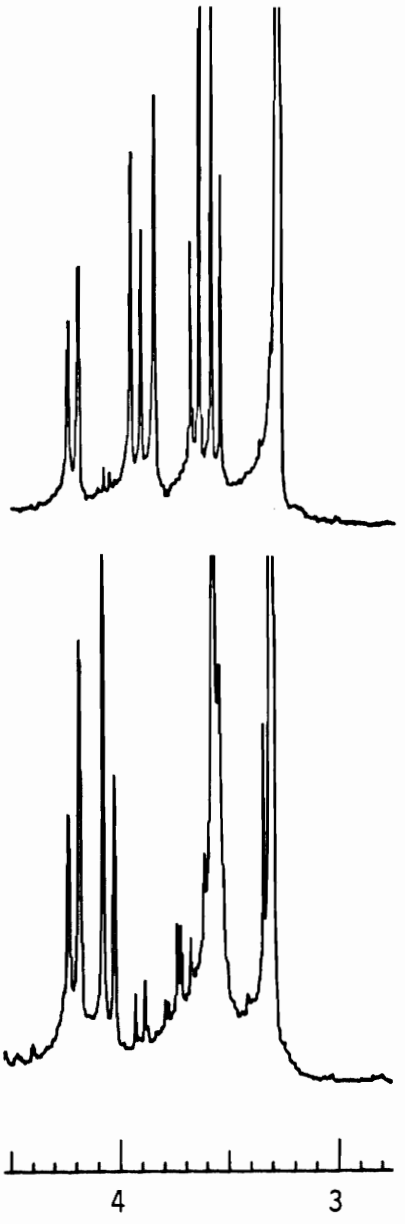

Figure 15. ^{1}H NMR of voeltzkowinol B (top) and voeltzkowinol C (bottom)

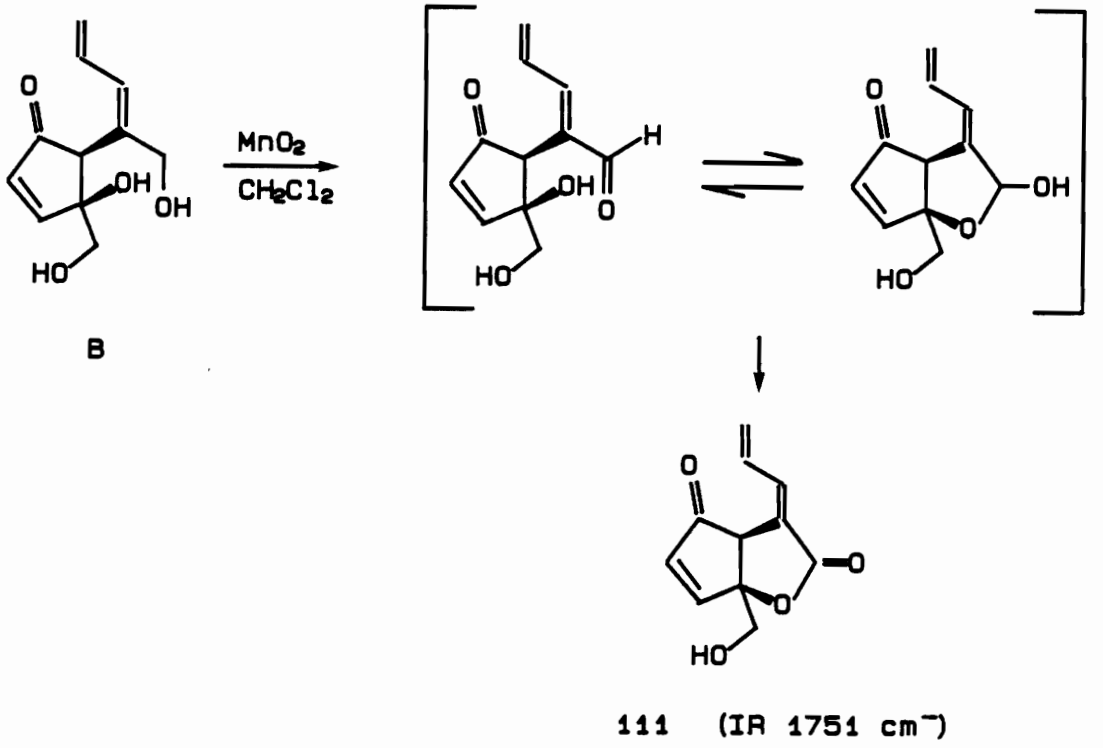

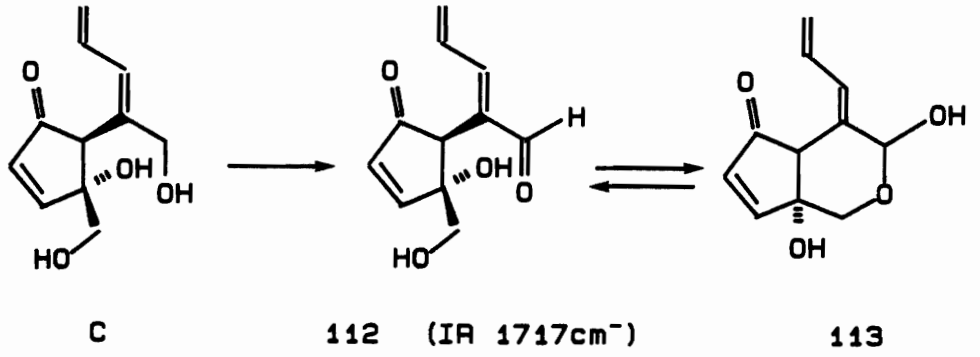

Figure 16. Allylic oxidation of B and C

intermediate formed is the aldehyde which spontaneously cyclizes to form the gamma-lactol. Because of the allylic nature of the lactol it is further oxidized to the lactone [EIMS: m/z = 206; IR: 1750, 1719 cm^{-1}]. This chemistry is consistent only if the 3° alcohol and the diene side chain at C-5 are cis to one another. Conversely, allylic oxidation of voeltzkowinol C, under identical conditions, produced the aldehyde [112, EIMS: m/z = 208, ^{1}H NMR: δ9.46 (s, 1H), IR: 1720, 1680cm^{-1}] indicating that the 3° alcohol and the side chain are now trans to one another. The lack of formation of the δ-lactone can be explained kinetically and thermodynamically. House states that the rates of ring closure follow the order: 3 > 5 > 6 > 7 > 4,8.[86] In the voeltzkowinols the 3° alcohol has fewer degrees of rotation than the 1° alcohol. Therefore, the 3° alcohol spends more time in close proximity to the aldehyde allowing it to react quicker (lower ΔG) and more often. Constructing a model with the 1° alcohol or 3° alcohol cis to the diene side chain is also very informative (Figure 17). When the 3° alcohol is cis to the diene the repulsive forces due to electrostatic interactions between the oxygen atoms of the 3° alcohol and the aldehyde result in an orientation that strongly favors lactonization. The model in which the 1° alcohol and the diene are cis to one another immediately demonstrates the spatial problems arising from the additional degrees of freedom. Furthermore, the

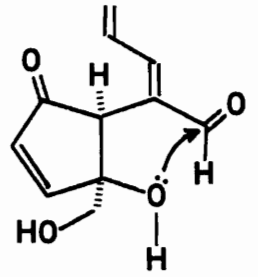

B

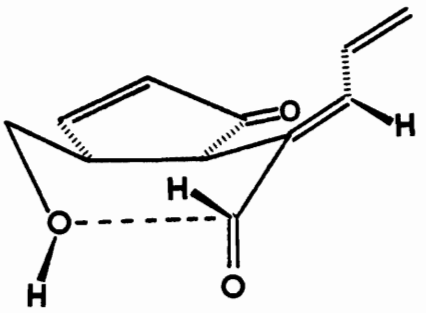

C

Figure 17. Postulated intermediates in the allylic oxidation of voeltzkowinol B and C

intermediate formed by initial attack of the primary hydroxyl on the aldehydic carbon exists in the unfavorable boat conformation. It is important to note that the equilibrium could be shifted from the aldehyde (112) to the δ-lactol [113, EIMS m/z = 208; ^{1}H NMR δ5.41 (s, 1H)] using MeOH. The hydroxyl proton is exchanging at a rate that enhances nucleophilicity of the oxygen. Protonation of the carbonyl causes increased electrophilicity of the carbonyl carbon. The combination of these two factors may influence formation of the δ-lactol.

The diene side chain was drawn as shown based on spectral comparison of a structurally similar compound (100) also isolated from a didemnid tunicate in which the diene was assigned by x-ray analysis.[75] Since the ^{1}H NMR spectrum of compound 100 and voeltzkowinols B and C were very similar it was proposed that the diene systems possessed the same configuration.

To support this argument a 2D nuclear Overhauser effect experiment (NOESY)[87] was performed on voeltzkowinol B. The nOe is a dipole-dipole phenomenon in which magnetization is transferred through space from one proton to another proton. The efficiency of this cross-relaxation falls off to the sixth power of the distance between the protons. In general, the nOe is detectable for protons separated spatially by ∿4 Angstroms. In the 2D NOESY experiment all protons are preirradiated by a 90° ^{1}H pulse. This is

followed by a delay time that allows for the exchange of magnetization between dipole-dipole coupled protons. This delay time is set to the average T_1 value for the protons of interest. A disadvantage of the NOESY experiment is the appearance of crosspeaks in the 2D NOESY map for scalar coupled protons. To circumvent this problem the final delay is randomly varied by 20 msec. This, theoretically, reduces the scalar couplings. Normally, a correlation experiment (COSY) used to assign protons that are scalar coupled is run for comparison. Both experiments (NOESY, COSY) were performed on voeltzkowinol B (Figure 18). Since the interpretation of the results involves a direct comparison of the two experiments, all ^1H pulses in both experiments were set to promote a 90° phase shift. The interpretation of both contour maps is essentially the same. The diagonal represents the 1D ^1H NMR spectrum. Crosspeaks that lie symmetrically above and below the diagonal can be thought of as occupying two corners of a box. Where the remaining two corners fall on the diagonal represents the protons that are scalar coupled (COSY) or dipole-dipole coupled (NOESY). If the assignment of the diene is correct, crosspeaks should appear in the NOESY map correlating the methinyl proton at C-5 (δ3.88 ppm) and the olefinic proton at C-8 (δ6.65 ppm). The arrows in the NOESY map indicate the presence of these two crosspeaks. The protons at C-5 and C-8 are separated by five bonds. Therefore. it is possible that these crosspeaks

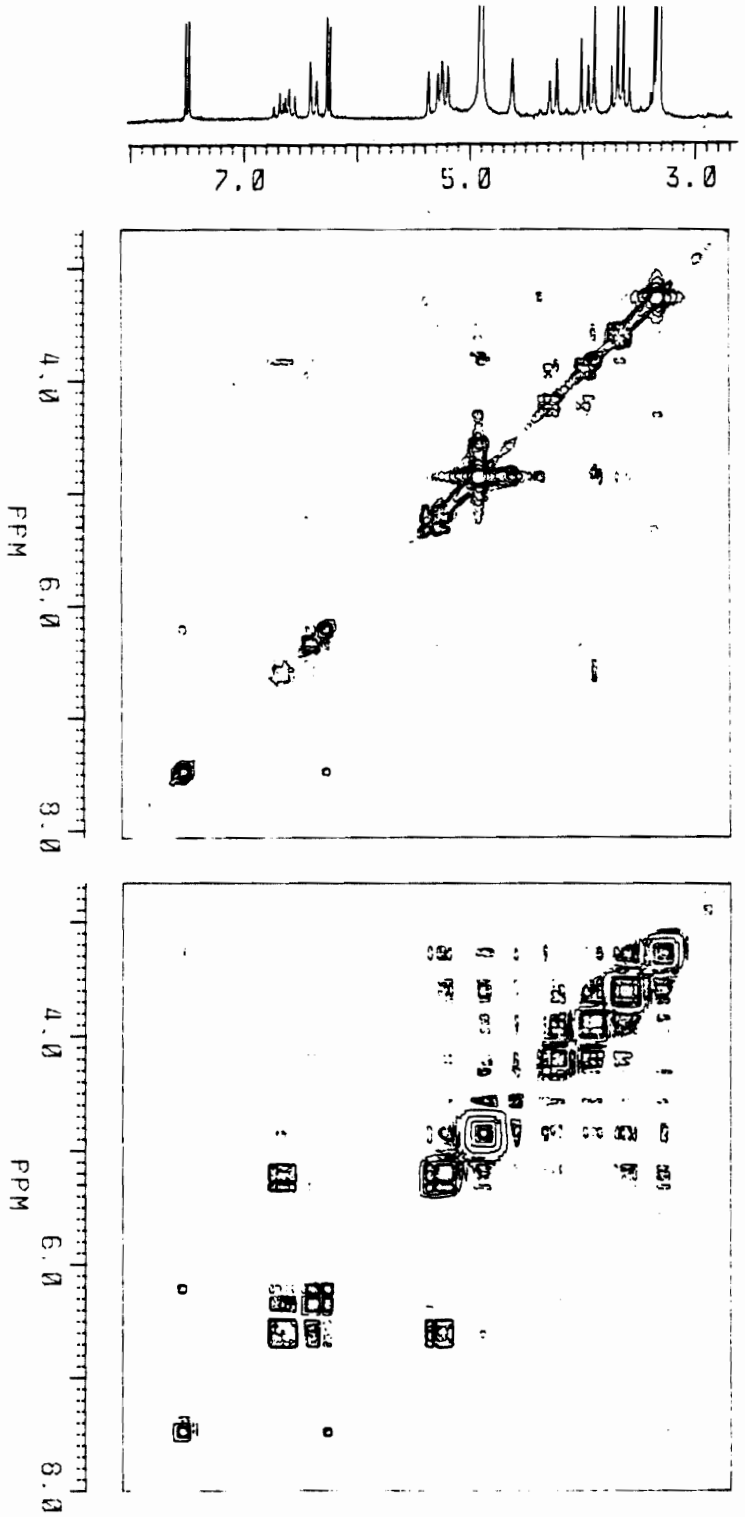

Figure 18. 2D NOESY (top) and COSY (bottom) spectra of voeltzkowinol B

could represent $^{5}J_{H-H}$. However, crosspeaks for this scalar interaction are absent in the COSY map.

Additional evidence supporting the attachment of the diene side chain at C-5 is the detection of W coupling (2.2 Hz) in the γ-lactone between the methinyl proton at C-5 and the olefinic proton at C-7. This coupling was not observed in the natural product.

Voeltzkowinol D (99) was also found to be isomeric with voeltzkowinol B. The UV spectrum showed two absorption maxima at 233 (ε 11,000) and 307 (ε 10,000) nm. The UV absorption at 233 nm along with the ^{1}H and ^{13}C NMR data [^{1}H: δ6.29 (d, 1H, J = 6 Hz), 7.40 (d, 1H, J = 6 Hz); ^{13}C: δ 199.1 (s), 161.5 (d), 128.4 (d)] established the presence of the cyclopentenone ring. The UV absorption at 307 nm and an IR stretch at 1680 cm^{-1} indicated that the diene had moved into conjugation with the cyclopentenone. The ^{1}H NMR spectrum is shown in Figure 19. Absent is the sharp singlet at 3.88 ppm that was previously assigned to the methinyl proton at C-5. Also missing are the two terminal methylene protons at 5.1 and 5.2 ppm. Replacing them are signals defining a trans disubstituted double bond [δ7.83 (dd, 1H, J = 16, 1.3 Hz), 6.52 (dq, 1H, J = 16, 7 Hz), 1.90 (dd, 3H, J = 7, 1.3 Hz)]. The ^{13}C NMR spectrum shows signals for a new tetra substituted double bond conjugated to a carbonyl. The α- and β-carbons appear at 134.2 and 146.8 ppm respectively. Of equal importance is the absence of a methinyl carbon

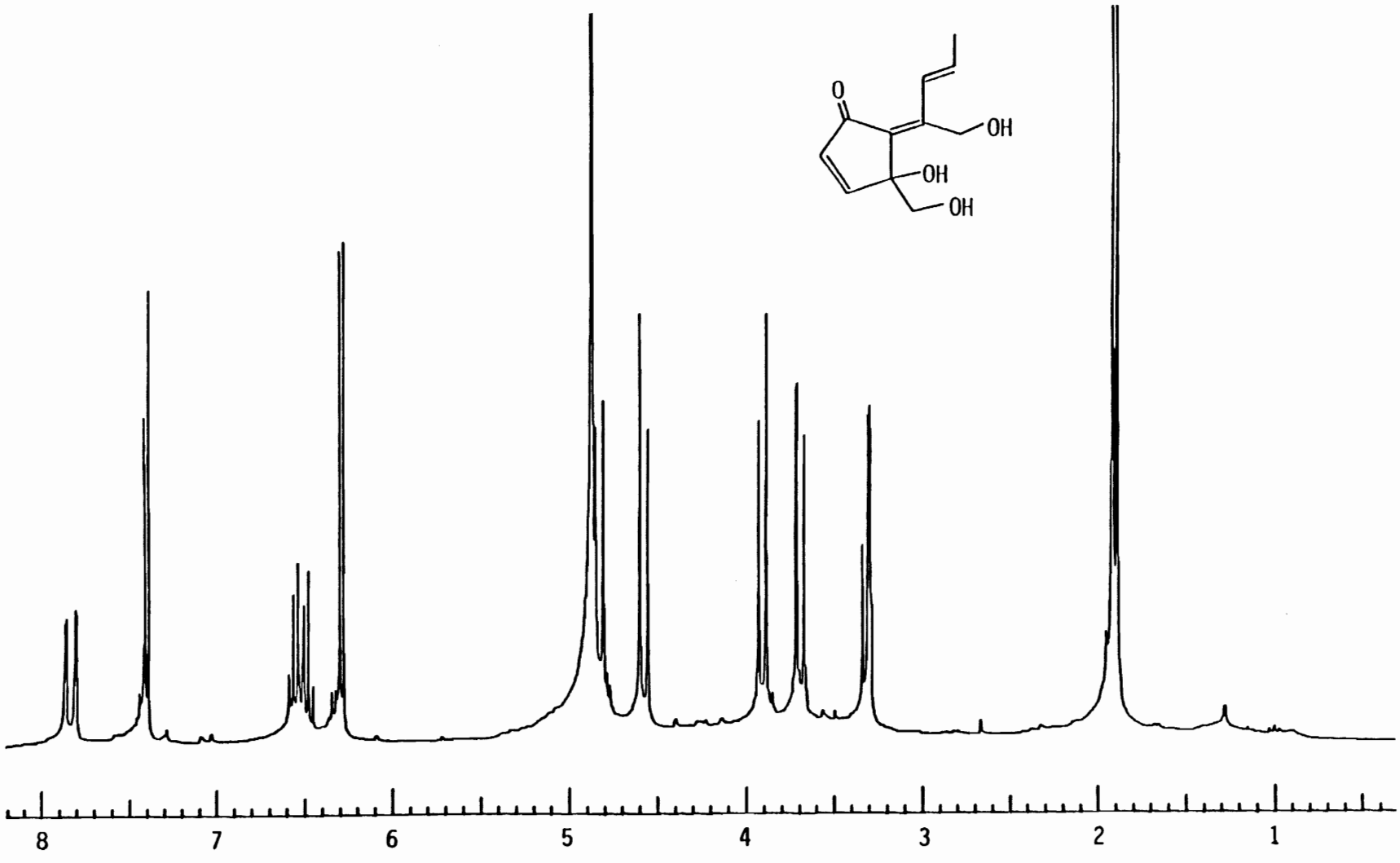

Figure 19. ^{1}H NMR of voeltzkowinol D

between 50-55 ppm and an upfield shift of the pentenone carbonyl (δ199 ppm) supporting conjugation of the diene to the carbonyl.

The presence of two primary alcohols and one tertiary alcohol was confirmed by interpretation of the spectral data [IR: 3600cm^{-1}; ^{13}C NMR: δ 82.0 (s), 68.2 (t), 58.3 (t); ^{1}H NMR: δ 4.83 (d, 1H, J = 11.8 Hz), 4.57 (d, 1H, J = 11.8 Hz), 3.90 (d, 1H, J = 12 Hz), 3.69 (d, 1H, J = 12 Hz)] and by acetylation of voeltzkowinol D (AC_2O, pyridine) to a diacetate [114, EIMS: m/z = 294; ^{1}H NMR: δ 2.03, (s, 6H)] and a small amount of a triacetate [115, EIMS: m/z = 336; ^{1}H NMR: δ2.06 (s, 3H), 2.04 (s, 3H), 2.02 (s, 3H)].

The tetra substituted double bond was assigned the E geometry based on the following argument. The gamma position of a dienone is normally a shielded position. The unusual downfield shift of the gamma proton at 7.83 ppm implies that it lies in the deshielding cone of the carbonyl; a situation that could exist only if the tetrasubstituted double bond adopts the E geometry. This assignment is in complete agreement with Kitagawa's assignment of the diene geometry in claviridenone 1 (116) and 3 (117).[88] In claviridenone 1, the gamma proton appears at 7.62 ppm whereas in claviridenone 3 the same proton appears at 6.74 ppm. Kitagawa also attributed this anomaly to the anisotropy effect from the carbonyl. The 7-ene moiety of voeltzkowinol D was assigned the E geometry based

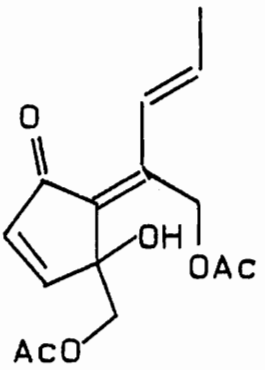

114

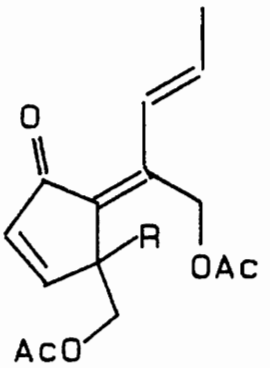

115 R = OAc

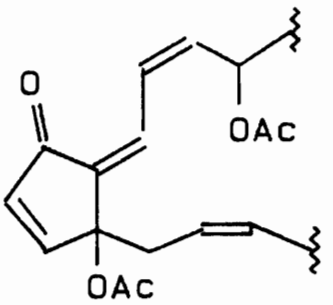

116

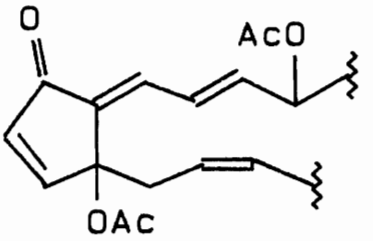

117

on the 16 Hz coupling constant between H-7 and H-8. This was also in complete agreement with the analogous coupling constants in claviridenone 1 and 3.[88]

With the gross structures of voeltzkowinol B, C and D secured, all that remains is the determination of their relative and absolute stereochemistry. The allylic oxidation of B and C only established that the 3° alcohol is cis to the diene side chain in B and trans to the diene side chain in C. The stereochemistry as illustrated in the structures for B (97) and C (98) is purely arbitrary. The enantiomers of B (118) and C (119) could also be drawn.

The proton at C-5 (B and C) should be very labile making C-5 the more reactive center. Removal of the proton at C-5 would result in the formation of a carbanion stabilized by the neighboring diene system and carbonyl. Reprotonation could then occur from either face yielding B and/or C. Therefore, it is theorized that the epimeric center is C-5 and not C-4. The lability of the proton at C-5 provides a handle for proving this theory. Epimerization of this center should be effected under acidic (0.1M HCOOH) or basic (1% Na_2CO_3, MeOH) conditions. Assuming that voeltzkowinol B (97) is the starting material, the reaction mixture should contain B (97) and C (98) or the enantiomer of C (119). A comparison of the optical rotation of the reaction product with that of the natural product should establish the relative stereochemistry of B and C. Under

the reaction conditions only C-5 should epimerize. Therefore, if the optical rotation of voeltzkowinol C (obtained from the reaction mixture) is identical to that of the natural product then C is structure 98 and B and C are epimeric at C-5. If the optical rotations are different then B and C are epimeric at C-4.

To determine absolute stereochemistry requires that the absolute configuration of one of the chiral centers be known. It should be possible (under stronger conditions) to cross-conjugate the diene and the carbonyl of B (or C) and form D (99) or its enantiomer (120). If the absolute stereochemistry of D and the relationship of B (or C) and D at C-4 can be established then voeltzkowinols B, C and D can be drawn with absolute stereochemistry.

Claviridenone 4 (121) is a structurally similar compound to voeltzkowinol D. A Japanese group established the absolute stereochemistry of (121) by the following procedure (Figure 20).[89] Reduction of 121 with $NaBH_4$ in MeOH at room temperature yielded two epimeric alcohols (122) and (123). The relative stereochemistry at C-9 and C-12 was determined by evaluation of their ^1H NMR spectra and also by the observation of intramolecular H-bonding between the hydroxyl proton at C-9 and the carbonyl oxygen at C-12. Compounds 122 and 123 were treated with p-bromobenzoylchloride in CCl_4 in the presence of triethylamine and N,N-dimethylaminopyridine. Analysis of

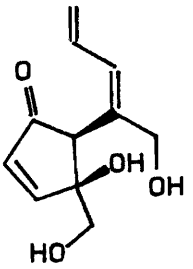

97

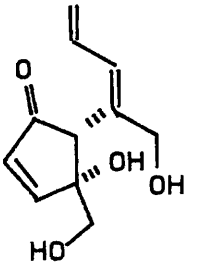

118

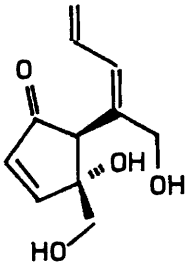

98

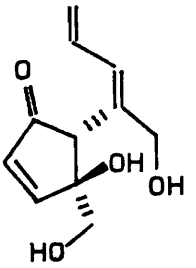

119

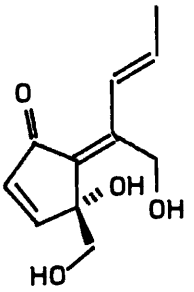

99

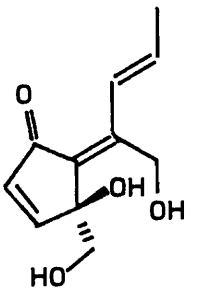

120

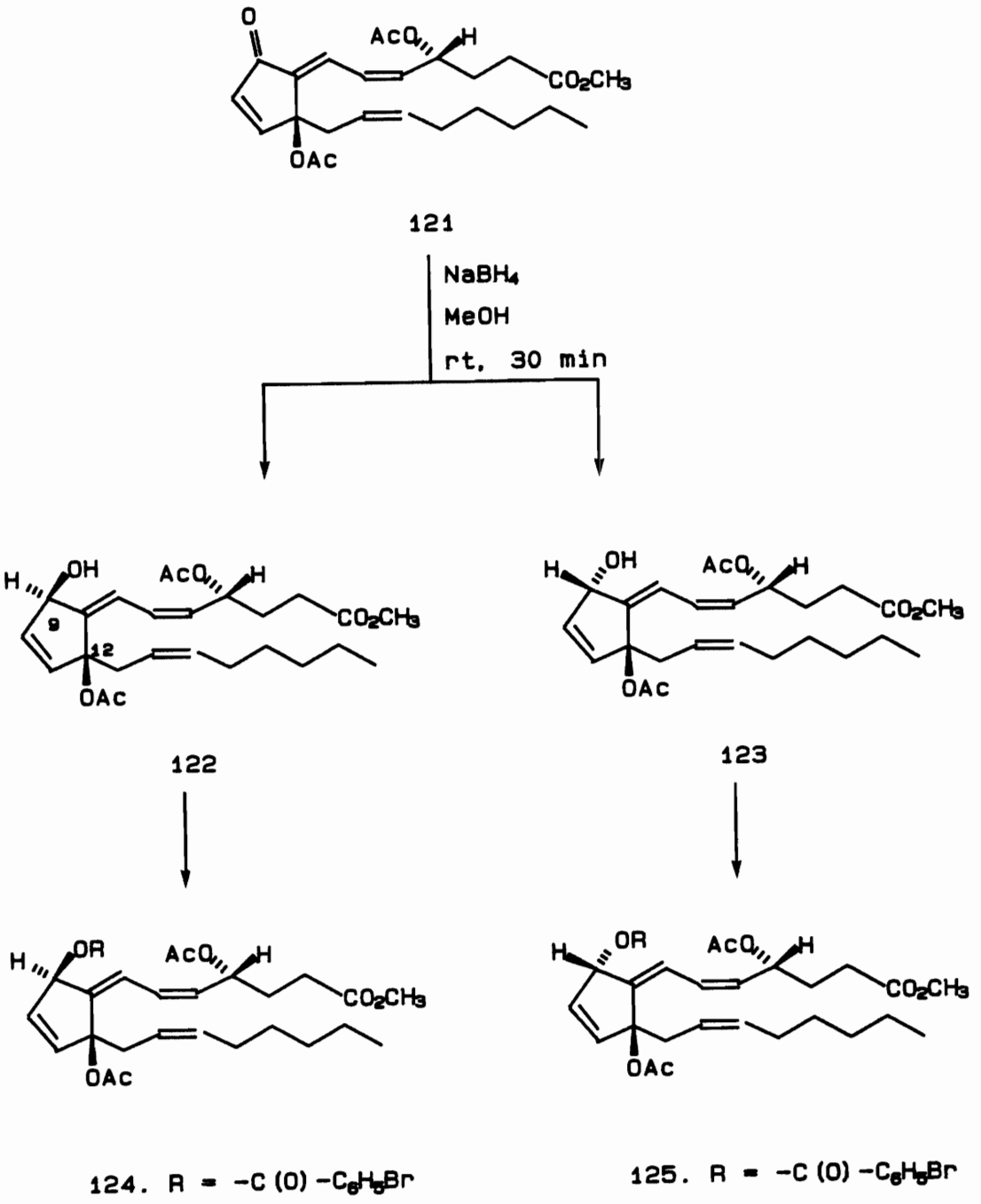

Figure 20. Determining absolute stereochemistry of claviridenone 4

the CD spectra of the resulting p-bromobenzoates (124) and (125) established the absolute stereochemistry at C-9 and C-12. This methodology should be applicable to voeltzkowinol D.

Voeltzkowinol A (96) represented the least polar metabolite in the family. It was assigned a molecular formula $C_{11}H_{12}O_3$ (HREIMS: obs. 192.0786, calc. 192.0783) indicating six degrees of unsaturation. Acetylation of 96 yielded a monoacetate [126, ^{1}H nmr: δ2.10 (s, 3H)] indicating the presence of one primary alcohol. A UV λmax of 270 nm and 6 olefinic signals in the carbon spectrum [δ155.9 (d), 152.1 (s), 147.9 (d), 128.8 (s),127.3 (d), 117.9 (s)] indicated the presence of a conjugated triene. The absence of a carbonyl stretch in the IR spectrum established that voeltzkowinol A was tricyclic. Present in the ^{1}H NMR spectrum is an isolated AB spin system [δ5.89 (d, 1H, J = 6 Hz), 7.71 (d, 1H, J = 6 Hz)] reminiscent of the cyclopentenone, an AB spin system [δ4.67 (d, 1H, J = 15 Hz), 4.92 (d, 1H, J = 15 Hz)] for one primary alcohol, and a sharp singlet at 6.93 ppm assignable to an enolic olefinic proton. Also present is a new spin system comprised of a methine bearing oxygen at 4.3 ppm (dd, 1H, J = 9.9, 5.7 Hz), two allylic methylene protons at 2.7 (dd, 1H, J = 18.5, 7.9 Hz) and 3.1 ppm (d, 1H, J = 18.5 Hz) and a doublet methyl at 1.42 ppm (d, 3H, J = 5.9 Hz) which defines partial structure 126.

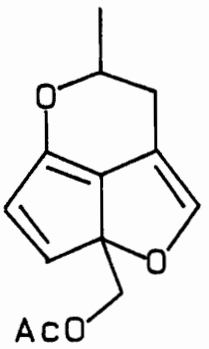

126

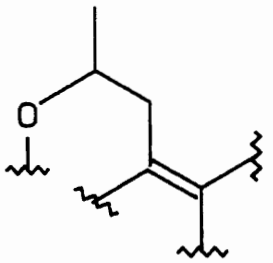

127

The skeletal structure of voeltzkowinols B, C and D served as a template for constructing voeltzkowinol A. The diene system was replaced with partial structure 127. Since only one of the allylic methylene protons (δ2.7 ppm) showed coupling to the adjacent methine protons, 127 must exist in a very rigid ring. The absence of a carbonyl supported the formation of a 6-membered cyclic ether. The appearance of a carbon doublet at 156 ppm and the disappearance of one of the primary alcohol carbon signals ($\sim$60 ppm) defined the location of the third ring. A strong fragment ion at m/z 163 (M^+ - CH_2-OH) secured the presence of the furan ring and negated the possibility of a pyran ring present in voeltzkowinol A.

A chemically plausible biogenesis of voeltzkowinol A from voeltzkowinol D was proposed (Figure 21). Compound 128 represents the hemi-acetal form of voeltzkowinol D. A 4 + 2 intramolecular cyclization results in the formation of intermediate 129. Hydride attack at the olefinic carbon followed by the ensuing flow of electrons and the expulsion of a hydroxyl group would produce voeltzkowinol A.

The voeltzkowinols exhibited varying degrees of cytotoxicity when tested *in vitro* against the L1210 murine leukemia cell line (A, 3.4 µg/ml; B, 5.6 µg/ml; C, 5.6 µg/ml; D, 0.56 µg/ml). This activity may be attributed to their ability to serve as Michael acceptors.

Voeltzkowinols B-D structurally resemble the

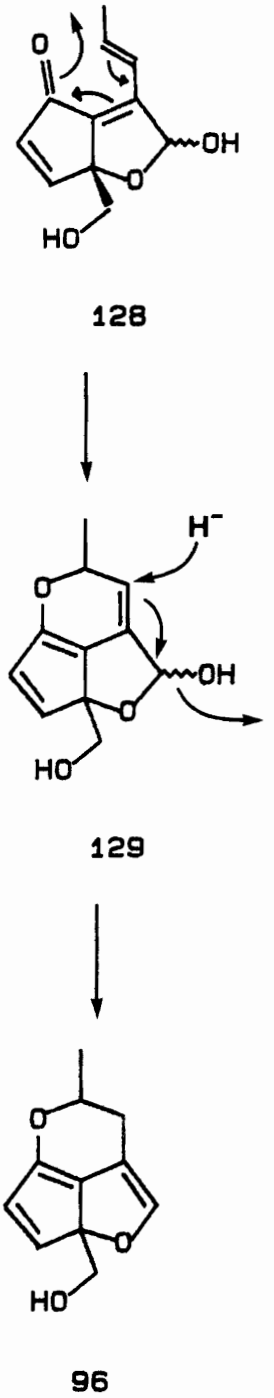

Figure 21. Proposed biogenesis of voeltzkowinol A

prostaglandins, a family of organic acids containing a five membered ring and derived from essential fatty acids via arachidonic acid. Prostaglandins exhibit different effects on several major bodily functions (i.e., nervous system, reproductive system, inflammation-gastrointestinal tract).[90] There have been several reports of eicosanoids isolated from marine sources[88,91-94] many of which possess significant biological activity. One of the punaglandins (130)[91] exhibited an IC_{50} value of 0.02 µg/ml (L1210 assay). The clavulones showed antiinflammatory effects at 30 µg/ml in the fertile egg test and were reported to possess remarkable anticancer activity.[95] The clavulones and the punaglandins all contain extended conjugated systems. This structural feature is present only in voeltzkowinol D and may explain the enhanced cytotoxicity of voeltzkowinol D over B and C.

The major metabolite isolated from Didemnum voeltzkowi was tributyl tin chloride (131). It was isolated as a pure compound or complexed in differing percentages with each of the four voeltzkowinols. Signals in the ^1H [δ1.66 (m, 1H), 1.35 (m, 2H), 1.20 (t, 2H, J = 8.6 Hz) , 0.93 (t, 3H, J = 7.5 Hz)] and ^{13}C NMR spectrum [27.8 (t), 26.8 (t), 17.5 (t), 13.6(q)] indicated the presence of a butyl group. The major peaks in the EI mass spectrum were m/z 326(M^+), 291, 269(B), 234, 213, 177, 155, 121, 57. A daughter plot established that all these peaks were derived from the same molecule. The difference between the molecular ion (326) and the base

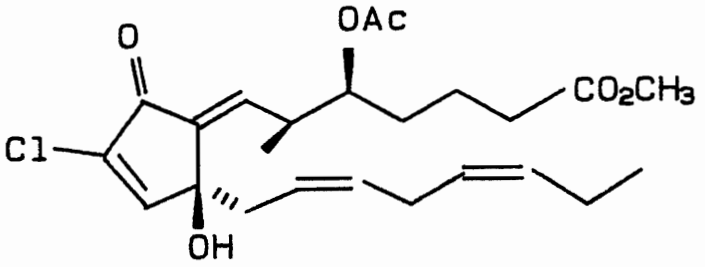

130

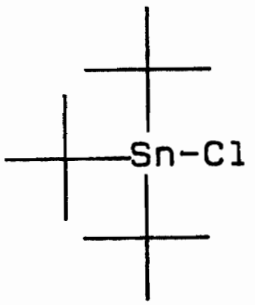

131

peak (269) is 57 amu's confirming that the structure was a butyl derivative. Another frequent loss was 35 amu's indicating the presence of chlorine. The molecular ion appeared as an intricate isotope pattern that was unlike any of the common chlorine clusters that one normally encounters. Based on the ability of tunicates to sequester transition metals from sea water, metal ions with isotope ratios that could produce the observed isotope pattern were sought. Tin was a logical candidate because of its many isotopes (^{116}Sn-^{124}Sn). Computer-derived isotope distribution ratios for m/z 326 ($C_{12}H_{27}SnCl$) and m/z 269 ($C_8H_{18}SnCl$) matched perfectly with the observed isotope distribution in the real spectrum supporting our assignment. The structure of tributyl tin chloride was subsequently confirmed by comparison with an authentic sample.

The source of tributyl tin chloride in the extract is unknown. It is unlikely that tributyl tin chloride is a natural product. Contamination of the sample during the isolation procedure is also unlikely because the tunicate was frozen immediately at the collection site in Fiji and no bottles of tributyl tin chloride were found in Dr. Ireland's lab. Interestingly, tributyl tin chloride is an additive in marine paints and also in the coatings on underwater cables. Tunicates have the ability to sequester metals from sea water and Didemnum voeltzkowi was collected on a coral reef approximately 50 yards from a drilling site.

The Chemistry of Lissoclinum patella*

Lissoclinum patella is a compound tunicate with an easily recognizable body. Colonies of L. patella have been collected in the Western Caroline Islands by snorkeling (-2m) and during a recent expedition off the coast of Suva, Fiji by SCUBA (-3m). Like many didemnid tunicates, L. patella harbors symbiotic algae as evidenced by the green hue showing through the translucent mantle.

The initial investigation of Lissoclinum patella yielded eight cyclic peptides characterized by the presence of oxazoline and thiazole amino acids.[54-56] My contribution to the investigation of Lissoclinum patella has focused on the structure revision of the patellamides using the COSY 45 technique. In addition to evaluating the patellamide structures, three new cyclic peptides were isolated from L. patella.[59] Interestingly, their structures were remarkably similar to three known lissoclinum peptides. The new metabolites all contain a thiazole amino acid. In place of the oxazoline ring, however, is its threonine precursor.

Germane to this discussion is a brief overview of the events leading to the structure revision of the patellamides. Ulicyclamide 132 and ulithiacyclamide 55 were the first two cyclic peptides isolated from L. patella.[54] Their amino acid composition was determined based on

---

*Tables of ^{1}H and ^{13}C NMR data for the lissoclinum peptides can be found in the appendix.

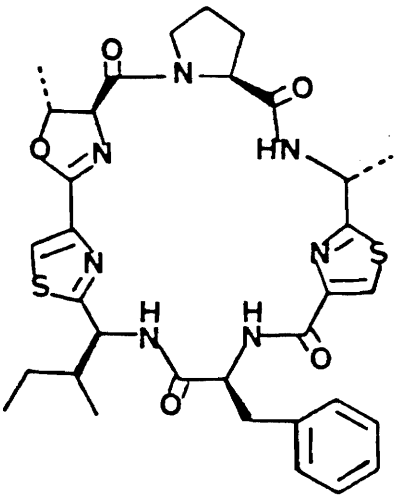

132

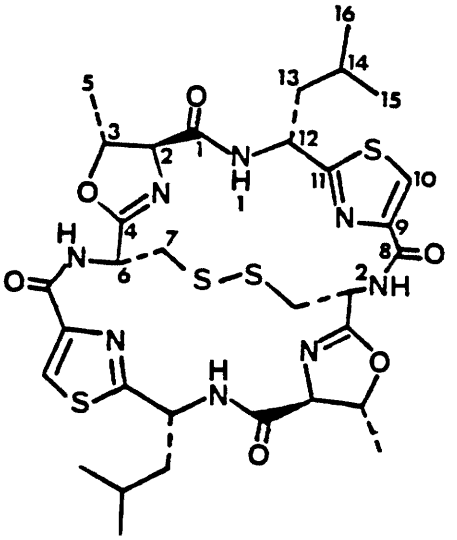

55

spectral analysis of the intact peptide and comparison of the acid hydrolysis products with authentic material. Their amino acid sequence was established from EIMS fragmentation patterns. Of equal importance was the multiplicity of the alpha amino proton (H-2) of the $\Delta^{2,3}$ oxazoline ring which served as an indicator for the type of substituent at C-4. Weinberger reported homoallylic (five bond) coupling (1.5 Hz) in 2-methyl-Δ^2-oxazoline between the proton at C-4 and the methyl protons.[96] The alpha amino proton (H-2) of ulicyclamide (132) appeared as a simple doublet (J = 4 Hz) suggesting that there were no protons on the carbon attached to C-4 and confirming placement of the thiazole at that position. In ulithiacyclamide (55) the alpha amino proton of the oxazoline ring appeared as a doublet of doublets with coupling constants of 8 and 2 Hz. The 2 Hz coupling constant represented homoallylic coupling through the oxazoline ring between H-2 and the proton on the carbon attached at C-6. Subsequent decoupling studies revealed that irradiation of the α-cysteinyl proton at 5.3 ppm resulted in a sharpening of the α-oxazoline proton (4.25 ppm) indicating that the substituent at C-6 was cysteine.

In 1982 Ireland and co-workers reported the structures of patellamides A, B and C (56-58), all of which contained fused oxazoline-thiazole ring systems.[55] EI mass spectral analysis of the tripeptide obtained by selective hydrolysis of the cyclic peptide was consistent for two sets of

structures 56-58 and 65-67. The alpha amino protons of the oxazoline rings appeared as sharp doublets (^{1}H: 4.30, d, J = 4 Hz) reminiscent of the oxazoline proton in ulicyclamide (^{1}H: 4.26, d, J = 4 Hz). Irradiation studies failed to show homoallylic coupling to the oxazoline protons via a sharpening of their signals. Therefore structures (56-58) containing fused oxazoline-thiazole ring systems were chosen based on the absence of homoallylic coupling.

In 1983 Ireland reported the structures of Lissoclinamide 1,2 and 3 (59-61).[56] Note that the structures contain no fused oxazoline-thiazoles even though, in the ^{1}H NMR spectrum, the alpha amino protons of the oxazoline ring appear as doublets (^{1}H: 4.30, d, J = 4 Hz). The amino acid sequences were secured by interpretation of FAB mass spectral data of a selective hydrolysis product. Interestingly, the amino acid composition of lissoclinamide 2 (60) and 3 (61) was identical to ulicyclamide (132). The lack of homoallylic coupling in the lissoclinamides and the availability of FABMS (which is a softer and oftentimes more informative mode of ionization) prompted a reevaluation of the structural assignment of ulicyclamide. After examination of the selective hydrolysis product from ulicyclamide by HRFABMS, ulicyclamide was reassigned structure 54.[56] The new structure did not contain a fused oxazoline-thiazole ring system. Conventional decoupling studies had failed to detect homoallylic coupling because

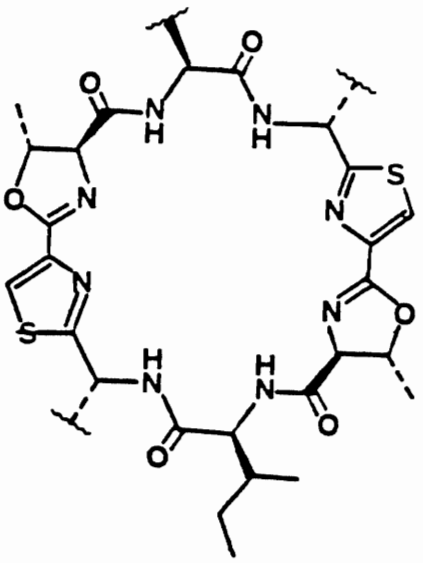

56-58

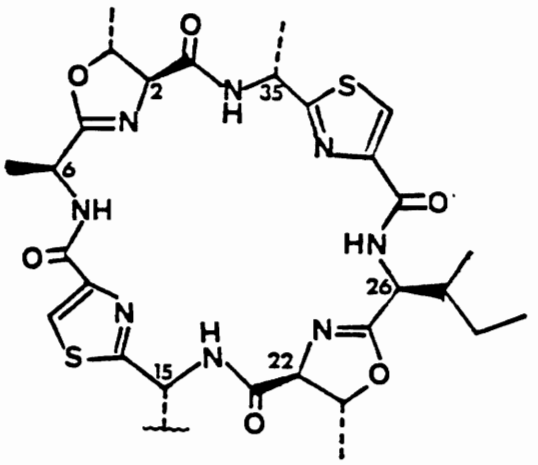

65-67

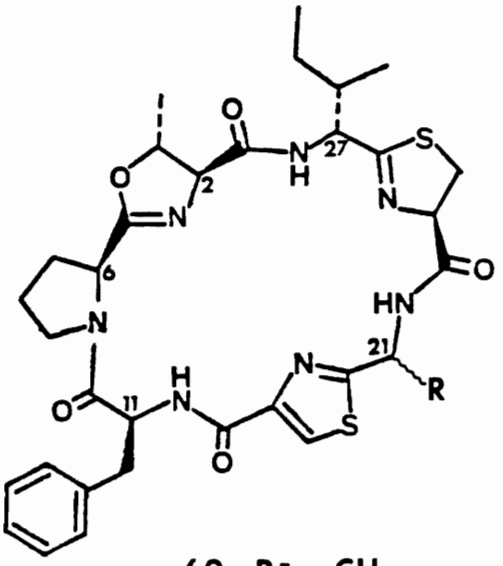

60 R = ⋯ CH_3

61 R = — CH_3

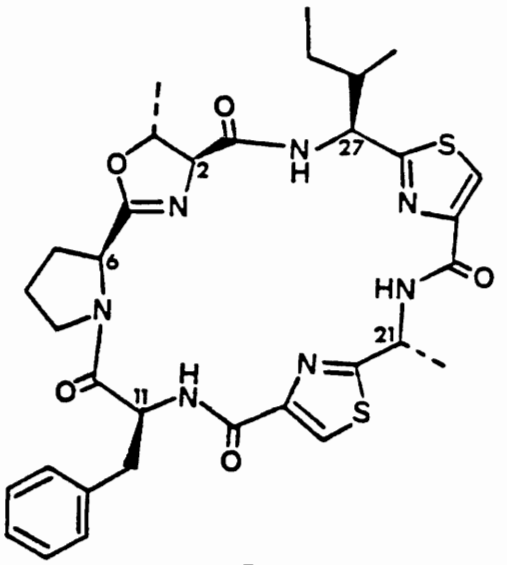

54

the coupling was too small (J < 0.5Hz). Since the same criterion was used to assign the structures of patellamides A, B and C (in particular the fused oxazoline-thiazole sub-structure), it was decided that a reinvestigation of the patellamides was necessary. In the case of the patellamides FABMS data did not distinguish between the two sets of possible structures. Therefore, a method was needed that could detect small couplings (J < 0.5 Hz) between alpha amino protons. Two dimensional homonuclear correlation experiments held the distinction of detecting long range couplings that were difficult or impossible to detect by conventional 1D methods.[97,98] Coincidental with the renewed interest in the patellamides was the arrival of the IBM 200 MHz NMR equipped with 2D software. Several different homonuclear correlation experiments were tried using ulicyclamide as a model compound: COSY 90, COSY 45, long range COSY and phase sensitive COSY. After comparative analysis of the contour maps obtained from each experiment the COSY 45 pulse sequence was chosen. It provided more long range coupling information in addition to suppressing diagonal distortions. A SECSY experiment was also run on ulicyclamide. Although comparable to the COSY 45 experiment in detecting homoallylic coupling, the data as presented led to ambiguous assignments.

Before revealing the results of the NMR study a brief discussion of the basic theory behind a 2D NMR experiment

will be presented.[99] The combination of fourier transformation and programmable pulse transmitters was directly responsible for the development of the 2D NMR experiment. The breakdown of a typical NMR experiment into its three time periods is shown in Figure 22 (top). The preparation time simply prepares the spins for evolution. During the evolution period the spins are allowed to evolve or dephase with their coupling constants, chemical shift or both. At the end of the evolution period, the signal is detected and an FID recorded. In a 1D NMR experiment t_1 is fixed. In a 2D NMR experiment t_1 varies.

A simplified representation of 2D NMR spectroscopy is shown in Figure 22 (bottom). The left diagram represents amplitude modulation, the right diagram represents phase modulation. However, the explanation is the same in both cases. Each row represents a 1D NMR spectrum. The signal intensity is different in each spectrum because it depends on how long the spin systems have been allowed to evolve. Since t_1, the evolution time, varies so does the signal intensity. A sine wave is formed by connecting the apex of each peak. A fourier transformation of this new sine wave results in the formation of an NMR spectrum in the 2^{nd} dimension. Simply put, 2D NMR is a fourier transformation of a series of fourier transformations.

The pulse train for a COSY 45 experiment along with its vector diagram analysis is shown in Figure 23. At point A

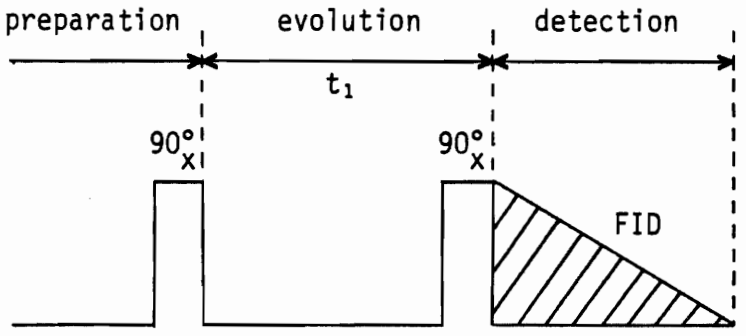

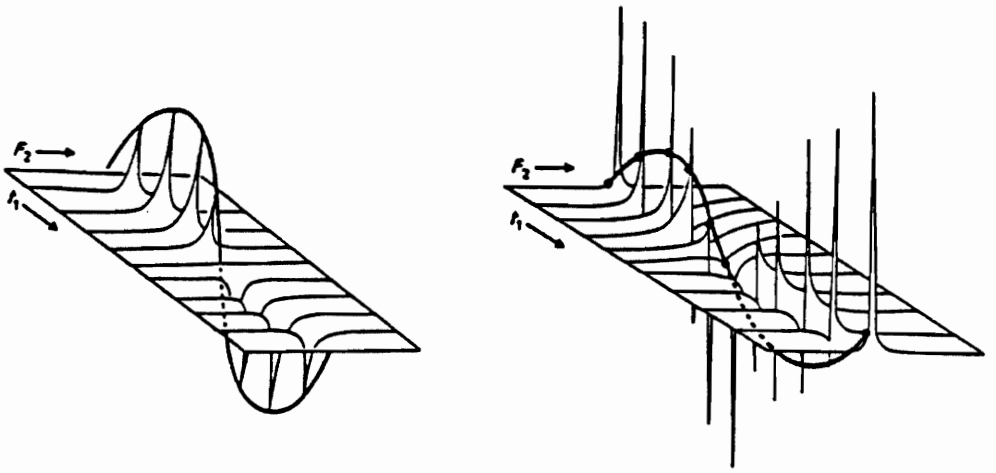

Figure 22. 2D NMR spectroscopy

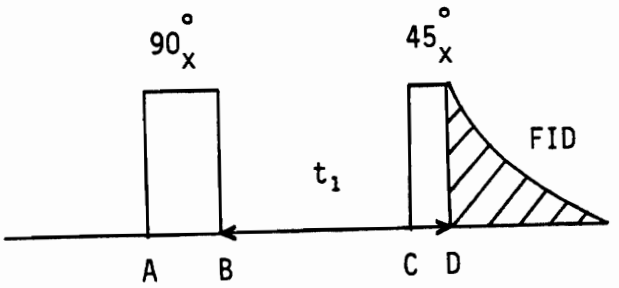

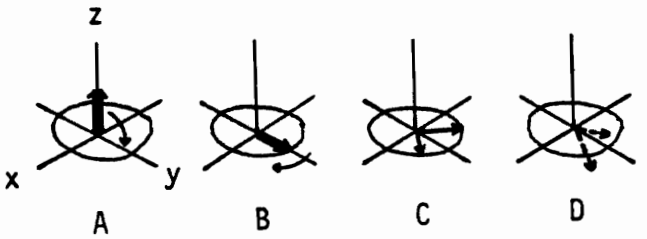

Figure 23. Pulse train and vector analysis for the COSY 45 experiment

all the spins are aligned with the field along the Z-axis. The first 90° pulse flips all the spins along the x-y plane thereby creating transverse magnetization. The spins are allowed to evolve for a time t_1 before the second 45° pulse is applied. This pulse serves as a mixing pulse and results in the exchange of magnetization between coupled nuclei. An FID is collected, t_1 is incremented a predetermined amount and the entire pulse sequence is repeated. At the end of the experiment a computer performs the necessary FT calculations and the data are presented as a contour map.

The first compound to be tested was ulicyclamide. A 32W by 1K data matrix was generated in thirty minutes. A portion of the COSY 45 spectrum is shown in Figure 24. As mentioned earlier, the diagonal represents the 1D spectrum. Symmetrical crosspeaks above and below the diagonal connect protons that are coupled.* Present in the COSY 45 spectrum of ulicyclamide are crosspeaks connecting the α-oxazoline proton (H-2) and the α-Ile proton (H-27). Interestingly, this connection represents homoallylic coupling through the amide linkage rather than through the oxazoline ring. This proved to be a very informative observation because it provided an additional handle for establishing the correct amino acid sequence of the cyclic peptides. There is precedence in the literature for the observation of

---

*A table of $^5J_{H-H}$ connectivities for the lissoclinum peptides can be found in the appendix.

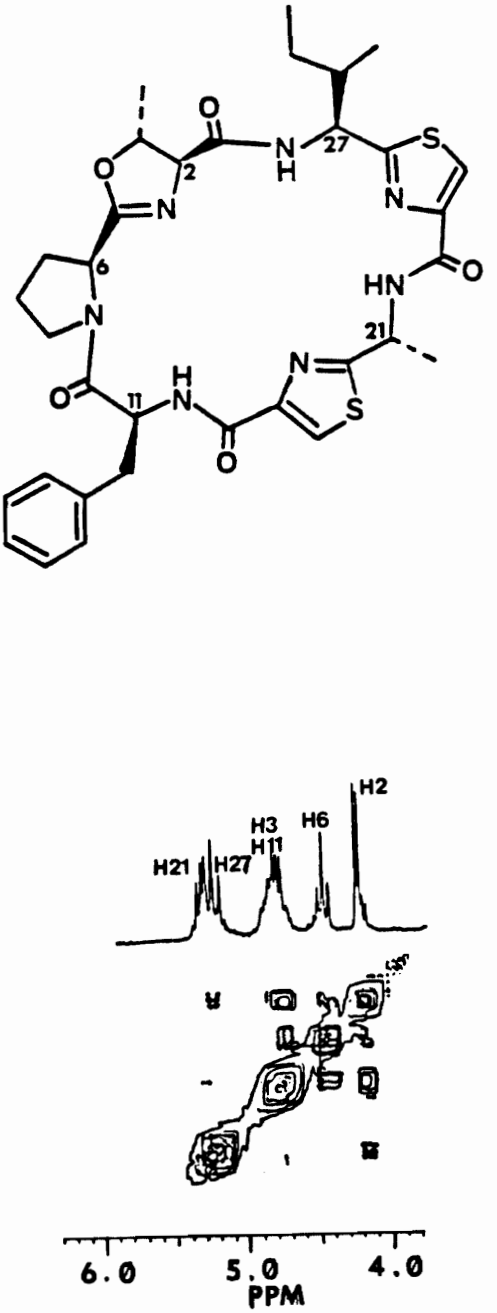

Figure 24. COSY 45 spectrum of ulicyclamide

homoallylic coupling through an amide bond. Barfield reported the presence of $^{5}J_{H-H}$ using spin tickling on model compounds 133-135[100] and Kessler detected similar couplings in cyclo-(L-Pro-L-Pro-D-Pro) (136) using the sophisticated 2D spin-echo homonuclear correlated (SECSY) experiment.[101] A logical explanation for the detection of homoallylic coupling through the amide linkage could be the imino character associated with the amide bond. Unfortunately, crosspeaks connecting H-2 and the α-Pro proton (H-27) through the oxazoline ring were missing. The absence of coupling in this case probably reflects a 90° orientation between H-2 and H-27.

The next compound to be tested was patellamide B. The COSY 45 spectrum is shown in Figure 25 along with its 1D ^{1}H NMR spectrum. The key features in the 1D NMR spectrum are the two sharp doublets for the two α-oxazoline protons [(H-2, 4.38, d, J = 4 Hz), (H-22, 4.29, d, J = 4 Hz)] the signals for the α-Ile (H-26, 4.77 dd, J = 11, 7 Hz), α-Leu (H-6, 5.01, m), and the α-Ala and α-Phe thiazole protons [(H-35, 5.39, dq, J = 9, 7 Hz), (H-15, 5.50, ddd, J = 10, 10, 7 Hz)] respectively. Present are four crosspeaks of varying intensity between 4.7 and 5.7 ppm. These crosspeaks represent connectivities via homoallylic coupling between H-2 <--> H-6 and H-22 <--> H-26 through the oxazoline ring and H-2 <--> H-35 and H-22 <--> H-15 through the amide linkage. These new pieces of data supported revised structure 66 for

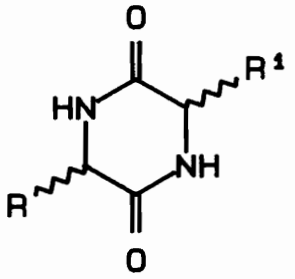

133. R = R¹ = H

134. R = H; R¹ = $CH_2C_6H_4OH$

135. R = H; R¹ = C_6H_5

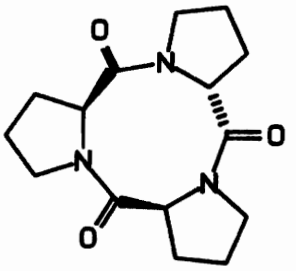

136

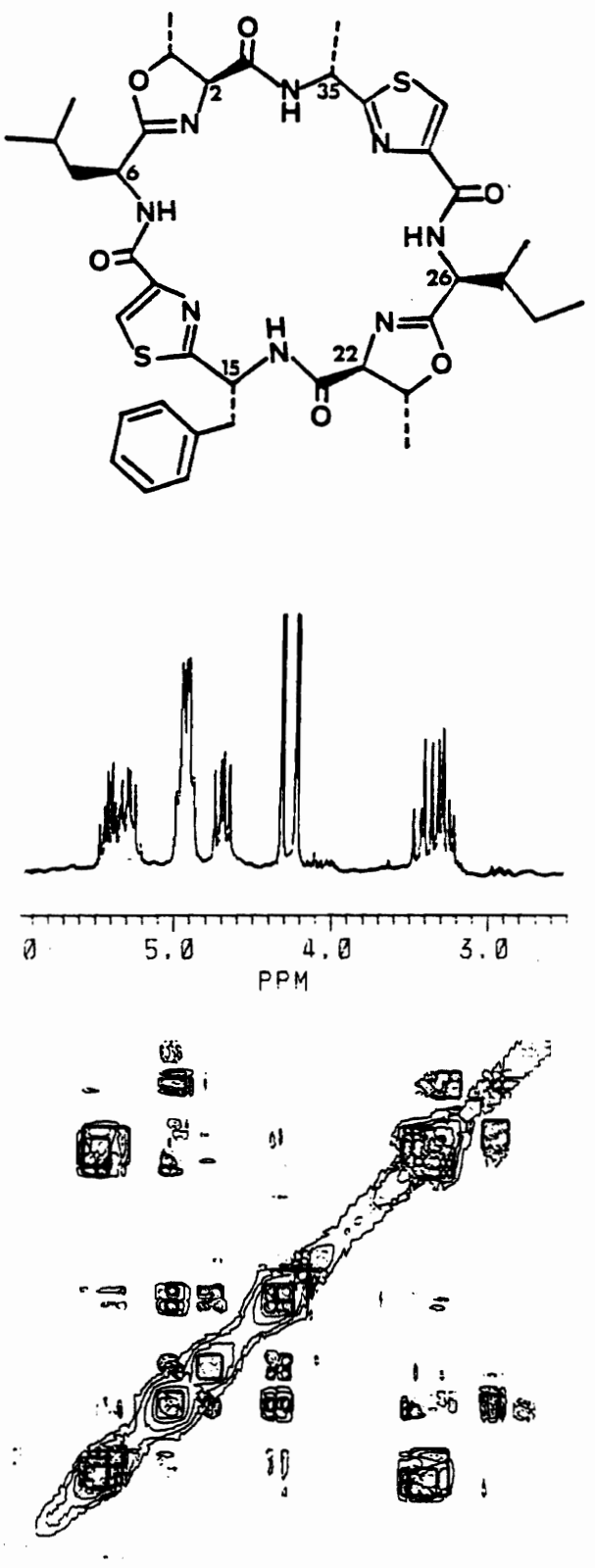

Figure 25. COSY 45 spectum of patellamide B

patellamide B. The revised structure was also supported by FAB MS/MS daughter ion analysis of a tripeptide obtained by selective hydrolysis of patellamide B (Figure 26). The tandem MS measurements were recorded on a VG ZAB 4F instrument. An in-depth analysis of the resulting mass spectrum was provided by Dr. Simon Gaskell. The sequence on the left is the interpretation based on the tripeptide derived from the revised structure. The sequence on the right is the interpretation based on the tripeptide derived from the original structure. The analysis is the same until assignments are made for the ions at m/z 138 and 155. The generation of these ions from the 223 ion is plausible only in sequence A and the revised structure vida infra. It should be noted that it is possible to generate ions with m/z 138 and 155 from fragment structures in column B. However, it is not possible to generate these ions (m/z 138, 155) from the 223 ion. Therefore, conventional FAB MS data does not distinguish between the two possible structures for the patellamides.

The COSY 45 spectrum of patellamide A was supportive of revised structure 65. A sample of patellamide C was not available. However, due to its spectral similarities with patellamide B it was reassigned structure 66. Concurrent with this work, Professor Shioiri confirmed the revised structures of the patellamides by an elegant synthetic approach.[60]

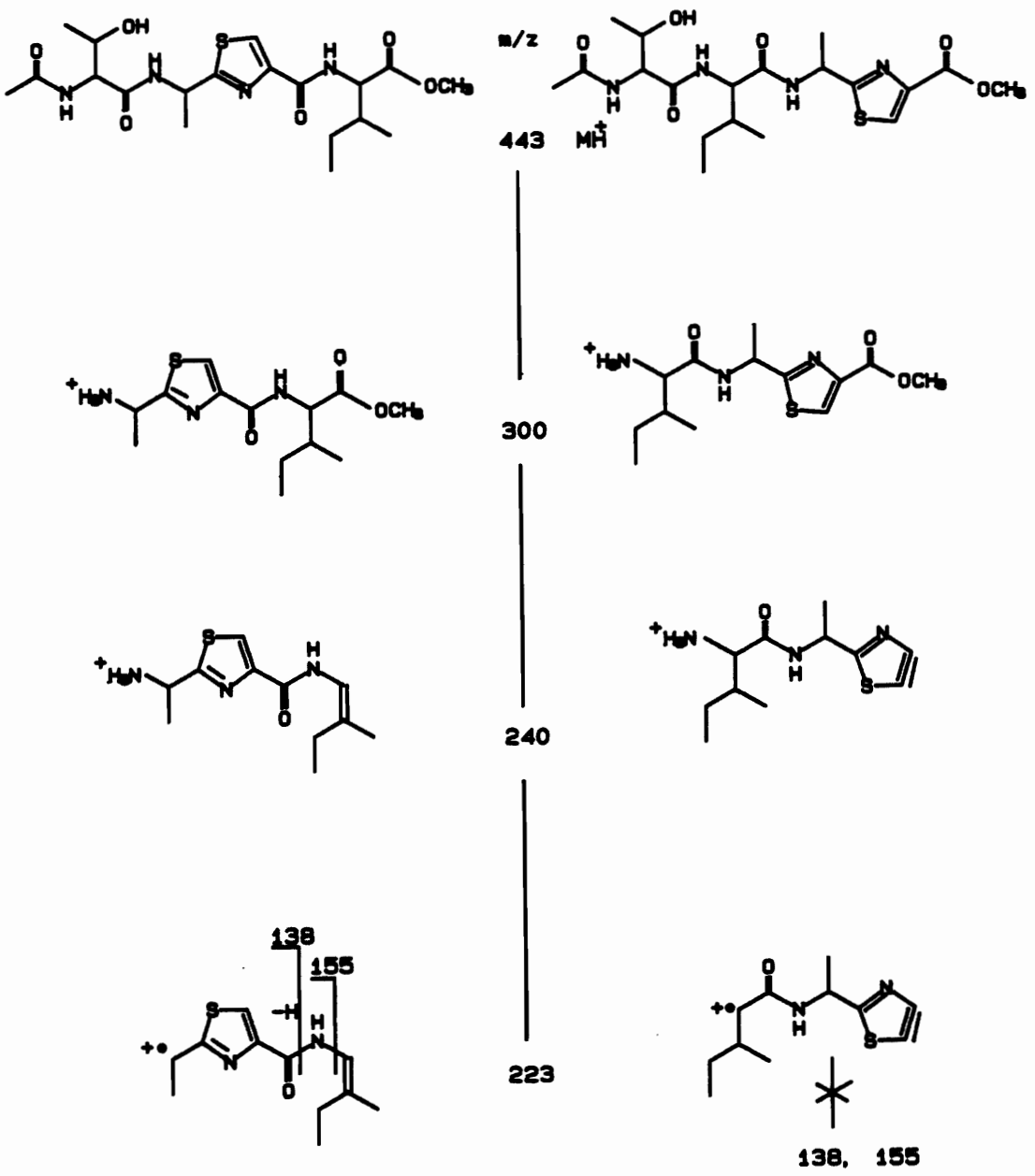

Figure 26. MS/MS analysis of a tripeptide obtained from patellamide B

The detection of five-bond coupling is not unique to the patellamides. Present in the COSY 45 contour map of lissoclinamide 2 are crosspeaks connecting the α-oxazoline proton (H-2, 4.27, d, J = 5 Hz) to the α-Pro proton (H-6, 4.59, t, J = 8 Hz) through the oxazoline ring and also H-2 to the α-Ile proton (H-27, 4.81, m) through the amide linkage.

Samples of the lissoclinum peptides used in the COSY 45 experiments were obtained by RP-HPLC of extracts from two previous workups of L. patella (Whatman ODS-2; 80:20, MeOH:H_2O). The HPLC chromatography also provided three new peptides: prelissoclinamide-2 (62, 33mg, 0.5% of extract), prepatellamide-B-formate (63, 13 mg, 0.2%) and preulicyclamide (64, 13 mg., 0.2%).

The first minor metabolite was named prelissoclinamide-2 62 because it had the same amino acid sequence and stereochemistry as lissoclinamide-2 60 but the oxazoline was now opened. It was assigned a molecular formula $C_{33}H_{43}N_7O_6S_2$ by HRFABMS measurements (obs. 698.2828; MH^+ requires 698.2793) suggesting that it differed from the lissoclinamides (MW 679) by the addition of water. IR stretches at 1680 and 1660 cm^{-1} and five carbon resonances between 170 and 180 ppm indicated a penta-peptide system. Interpretation of the ^1H and ^{13}NMR data of the new peptide confirmed the presence of an Ala-thiazole [^1H δ7.95 (s), 5.28 (dq, 1H, J = 10, 7 Hz), 1.58 (d, 3H, J = 7 Hz); ^{13}C

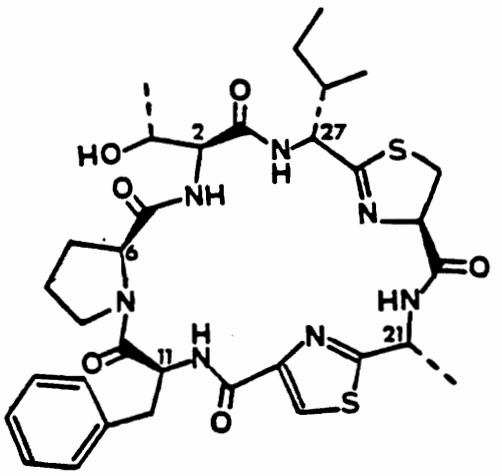

62

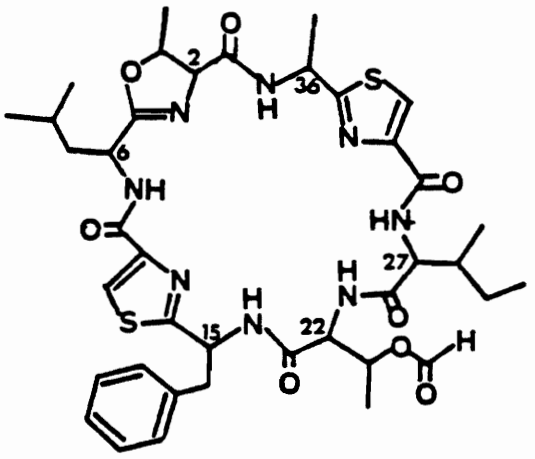

63

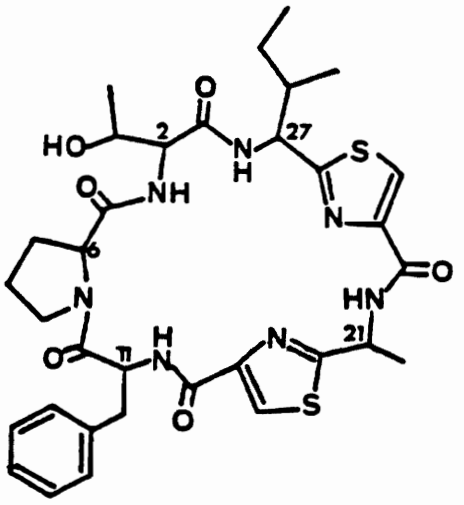

64

δ148.2, 123.5, 159.6, 47.4, 22.1] Ile-thiazoline [^{1}H δ5.25 (m, 1H), 3.59 (m, 2H), 5.33 (dd, 1H, J = 8.5, 8 Hz), 2.58 (m, 1H,), 1.40 (m, 2H), 0.97 (t, 3H, J = 7.3 Hz), 1.12 (d, 3H, J = 7 Hz); ^{13}C δ79.8, 35.4, 171.0, 55.0, 37.9, 26.6, 12.0, 14.7], Phe [^{1}H δ 5.18 (ddd, 1H, J = 9, 7, 7 Hz), 3.15, (dd, 1H, J = 14, 7 Hz), 3.09 (dd, 1H, J = 14, 7 Hz), 7.36 (m, 5H); ^{13}C δ 52.4, 40.7, 136.1, 128.9 (2C), 129.3 (2C), 127.4] and Pro [^{1}H δ 4.30 (t, 1H, J = 8 Hz), 1.84, (m, 1H), 2.39 (m, 1H), 1.84 (m, 1H), 3.59 (m, 1H), 2.58 (m, 1H); ^{13}C δ63.2, 29.8, 25.3, 47.8]. The remaining spin systems in the ^{1}H NMR [δ 6.45 (d, 1H, J = 8.7 Hz), 4.43 (d, 1H, J = 8.7 Hz), 4.84 (q, 1H, J = 6.5 Hz) and 1.29 (d, 3H, J = 6.5 Hz] defined an open Thr unit. The α- and β-protons of the Thr unit failed to show coupling indicating that they exist in a fixed conformation with the angle between the two protons approaching 90°.[102] Complete assignment of the NMR signals was based on conventional decoupling experiments, heteronuclear correlation experiments that indicated C-H connectivities and the COSY 45 experiment that not only confirmed the results of the conventional decoupling study but was very useful in establishing the amino acid sequence. Crosspeaks were present connecting the α-Ile thiazoline proton (H-27) to the α-Thr proton (H-2) which showed connections to the α-Pro proton (H-6) which showed an additional connection to the α-Phe proton (H-11) establishing the sequence Ile thiazoline-Thr-Pro-Phe present

in the molecule.

The structure and stereochemistry of prelissoclinamide-2 was confirmed by the reaction sequence shown in Figure 27. Lissoclinamide-2 (60) was refluxed in 5% H_2SO_4/MeOH forming the amino lactone intermediate 127 which then underwent transacylation in strong base yielding prelissoclinamide-2. The spectral data and optical rotation of the degradation product and the natural product were found to be identical.

The second minor metabolite was named prepatellamide-B-formate (63) based on its compositional similarity to patellamide B. It was assigned a molecular formula $C_{39}H_{50}N_8O_8S_2$ by HRFABMS (obs. 823.3254, MH^+ requires 823.3271). Comparison of the spectral data of prepatellamide-B-formate with patellamide B indicated the presence of Ala and Phe thiazoles, Leu, Ile but only one oxazoline [^{1}H NMR: δ 4.27 (d, J = 2.6 Hz), 4.95 (dq, 1H, J = 5.3, 2.6 Hz), 1.41 (q, 3H, J = 5.3 Hz)]. The major changes in the ^{1}H NMR spectrum, Figure 28, are 1) a new amide NH proton at 7.04 ppm (d, J = 9Hz), 2) a downfield shift of what was one of the oxazoline protons (δ 4.29 in the patellamide B spectrum) to 4.76 ppm (d, J = Hz), 3) a methinyl quartet at 5.76 ppm (q, J = 6.6 Hz) and 4) a doublet methyl at 1.43 ppm (d, J = 6.6 Hz) all of which defines a threonine unit and 5) a singlet at 8.5 ppm that correlates via a HETCOR experiment to a carbon signal at 161 ppm defining the O-formyl-Thr unit. Evidence for

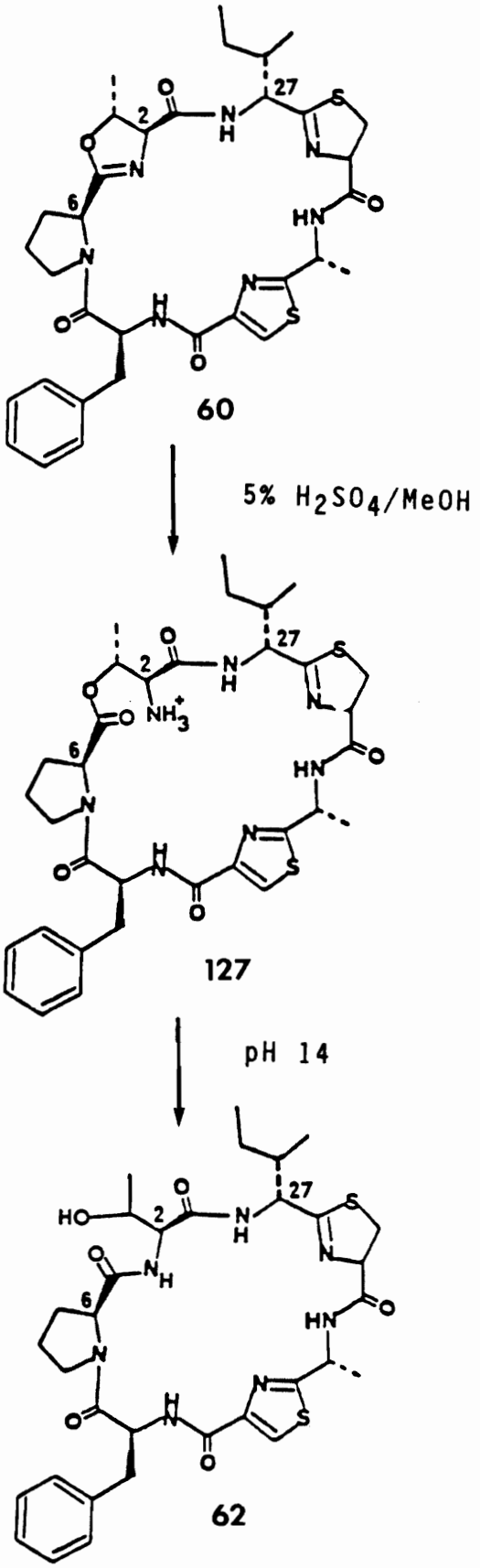

Figure 27. Conversion of lissoclinamide 2 (60) to prelissoclinamide-2 (62)

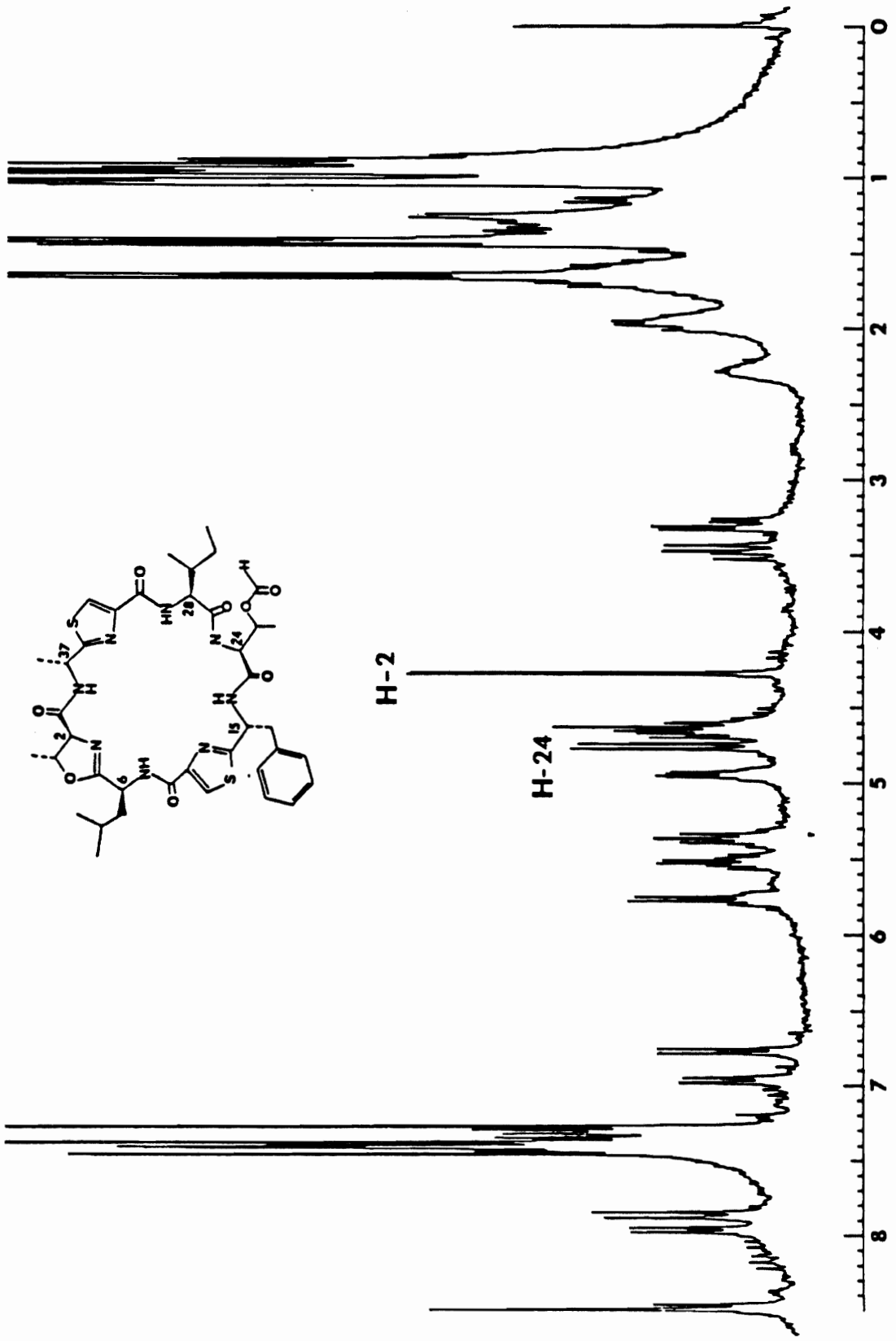

Figure 28. ^{1}H NMR of prepatellamide-B-formate

preferential ring opening of one of the oxazoline rings was obtained from the COSY 45 spectrum (Figure 29). The oxazoline proton (H-2) shows a connectivity to the α-Ala-thiazole proton (H-36) and to the α-Ile proton (H-6). No coupling was observed between the α- and β-protons of the Thr unit indicating that it too exists in a fixed conformation.

The third minor metabolite was named preulicyclamide (64) and assigned a molecular formula $C_{33}H_{41}N_7O_6S_2$ by high resolution FAB mass measurement (obs. 696.2652, MH^+ requires 696.2622). Initial inspection of the ^1H and ^{13}C NMR data revealed the presence of Ala and Ile thiazoles, Phe, Pro and again an oxazoline replaced by a Thr unit [^1H δ6.99 (d, NH, J = 6.6 Hz), 4.03 (dd, 1H, J = 7.4, 6.6 Hz), 4.70 (dq, 1H, J = 7.4, 6.6 Hz), 1.19 (d, 3H, J = 6.6 Hz)]. The 7.4 Hz coupling constant represents $^3J_{H-H}$ between the α-and β-protons of threonine indicating that in preulicyclamide the Thr exists as a freely rotating unit. The COSY 45 spectrum established the sequence Ile thiazole-Thr-Pro-Phe confirming the proposed structure.

Harsh conditions are necessary to effect ring opening of the oxazoline ring. Therefore, it is proposed that the three new lissoclinum peptides are not artefacts of the work-up procedure. Rather, they are postulated precursors in the biosynthetic pathway leading to formation of the lissoclinum peptides in which the final step is possibly

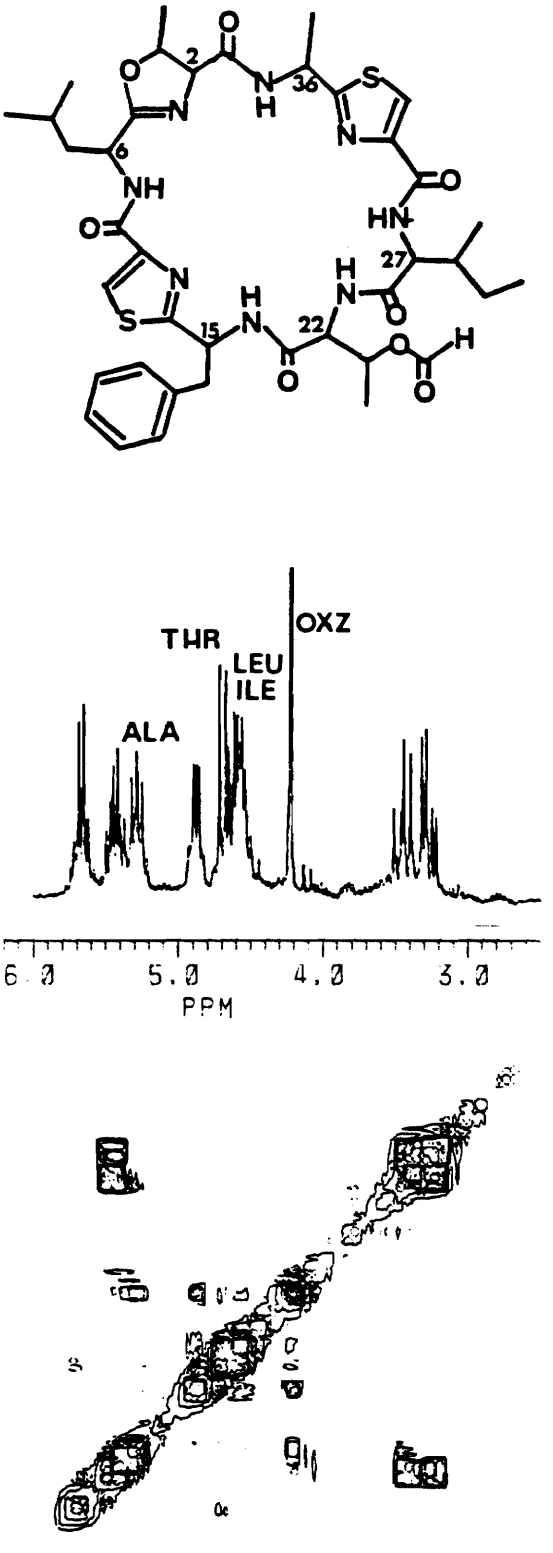

Figure 29. COSY 45 spectrum of prepatellamide-B-formate

formation of the oxazoline ring.

The lissoclinum peptides were tested *in vitro* against the L1210 murine leukemia cell line. The results, shown in Table 2, are very perplexing. Prelissoclinamide-2 exhibited good biological activity (IC_{50} 2.7 μg/ml) whereas lissoclinamide 2 was completely inactive (IC_{50} >10 μg/ml). These results indicate that the threonine unit may be responsible for the biological activity. If this were true then prepatellamide-B-formate and preulicyclamide should be more active then patellamide B or ulicyclamide respectively. However, the exact opposite is observed. In fact, prepatellamide-B-formate and preulicyclamide were completely inactive. Therefore, the threonine unit is probably not responsible for the activity and the explanation for the observed activities or lack thereof remains a mystery.

Table 2

L1210 values for the lissoclinum peptides

Compound	IC_{50}, μg/ml
ulicyclamide	7.2
ulithiacyclamide	0.35
patellamide A	3.9
patellamide B	2.0
patellamide C	3.2
lissoclinamide 1	>10
lissoclinamide 2	>10
lissoclinamide 3	>10
prelissoclinamide 2	2.7
prepatellamide B formate	>10
preulicyclamide	>10

EXPERIMENTAL

Instrumentation

Infrared spectra were recorded on a Beckman 620 MX spectrophotometer. UV spectra were recorded on a Beckman DU-8 spectrophotometer. ^{1}H and ^{13}C NMR spectra were recorded on a Bruker WM 500 spectrometer at Yale University, a JEOL 270 or an IBM 200 spectrometer. All 2D NMR spectra were recorded on the IBM 200 MHz spectrometer equipped with an Aspect 3000 computer. Chemical shifts are reported in ppms downfield from Me_4Si ($\delta=0$) for proton spectra or using the central line of the $^{2}HCCl_3$ triplet (77.0 ppm) as the internal reference for ^{13}C measurements. Electron ionization mass spectra were recorded on an AEI MS-902 (University of Connecticut) or on a Varian MAT 112S spectrometer. Low resolution CI and FAB mass spectra were also recorded on the Varian MAT 112S spectrometer. High resolution FAB/MS measurements were made using a Varian MAT 731 spectrometer. Tandem MS/MS measurements were recorded on a VG ZAB 4F instrument. Optical rotations were recorded on a Perkin-Elmer 241MC polarimeter. HPLC separations (analytical and preparatory) were performed on a Waters system equipped with a U6K injector, a 501 pump and an R401 differential refractometer. Melting points were measured on a Thomas capillary melting point apparatus.

L1210 assays were performed at the University of Vermont under the direction of Dr. Miles Hacker. The L1210 murine leukemia cells were grown as a stationary suspension cultured in vitro in McCoy's 5A medium supplemented with 10% newborn calf serum, penicillin (100 µg/ml), streptomycin (100 µg/ml) and fungizone (0.25 µg/ml). Cultures were maintained at 37° in a humidified atmosphere of 90% air/10% CO_2. L1210 cells grown under these conditions have a doubling time of approximately 18h.

Compounds were dissolved in sterile DMSO at concentrations such that a 40 µl addition of the solution to 4 ml of cell suspension delivered the desired final concentration of test compound. Routinely, 4 ml of L1210 cells (10^5cells/ml) were added to 15 ml of disposable tissue culture tubes. The test compound was then added to the cells, and the cultures were incubated for 96h. Cell concentration was measured electronically by using a Coulter particle counter (Model ZB_F).

Baseline separation was achieved in the HPLC purification of the voeltzkowinols and the lissoclinum peptides. This insured 95% purity for each metabolite. The ^1H NMR spectrum of all the metabolites also established their purity.

The Chemistry of an Unidentified Tunicate

Collection, extraction and chromatography. The encrusting tunicate was collected on exposed rocks at the

northwest end of Cocos lagoon, Guam. It was placed in a freezer bag and kept frozen until work-up. The tunicate was freeze-dried (116g, dry weight) and extracted in a Soxhlet extraction apparatus with petroleum ether, CCl_4 and then $CHCl_3$. The freeze-dried material was then placed in 500 ml of MeOH and extracted overnight. On standing, a precipitate began to appear in the $CHCl_3$ extract. It was subsequently identified as 3,5-diiodo-4-methoxyphenethylamine (45) (453 mg, 0.39% dry weight). The $CHCl_3$ extract was refrigerated and a second compound, identified as the urea analog (46) (20 mg, 0.017% dry weight) precipitated from solution. Each precipitate was collected by vacuum filtration. The solvent from each extract was removed *in vacuo* and the resulting oil was dissolved in $CHCl_3$ or MeOH and refrigerated. A 1mg sample from each extract was sent to the University of Vermont for cytotoxic evaluation in the L1210 assay.

3,5-diiodo-4-methoxyphenethylamine (45). mp obs 209-212°C, lit 213°C; UV 265nm (ε 2200); IR (KBr) 3650-3200, 3000, 2920, 1000, 860, 710 cm^{-1}; ^1H NMR (DMSO) δ8.26 (s, 2H), 7.76 (s, 2H), 3.73 (s, 3H), 3.03 (t, 2H, J = 8 Hz), 2.86 (t, 2H, J = 7 Hz); ^{13}C NMR (DMSO) δ157.1 (s), 139.7 (d), 139.66 (d), 137.7 (s), 91.5 (2C, s), 60.1 (q), 39.4 (t), 30.8 (t); HREIMS m/z 402.8941, $C_9H_{11}NOI_2$ requires 402.8929; EIMS m/z 403 (M^+), 386, 374 (B), 359.

Bis 3,5-diiodo-4-methoxyphenethylurea (46). mp 224-225 °C; ^1H NMR (DMSO) δ7.56 (s, 2H), 5.78 (t, 1H, J = 6 Hz),

3.62 (s, 3H), 3.08 (dt, 2H, J = 7, 6 Hz), 2.49 (t, 2H, J = 7 Hz); ^{13}C NMR (DMSO) δ157.8 (s), 156.6 (s), 140.2 (d), 139.6 (d), 91.0 (s), 60.1 (q), 40.4, (t), 34.1 (t); HREIMS m/z 831.7699, $C_{19}H_{20}N_2O_3I_4$ requires 831.7675; EIMS m/z 832 (M^+), 705, 429, 403, 373 (B).

Formation of N-acetyltyramine (106). In a 50 ml 3-necked rbf was suspended tyramine (Aldrich, 200 mg) in 10 ml distilled H_2O. The contents of the flask were heated to 90-95 °C at which temperature 1100 µl acetic anhydride was added in 8 portions (137 µl each) over a 3 minute period. The reaction was monitored by TLC (Silica gel, EtOAc). After 3 hours heating was discontinued and the volatiles were removed in vacuo. The product was purified using vacuum filtration through silica (silica gel, EtOAC). The overall yield was 97%.

N-Acetyltyramine (106). IR ($CHCl_3$) 1625 cm^{-1}; ^1H NMR (60 MHz, DMSO) δ7.4 (br s, 2H), 6.5 (dd, 2H), 2.9 (m, 2H), 2.4 (m, 2H), 1.6 (s, 3H).

Formation of 3,5-diiodo-N-acetyl tyramine (107). To a 50 ml rbf containing a solution of N-acetyl tyramine (80 mg; 0.45mM) dissolved in gl acetic acid (1.5ml) was added with stirring, ICl (75 µl; 1.44 mM). The reaction was heated to 80°C and allowed to react for 17 hours. The solvent was removed in vacuo and the product was purified using vacuum filtration (3/4" bed of silica gel 60 eluted with EtOAc). The overall yield was 37%.

3,5-diiodo-N-acetyl tyramine (107). ^{1}H NMR (60 MHz, d_6-acetone) δ7.1 (s, 2H) 2.84 (m, 2H), 2.16 (m, 2H), 1.28 (s, 3H); EIMS m/z 431 (M^+), 372, 359, 305, 246, 233; HREIMS m/z 430.8880, $C_{10}H_{11}NO_2I_2$ requires 430.8890.

Formation of 3,5-diiodo-4-methoxy-N-acetyl tyramine (108). To a 50 ml rbf containing 3,5-diiodo-N-acetyl tyramine (45 mg; 0.104 mM) in EtOAc (5 ml) was added with stirring, NaH (6 mg; 0.125 mM) and dimethyl sulfate (15 µl; 20 mg; 0.158 mM). The reaction was held at reflux for 15 hrs. At the end of the reaction time, the solvent was removed in vacuo and the residue concentrated on the vacuum pump for 10 min. The contents of the flask were then dissolved in MeOH. Analysis of this solution by TLC (silica gel, EtOAc) showed one spot that was less polar than the starting material. The yield of this reaction was 67%.

3,5-diiodo-4-methoxy-N-acetyltyramine (108). ^{1}H NMR (60 MHz, $CDCl_3$) δ 7.5 (s, 2H), 3.8 (s, 3H), 3.3 (m, 2H), 2.7 (m, 2H), 1.9 (s, 3H).

Formation of 3,5-diiodo-4-methoxyphenethylamine (45). Approximately 28 mg of 3,5-diiodo-4-methoxy-N-acetyltyramine was transferred to a threaded test tube in MeOH. The solvent was removed under N_2 and five ml of 6N HCl was added to the residue. The reaction vessel was capped and placed in a 110°C oven and left overnight. After 12 hours the tube was removed from the oven and allowed to cool to room temperature before the solvent was removed in vacuo. The

residue was dissolved in DMSO for ^1H NMR analysis and structural conformation. The yield was 80%.

The Chemistry of Didemnum voeltzkowi

Collection, isolation and chromatography. Didemnum voeltzkowi was collected at low tide on a coral reef approximately one mile off the coast of Suva, Fiji. The freeze-dried tunicate (625 g, dry weight) was homogenized with 1.25 L of MeOH. The homogenate was divided into three equal portions, transferred to erlenmeyer flasks and allowed to extract in the refrigerator overnight. The solvent was removed in vacuo leaving a dark green oil that contained several UV-active compounds. The oil was dissolved in MeOH (100 ml) and partitioned with $CHCl_3$ (3 x 125ml). Examination of the $CHCl_3$ and MeOH fractions by TLC (silica gel, EtOAc) indicated that the voeltzkowinols were present in the MeOH fraction. The contents of the MeOH fraction (3.9 g) were partitioned between BuOH/H_2O. The butanol fraction was chromatographed on a 6 ft. Sephadex column (LH-20, $CHCl_3$:MeOH, 1:1). The voeltzkowinols eluted together in a light yellow band immediately following a dark green pigment-containing band. The appropriate fractions were combined and concentrated to a light yellow oil (756 mg). The oil was further purified by HPLC (μ partisil M9 10/50, EtOAc:TMP, 8:2) yielding voeltzkowinol A (96, 4 mg, 0.002% dry weight), B (97, 22 mg, 0.007% dry weight), C(98, 13 mg,

0.006% dry weight) and D (99, 47 mg, 0.02% dry weight). Voeltzkowinols A-D are easily identified by their characteristic R_f values of 0.4, 0.2, 0.15 and 0.08 respectively.

Voeltzkowinol A (96). $[\alpha]_D$ +43.4°; IR ($CHCl_3$) 3620 cm^{-1} UV (MeOH) 354 (ε 6500), 270 (ε 20000), 231 nm (ε 22000); ^1H NMR($CDCl_3$) δ1.42 (d, 3H, J = 5.9 Hz), 2.70 (dd, 1H, J=18.5, 7.9 Hz), 3.05 (d, 1H, J = 18.5 Hz), 4.32 (m, 1H, J = 7.9, 5.9 Hz), 4.67 (d, 1H, J = 15 Hz), 4.92 (d, 1H, J = 15 Hz), 5.89 (d, 1H, J = 6 Hz), 6.93 (s, 1H), 7.71 (d, 1H, J = 6 Hz); ^{13}C NMR ($CDCl_3$) δ 22.0 (q), 41.5 (t), 60.8 (t), 78.6 (d), 117.9 (s), 127.3 (d), 128.8 (s), 147.9 (d) 152.1 (s) 155.9 (d); HREIMS m/z 192.0786, $C_{11}H_{12}O_3$ requires 192.0783.

Voeltzkowinol B (97). $[\alpha]_D$ -25.3°; IR (MeOH) 3600-3200, 1704 cm^{-1}; UV (MeOH) 231 nm (ε 1600); ^1H NMR(d_4-MeOH) δ3.59 (d, 1H, J = 10.5 Hz), 3.69 (d, 1H, J = 10.5 Hz), 3.88 (s, 1H), 3.96 (d, 1H, J = 12.6 Hz), 4.24 (d, 1H, J = 12.6 Hz). 5.21 (d, 1H, J = 10.6 Hz), 5.31 (d, 1H, J = 16.5 Hz), 6.25 (d, 1H, J = 6 Hz), 6.38 (d, 1H, J = 11.2 Hz), 6.65 (ddd, 1H, J=16.5, 11.2, 10.6 Hz), 7.51 (d, 1H, J = 6 Hz); ^{13}C NMR(d_4-MeOH) δ 53.0 (d), 65.3 (t), 66.6 (t), 82.2 (s), 119.8 (t), 133.5 (d), 133.7 (d), 135.0 (d), 136.1 (s), 166.4 (d), 210.0 (s); HREIMS m/z 210.0893, $C_{11}H_{14}O_4$ requires 210.0888.

Voeltzkowinol C (98). $[\alpha]_D$ -12.6°; IR ($CHCl_3$) 3600-3200 1708 cm^{-1}; UV (MeOH) 231 nm (ε 20000); ^1H NMR(d_4-MeOH) δ7.58 (d, 1H, J = 6 Hz), 6.41 (m, 1H, J = 16.4, 16, 10 Hz), 6.26

1H, J = 16 Hz), 6.15 (d, 1H, J = 6 Hz), 5.27 (d, 1H, J = 16.4 Hz), 5.16 (d, 1H, J = 10 Hz), 4.20 (d, 1H, J = 13.8 Hz), 4.05 (d, 1H, J = 13.8 Hz), 3.31 (s, 3H); ^{13}C NMR (d_4-MeOH) δ208.6 (s), 165.7 (d), 136.7 (s), 134.5 (d), 134.3 (d), 132.6 (d), 119.5 (t), 83.7 (s), 65.8 (t), 65.3 (t), 58.7 (d); HREIMS m/z 210.0900, $C_{11}H_{14}O_4$ requires 210.0888.

Voeltzkowinol D (99). $[\alpha]_D$ -16.4°; IR (MeOH) 3600-3000, 1690 cm^{-1}; UV (MeOH) 307 (ε 10000), 233 nm (ε 11000); ^1H NMR (d_4-MeOH) δ 1.90 (dd, 3H, J = 7, 1.3 Hz), 3.69 (d, 1H, J = 12 Hz), 3.90 (d, 1H, J = 12 Hz), 4.57 (d, 1H, J = 11.8 Hz), 4.83 (d, 1H, J = 11.8 Hz), 6.29 (d, 1H, J = 6 Hz), 6.52 (dq, 1H, J = 16, 7 Hz), 7.40 (d, 1H, J = 6 Hz), 7.83 (dd, 1H, J=16, 1.3 Hz); ^{13}C NMR (d_4-MeOH) δ19.4 (q), 58.3 (t), 68.2 (t), 82.0 (s), 128.4 (d), 134.2 (s), 136.5 (d), 136.6 (d), 146.8 (s), 161.5 (d), 199.1 (s); HREIMS m/z 210.0893, $C_{11}H_{14}O_4$ requires 210.0888.

Acetylation of the voeltzkowinols. To 3 mg of a voeltzkowinol dissolved in 200 µl of acetic anhydride was added 10 µl of pyridine. The reaction was stirred at RT and monitored by TLC (silica, EtOAc). After 30 minutes of reaction time the mixture was evaporated under vacuum and the residue partitioned between $CHCl_3$ (20, ml) and water (20 ml). The water layer was extracted 2X with $CHCl_3$ (20 ml each time). The combined $CHCl_3$ fractions were evaporated under vacuum and purified by HPLC (Partisil PXS 10/25, EtOAc:TMP, 1:1).

Voeltzkowinol A (126). (monoacetate) IR ($CHCl_3$) 1735 cm^{-1}; ^1H NMR ($CDCl_3$) δ5.61 (d, 1H, J = 12.5 Hz), 5.27 (d, 1H, J = 12.5 Hz), 2.10 (3, 3H).

Voeltzkowinol B (109). (diacetate) IR ($CHCl_3$) 3600-3000, 1735 cm^{-1}; EIMS m/z 294; ^1H NMR ($CDCl_3$) δ7.52 (d, 1H, J = 5.2 Hz) 6.47 (br s, 2H), 6.33 (d, 1H, J = 5.2 Hz), 5.41 (d,1H,J=10.5Hz), 5.32 (d, 1H, J = 17.9 Hz), 4.65 (d, 1H, J = 13.1 Hz), 4.53 (d,1H, J = 13.1 Hz), 4.53 (d, 1H, J = 13.1 Hz), 4.34 (d, 1H, J = 11.2Hz) 4.18 (d, 1H, J = 11.2 Hz), 3.70 (br s, 1HO, 2.09 (s, 3H), 2.04 (s, 3H); HREIMS m/z 294.1090, $C_{15}H_{18}O_6$ requires 294.1116.

Voeltzkowinol C (110). (diacetate) IR ($CHCl_3$) 1741, 1720 cm^{-1}; EIMS m/z 294; ^1H NMR ($CDCl_3$) δ4.77 (d, 1H, J = 13.8 Hz), 4.55 (d, 1H, J = 13.8 Hz), 4.16 (br s, 2H), 2.13 (s, 3H), 2.02 (s, 3H); HREIMS m/z 294.1098, $C_{15}H_{18}O_6$ requires 294.1116.

Voeltzkowinol D. [diacetate, (114)] IR ($CHCl_3$) 3600-3200, 1735 cm^{-1}; EIMS m/z 294; ^1H NMR ($CDCl_3$) δ7.72 (d, 1H, J = 15.9, 1.3 Hz), 7.32 (d, 1H, J = 6 Hz), 6.38 (m, J = 15.9, 7 Hz), 6.32 (d, 1H, J = 6 Hz), 5.47 (d, 1H, J = 12.5 Hz), 4.96 (d, 1H, J = 12.5Hz), 4.33 (d, 1H, J = 11.8 Hz), 4.15 d, 1H, J = 11.8 Hz), 2.03 (s, 6H), 1.91 (dd, 3H, J = 7, 1.3 Hz); HREIMS m/z 294.1098, $C_{15}H_{18}O_6$ requires 294.1116. [triacetate, (115)] IR ($CHCl_3$) 1741 (br), 1686 cm^{-1}; EIMS m/z 336; ^1H NMR ($CDCl_3$) δ7.83 (d, 1H, J = 15.8, 1.3 Hz), 7.39 (d, 1H, J = 6 Hz), 6.42 (d, 1H, J = 6 Hz), 6.26 (dq,

1H, J = 15.8, 6.5 Hz), 5.00 (s, 3HO, 4.57 (d, 1H, J = 11.2 Hz), 4.15 (d, 1H, J = 11.2 Hz), 2.06 (s, 3H), 2.04 (s, 3H), 2.02 (S, 3H), 1.90 (dd, 3H, J = 6.5, 1.3 Hz); HREIMS m/z 336.1212, $C_{17}H_{20}O_7$ requires 336.1203.

MnO_2 oxidation of the voeltzkowinols. To 1 equivalent of a voeltzkowinol partially dissolved in CH_2Cl_2 (2 ml) was slowly added with stirring 36 equivalents of activated MnO_2. The reaction was stirred at RT and monitored by TLC (silica gel, EtOAc). The reaction was complete in 50 minutes and the reaction mixture was filtered through a scintered glass funnel. The MnO_2 was rinsed 3X with CH_2Cl_2. The filtrate was evaporated under vacuum and purified by HPLC (Partisil PXS 10/25, EtOAc:TMP, 7:3).

Voeltzkowinol B. [(γ-lactone, (111)] IR ($CHCl_3$) 3600-3200, 1751, 1719 cm^{-1}; UV (MeOH) 268.9 (ε 6.2 x10^5); ^1H NMR ($CDCl_3$) δ 7.63 (d, 1H, J = 6 Hz), 7.30 (dd, 1H, J = 16, 2.2 Hz), 7.07 (m, 1H, J = 16, 11, 7.7 Hz), 6.39 (d, 1H. J = 6 HzO, 5.81 (d, 1H, J = 11 Hz), 5.76 (d, 1H, J = 7.7 Hz), 4.03 (d, 1H, J = 12 Hz), 3.86 (d, 1H, J = 12Hz), 3.81 (d, 1H, J = 2.2 Hz), 2.09 (br s, 1H, exchangeable); HREIMS m/z 206.0550, $C_{11}H_{10}O_4$ req 206.0576.

Voeltzkowinol C. [aldehyde, (112)] IR ($CHCl_3$) 3600-3200, 1720, 1680 cm^{-1}; UV (MeOH) 235.6 (ε 6000); UV ($CHCl_3$) 270.6nm (ε 4000); [aldehyde, (112)] ^1H NMR ($CDCl_3$) δ9.46 (s, .8H), 7.56 (d, .8H, J = 6 Hz), 6.36 (d, .8H, J = 6 Hz), 7.20 (d, .8H, J = 11 Hz), 6.72 (m, .8H, J = 17, 11, 9.5 Hz), 5.87

(d, .8H, J = 17 Hz, 5.76 (d, .8H, J = 9.5 Hz), 3.78 (d, .8H, J = 12 Hz, 3.63 (d, .8H, J = 12 Hz), 3.59 (s, .8H). [δ-lactol, (113)] δ7.41 (d, .2H, J = 5 Hz), 6.36 (d, .2H, J = 5 Hz), 5.48 (d, .2H, J = 16 Hz), 5.36 (d, .2H, J = 9.5 Hz), 5.41 (s, .2H), 3.56 (d, .2H, J = 11 Hz), 3.49 (d, 1H, J = 11 Hz), 3.51 (s, .2H); HREIMS m/z 208.0719, $C_{11}H_{12}O_4$ requires 208.0744.

Recording 2D NMR spectra. The NOESY spectrum was recorded using a 128W x 1K data matrix. Sixty scans were acquired for each experiment. The mixing delay was set at the average T_1 for the protons of interest (1.75 s) as determined by a standard inversion recovery experiment. Total measuring time was approximately 16 hours. The f_1 dimension was zero-filled to 512W to satisfy the equation : $Hz_1/Pt_1 = Hz_2/Pt_2 = 1$. The spectrum was obtained by applying a sinebell filtering function in each dimension followed by a symmetrization function.

For experimental details on the COSY experiment the reader is directed to the experimental section for Lissoclinum patella.

The Chemistry of Lissoclinum Patella

Extraction and chromatography. Recombined chromatography fractions containing "minor components" from two previous workups of L. patella (7.0 grams total extract) were chromatographed on RP HPLC (Whatman ODS-2; 80:20, MeOH:H_2O) to give prelissoclinamide-2 (62, 33 mg, 0.5% of

extract), prepatellamide-B-formate (63, 13 mg, 0.2% of extract) and a complex mixture of at least five additional peptides (53 mg). HPLC of this mixture (Whatman partisil-10; 96:4, $CHCl_3$:MeOH) gave preulicyclamide (64, 15 mg, 0.2% of extract).

Prelissoclinamide-2 (62). $[\alpha]_D$ +18.1° (c 2.24, $CHCl_3$); IR ($CHCl_3$) 3387, 3316, 2917, 1680, 1660, 1530 cm^{-1}; HRFABMS m/z 698.2828, $C_{33}H_{44}N_7O_6S_2$ (MH^+) requires 698.2793.

Prepatellamide-B-Formate (63). $[\alpha]_D$ +36.5° (c 0.3, $CHCl_3$); IR 3356, 3316, 2911, 1747, 1661, 1538 cm^{-1}; HRFABMS m/z 823.3254, $C_{39}H_{51}N_8O_8S_2$ (MH^+) requires 823.3217.

Preulicyclamide (64). $[\alpha]_D$ +5.4° (c 0.24, $CHCl_3$); IR ($CHCl_3$) 3369, 3345, 2919, 1660, 1623, 1530 cm^{-1}; HRFABMS m/z 696.2652, $C_{33}H_{42}N_7O_6S_2$ (MH^+) requires 696.2622.

The Conversion of Lissoclinamide 2 (60) to Prelissoclinamide-2 (62). Lissoclinamide 2 (3.5 mg) was refluxed in 5% H_2SO_4/MeOH for 1 hour. The reaction mixture was then added to a solution of 10% NaOH and allowed to stir overnight. The mixture was partitioned with $CHCl_3$ (3 X 50 ml). The $CHCl_3$ fraction was dried over anhydrous Na_2SO_4 and the solvent removed in vacuo. HPLC purification of the mixture (Whatman RP-18, 60:40, MeOH/H_2O) yielded Prelissoclinamide-2 [1 mg, $[\alpha]_D$ +22.5° (c 0.027, $CHCl_3$)].

Recording 2D-NMR Spectra The COSY 45 pulse sequence is 90 - τ - 45. COSY 45 spectra were recorded using a 32W X 1K data matrix, and 16 scans were acquired for each t_1

duration. Total measuring time for a COSY spectrum was approximately 30 minutes. The f_1 dimension was zero-filled to 512W to satisfy the equation: $Hz_1/Pt_1 = Hz_2/Pt_2 = 1$. Each spectrum was obtained by applying a sine bell filtering function in each dimension followed by a symmetrization function. The HETCOR spectra were recorded using a 64W X 1K data matrix and 600 scans were acquired for each t_1 duration. Total measuring time was approximately 6 hours. Each spectrum was obtained by applying a sine bell function in each dimension.

APPENDIX

NMR DATA FOR THE LISSOCLINUM PEPTIDES

Table 3. ^{1}H NMR Chemical Shift Assignments for the Lissoclinum Peptides Assignments are Based on Detailed Analysis of COSY 45 Data

H at C #	Patellamide A (65)	Patellamide B (66)
2	4.30 (dd, J = 8, 4 Hz)	4.38 (d, J = 4 Hz)
3	4.80 (m)	5.01 (m)
4		
5	4.56 (dd, J = 10, 8 Hz)	1.47 (d, J = 7 Hz)
6	1.96 (m)	5.01 (m)
7	1.58 (m)	1.61 (m)
8	0.73 (t, J = 7 Hz)	2.08 (m)
9	0.81 (d, J = 7 Hz)	1.07 (d, J = 6 Hz)
10		1.05 (d, J = 7 Hz)
11		
12	7.83 (s)	
13		7.49 (s)
14	5.22 (m)	
15	2.32 (m)	5.50 (ddd, J = 10, 10, 7 Hz)
16	1.13 (d, J = 7 Hz)	3.45 (dd, J = 14, 10 Hz)
		3.31 (dd, J = 14, 7 Hz)
17	1.08 (d, J = 7 Hz)	
18		7.30 (m, 5H)
19	4.30 (d, J = 4 Hz)	
20	4.89 (dg, J = 6, 4 Hz)	
21		
22	1.47 (d, J = 6 Hz)	4.29 (d, J = 4 Hz)
23	4.65 (dd, J = 8, 6 Hz)	5.01 (m)
24	1.96 (m)	
25	1.58 (m)	1.45 (d, J = 7 Hz)
26	0.75 (t, J = 7 Hz)	4.77 (dd, J = 11, 7 Hz)
27	0.81 (d, J = 7 Hz)	2.24 (m)
28		1.61 (m)
29		0.93 (t, J = 6 Hz)
30	7.83 (s)	1.09 (d, J = 7 Hz)
31		
32	5.22 (m)	
33	2.32 (m)	7.39 (s)
34	1.13 (d, J = 7 Hz)	
35	1.08 (d, J = 7 Hz)	5.39 (dq, J = 9, 7 Hz)
36		1.74 (d, J = 7 Hz)
37		
N-1	7.95 (m)	7.62 (d, J = 9 Hz)
N-2	7.41 (d, J = 10 Hz)	7.62 (m)
N-3	7.95 (m)	7.62 (d, J = 10 Hz)
N-4	7.41 (d, J = 8 Hz)	7.62 (d, J = 11 Hz)
N-5		

Table 3. Continued

H at C No.	Ulicylamide (54)	Ulithiacyclamide (55)
2	4.26 (d, J = 4 Hz)	4.05 (dd, J = 8, 2 Hz)
3	4.82 (dq, J = 7, 4 Hz)	4.71 (dg, J = 8, 7 Hz)
4		
5	1.44 (d, J = 7 Hz)	1.1 (d, J = 7 Hz)
6	4.52 (t, J = 8 Hz)	5.24 (ddd̄d, J = 9, 6, 4, 2 Hz)
7	1.9 (m)	3.22 (dd, J = 14, 6 Hz)
		3.02 (dd, J = 14, 4 Hz)
8	1.35 (m)	
9	3.25 (m, 3H)	
10		7.72 (s)
11	4.89 (m)	
12	3.25 (m, 3 Hz)	5.36 (m)
	2.93 (dd, J = 14, 10 Hz)	
13		1.66 (m)
14		1.35 (m)
15	7.30 (s, 5H)	0.78 (d, J = 7 Hz)
16		0.90 (d, J = 7 Hz)
17		
18		
19	8.03 (s)	
20		
21	5.38 (dq, J = 7, 5 Hz)	
22	1.71 (d, J = 7 Hz)	
23		
24		
25	8.08 (s)	
26		
27	5.26 (dd, J = 10, 7 Hz)	
28	2.65 (m)	
29	2.10 (m)	
	1.70 (m)	
30	0.85 (t, J = 7 Hz)	
31	0.73 (d, J = 7 Hz)	
32		
33		
34		
35		
36		
37		
N-1	7.85 (d, J = 10 Hz)	7.70 (d, J = 9 Hz)
N-2	8.67 (d, J = 7 Hz)	8.50 (d, J = 9 Hz)
N-3	9.06 (d, J = 5 Hz)	
N-4		
N-5		

Table 3. Continued

H at C No.	Lissoclinamide 1 (59)	Lissolinamide 2 (60)	Lissoclinamide 3 (61)
2	4.30 (d, J = 4 Hz)	4.27 (d, J = 5 Hz)	4.23 (d, J = 5 Hz)
3	4.87 (dq, J = 6, 4 Hz)	4.81 (dq, J = 6, 5 Hz)	4.77 (dq, J = 6, 5 Hz)
4			
5	1.46 (d, J = 6 Hz)	1.51 (d, J = 6 Hz)	1.46 (d, J = 6 Hz)
6	4.58 (t, J = 8 Hz)	4.62 (t, J = 7 Hz)	4.59 (t, J = 8 Hz)
7	1.87 (m)	2.01 (m)	1.80 (m)
		2.34 (m)	
8	1.61 (m)	2.01 (m)	2.16 (m)
		2.14 (m)	1.80 (m)
9	3.27 (m)	3.80 (m)	3.38 (m)
	2.31 (m)	3.42 (m)	2.35 (m)
10			
11	4.86 (m)	5.14 (m)	4.95 (ddd, J = 9, 8, 5 Hz)
12	3.28 (dd, J = 13, 5 Hz)	3.17 (dd, J = 14, 6 Hz)	3.21 (dd, J = 13, 5 Hz)
	2.91 (dd, J = 13, 10 Hz)	3.02 (dd, J = 14, 6 Hz)	2.95 (dd, J = 13, 9 Hz)
13			
14-16	7.31 (m, 5H)	7.18 (m, 5H)	7.30 (m 5H)
17			
18			
19	8.05 (s)[a]	7.99 (s)	8.07 (s)
20			
21	5.35 (dd, J = 9, 6 Hz)	5.33 (dq, J = 8, 7 Hz)	5.37 (dq, J = 7, 7 Hz)
22	2.22 (m)	1.56 (d, J = 7 Hz)	1.56 (d, J = 7 Hz)
23	1.70 (m)		
24	0.92 (t, J = 7 Hz)	5.21 (dd, J = 9.2, 4.6 Hz)	5.21 (dd, J = 6, 5.2 Hz)
25	1.04 (d, J = 7 Hz)	3.48 (dd, J = 13, 4.6 Hz)	3.73 (dd, J = 13.8, 5.2 Hz)
		3.42 (dd, J = 13, 9.2 Hz)	3.64 (dd, J = 13.8, 6 Hz)
26			
27		5.14 (m)	4.81 (m)
28	8.03 (s)[a]	2.45 (m)	2.35 (m)
29		1.43 (m)	1.60 (m)
		1.32 (m)	1.32 (m)
30	5.15 (t, J = 10 Hz)	0.93 (t, J = 8 Hz)	0.91 (t, J = 7 Hz)
31	2.78 (dqq, J = 10, 7, 7 Hz)	1.02 (d, J = 7 Hz)	0.95 (d, J = 7 Hz)
32	1.08 (d, J = 7 Hz)		
33	0.75 (d, J = 7 Hz)		
34			
35			
36			
37			
N-1	7.97 (d, J = 10 Hz)	7.56 (d, J = 10 Hz)	7.70 (d, J = 10 Hz)
N-2	8.73 (d, J = 6 Hz)	7.98 (d, J = 6 Hz)	8.58 (d, J = 8 Hz)
N-3	8.97 (d, J = 6 Hz)	6.70 (d, J = 8 Hz)	8.24 (d, J = 7 Hz)
N-4			
N-5			

Table 3. Continued

H at C#	Prepatellamide-B-Formate (63)	Prelissoclinamide-2 (62)	Preulicyclamide (64)
2	4.27 (d, J = 2.6 Hz)	4.43 (d, J = 8.7 Hz)	4.03 (dd, J = 7.4, 6.6 Hz)
3	4.95 (dq, J = 5.3, 2.6 Hz)	4.84 (q, J = 6.5 Hz)	4.70 (dq, J = 7.4, 6.6 Hz)
4	1.41 (q, J = 5.3 Hz)	1.29 (d, J = 6.5 Hz)	1.19 (d, J = 6.6 Hz)
5			
6	4.63 (m)	4.30 (t, J = 8 Hz)	4.17 (dd, J = 8, 7 Hz)
7	1.97 (m)	1.84 (m)	1.80 (m)
	1.30 (m)	2.39 (m)	2.17 (m)
8	1.50 (m)	1.84 (m)	3.31 (m)
9	1.03 (d, J = 6 Hz)	3.59 (m)	
		2.58 (m)	
10	0.95 (d, J = 6 Hz)		
11		5.18 (ddd, J = 9,7,7 Hz)	4.96 (ddd, J = 9.5, 8, 5 Hz)
12		3.15 (dd, J = 14, 7 Hz)	3.18 (dd, J = 13, 5 Hz)
		3.09 (dd, J = 14, 7 Hz)	2.98 (dd, J = 13, 9.5 Hz)
13	7.46 (s)		
14			
15	5.51 (ddd, J = 10, 10, 6 Hz)	7.36 (m, 5H)	7.35 (m, 5H)
16	3.29 (dd, J = 14, 6 Hz)		
	3.47 (dd, J = 14, 10 Hz)		
17			
18			
19	7.33 (m, 5H)	7.95 (s)	7.89 (s)
20			
21		5.28 (dq, J = 10, 7 Hz)	5.31 (dq, J = 6.6, 5 Hz)
22	4.76 (d, J = 9 Hz)	1.58 (d, J = 7 Hz)	1.64 (d, J = 6.6 Hz)
23	5.76 (q, J = 6.6 Hz)		
24	1.43 (d, J = 6.6 Hz)	5.25 (m)	
25	8.48 (s)	3.59 (m)	8.06 (s)
26			
27	4.65 (m)	5.33 (dd, J = 8.5, 8 Hz)	5.18 (dd, J = 10, 9 Hz)
28	2.32 (m)	2.58 (m)	2.70 (m)
29	1.30 (m)	1.40 (m)	1.80 (m)
30	0.86 (t, J = 7 Hz)	0.97 (t, J = 7.3 Hz)	0.86 (t, J = 7 Hz)
31	1.03 (d, J = 6 Hz)	1.12 (d, J = 7 Hz)	0.71 (d, J = 6.6 Hz)
32			
33			
34	7.42 (s)		
35			
36	5.35 (dq, J = 8.5, 7.3 Hz)		
37	1.65 (d, J = 7.3 Hz)		
N-1	6.78 (d, J = 8.5 Hz)	6.89 (d, J = 8 Hz)	8.28 (d, J = 9 Hz)
N-2	7.95 (d, J = 8 Hz)	6.45 (d, J = 8.7 Hz)	6.99 (d, J = 6.6 Hz)
N-3	7.86 (d, J = 10 Hz)	8.32 (d, J = 9 Hz)	8.68 (d, J = 8 Hz)
N-4	7.04 (d, J = 9 Hz)	8.18 (d, J = 10 Hz)	9.17 (d, J = 5 Hz)
N-5	8.47 (d, J = 5 Hz)		

Table 4. ^{13}C NMR Assignments for the Lissoclinam Peptides
Chemical Shift Assignments for Protonated Carbons are Based on Heteronuclear COSY Data

Carbon No.	Patellamide A (65)	Patellamide B (66)	Lissoclinamide 1 (59)	Lissoclinamide 2 (60)	Lissoclinamide 3 (61)
1	169.5[a]	173.3[a]	171.4[a]	182.6[a]	174.6[a]
2	67.4	73.8	75.0	75.6	74.9
3	72.2	82.5	82.6	80.8	81.7
4	169.1[a]	168.2[a]	167.6[a]	169.1[a]	169.0[a]
5	52.1	23.2	21.7	21.7[c]	21.6
6	33.3	47.8	56.5	56.7	56.3
7	24.7	39.0	28.7	28.7	29.3
8	10.6	25.1	24.7[d]	25.5	28.4
9	14.9	21.0	47.0	47.3	46.8
10	171.5[a]	21.0	170.9[a]	171.8[a]	170.7[a]
11	149.4[b]	173.0[a]	53.9	52.0[b]	52.8
12	123.0[c]	147.6[b]	40.5	37.8	40.3
13	160.5[d]	123.6[c]	136.0	135.6	135.5
14	54.9	161.8[d]	128.6 (2C)	128.2 (2C)	128.2 (2C)
15	37.1	53.3	129.7 (2C)	129.6 (2C)	129.6 (2C)
16	19.2	40.7	127.2	126.7	126.9
17	19.2	136.1	169.8[a]	171.8[a]	170.6[a]
18	171.5[a]	128.7 (2C)	150.5[c]	148.3	148.0
19	73.6	129.2 (2C)	122.9	123.7	123.3
20	81.6	127.1	160.8[b]	159.6	159.1
21	168.5[a]	172.8[a]	56.8	47.0	47.3
22	21.7	73.8	40.8	22.0[c]	24.4
23	52.4	82.1	25.0[d]	171.7[a]	170.6[a]
24	33.3	168.0[a]	11.9	78.7	78.7
25	24.9	21.8	15.2	36.2	35.2
26	11.1	52.5	168.5[a]	169.1[a]	169.9[a]
27	15.0	32.9	148.1[c]	54.2[b]	53.2
28	171.8[a]	25.1	122.9	38.5	38.9
29	149.4[b]	8.8	159.9[b]	26.6	24.9
30	123.0[c]	15.0	55.5	11.7	10.2
31	160.5[d]	170.8[a]	33.0	14.0	14.8
32	54.9	147.2[b]	20.2		
33	36.8	123.6[c]	20.0		
34	17.9	161.6[d]			
35	17.9	46.7			
36		21.0			
37					

Table 4. Continued

Carbon #	Ulicyclamide (54)	Ulithiacyclamide (55)	Prepatellamide-B-Formate (63)	Prelissoclinamide-2 (62)	Preulicyclamide (64)
1	171.9[b]	170.0[a]	173.6[a]	180.1[a]	172.8[a]
2	76.3	74.1	74.0	58.8	63.2
3	83.3	81.7	81.9	67.2	66.9
4	167.7	167.3	168.6	20.0	20.2
5	22.9	22.1	21.0	170.4[a]	171.6[a]
6	57.5	48.4[b]	51.6	63.2	62.6
7	29.8	46.5	39.9	29.8	29.8
8	25.9[e]	170.5[a]	25.0	25.3	25.4
9	54.4[a]	160.1	22.2	47.8	47.4
10	171.9[b]	124.1	22.5	172.8[a]	171.0[a]
11	54.4[a]	149.2	172.2[a]	52.4	53.5
12	41.8	48.5[b]	149.2[b]	40.7	41.0
13	136.8	46.5	122.8[c]	136.1	135.9
14	129.5 (2C)	25.3	162.3[d]	128.9 (2C)	128.9 (2C)
15	130.6 (2C)	22.7[c]	52.5	129.3 (2C)	129.8 (2C)
16	128.2	22.8[c]	40.8	127.4	127.4
17	171.9[b]		136.3	172.0[a]	169.8[a]
18	161.1[c]		128.8 (2C)	148.2	159.5[b]
19	124.3[d]		129.4 (2C)	123.5	122.9[c]
20	151.4[c]		127.2	159.6	148.0[d]
21	49.6		171.7[a]	47.4	48.6
22	25.4		56.9	22.1	24.2
23	170.5[b]		69.5	172.0[a]	169.0[a]
24	160.5[c]		18.9	79.8	160.7[b]
25	123.8[d]		161.4	35.4	123.5[c]
26	148.9[e]		171.1[a]	171.0[a]	150.2[d]
27	48.1		54.3	55.0	54.3
28	39.0		33.2	37.9	36.3
29	26.0[e]		25.3	26.6	25.3
30	10.9		9.9	12.0	16.0
31	16.2		15.3	14.7	8.8
32			168.6[a]		
33			146.7[b]		
34			123.8[c]		
35			161.6[d]		
36			46.8		
37			21.9		

a interchangeable signals
b interchangeable signals
e interchangeable signals
c interchangeable signals
d interchangeable signals

Table 5. COSY 45 Connectivities for the α-Amino Protons in Lissoclinum Peptides

COMPOUND	CONNECTIONS	
Ulicyclamide (54)	H2	H6
	H2	H27
	H6	H11
Ulithiacylcamide (55)	H2	H6*
	H2	H12
Patellamide-A (65)	H2	H5
	H2	H32
	H19	H14
	H19	H23
Patellamide-B (66)	H2	H6
	H2	H35
	H22	H26
Lissoclinamide-1 (59)	H2	H6
	H2	H30
Lissoclinamide-2 (60)	H2	H6
	H2	H27
Lissoclinamide-3 (61)	H2	H6
	H2	H27
Prelissoclinamide-2 (62)	H2	H6
	H2	H27
	H6	H11
Prepatellamide-B-Formate (63)	H2	H36
	H22	H15
	H22	H27
Preulicyclamide (64)	H2	H6
	H2	H27

* Coupling observable in ID Spectrum.

REFERENCES

1. Chiasson, R.B., Laboratory Anatomy of the Elementary Chordates; Wm.L. Brown Co. Publishers: Dubuque, 1969; pp 1-4.

2. Barrington, E.J.W.; Thorpe, A. Gen. Comp. Endocrinol. 1960, 5, 373-385.

3. Suzuki, S.; Kondo, Y. Gen. Comp. Endocrinol. 1971, 17, 402-406.

4. Salvatore, G. Gen. Comp. Endocrinol., Suppl. 1969, 2, 535-552.

5. Suzuki, S. Jap. J. Develop, Biol. 1969, 23, 16-17.

6. Pearse, A.G.E.; Carvalheira, A.F. Nature 1967, 214, 925-930.

7. Kalk, M. Nature 1963 198, 1010-1011.

8. Danskin, G.P. Can. J. Zool. 1978, 56, 547-551.

9. Burton, J.D.; Massie, K.S. J. Man. Biol. Ass. U.K. 1971, 51, 679-683.

10. Kustin, K.; Toppen, D.L. Limnol. Oceanogr. 1975, 20, 491-493.

11. Dingley, A.L.; Kustin, K.; Macara, I.G.; McLead, G.C. Biochem. Biophys. Acta. 1981, 649, 493-502.

12. Barrington, E.J.W. In Comparative Endocrinology; Gorbman, A., Ed.,; Wiley: New York, 1959; p 80.

13. Willey, A. Amphioxus and the Ancestry of the Vertebrates; Macmillan and Co.: New York, 1894; pp 180-241.

14. Plough, H.H., Sea Squirts of the Atlantic Continental Shelf from Maine to Texas; The Johns Hopkins University Press: Baltimore, 1978; pp 1-111.

15. Young, J.Z., The Life of Vertebrates; Clarendon Press: Oxford, 1981; pp 57-69.

16. Orr, R.T., Vertebrate Biology; Saunders College Publishing Co.: New York, 1982; p. 7.

17. Smith, H.G. Ann. Mag. Nat. Hist. 1935, 15, 615-626.

18. Tokioka, T. Palau Tropical Biological Station Studies 1942, 2, 499-507.

19. Lewin, R.A. Nature 1976, 261, 697-698.

20. Lewin, R.A. Phycologia 1977, 16, 217.

21. Sargent, M.S.; Austin, T.S. Geol. Surv. Prof. Paper 1954, 260-E, 293.

22. Odom, H.T.; Odom, H.P. Ecol. Mono. 1955, 25, 291.

23. Akazawa, T.; Newcomb, E.H.; Osmond, C.B. Mar. Biol. 1978, 47, 325-330.

24. Pardy, R.L.; Lewin, R.A. Bull. Mar. Sci. 1981, 81, 817-823.

25. Davis, B.D.; Dulbecco, R.; Eisen, H.N.; Ginsberg, H.S. Microbiology; 3rd Ed; Harper and Row, publishers: Hagerstown, 1980; p 43.

26. Bruening, R.C.; Oltz, E.M.; Furukawa, J.; Nakanishi, K. J. Am. Chem. Soc. 1985, 107, 5298-5300.

27. Chlorinated metabolites of Dysidea Herbacea (dysidin) strongly resemble the tetramic acid portion of a metabolite from Lyngbya Majuscula (malyngamide A).

28. Bancroft, F.W. Proc. Calif. Acad. Sci. 1905, 3, 138-144.

29. Withers, N.; Vidaver, W.; Lewin, R.A. Phycologia 1978, 17, 167-171.

30. Patterson, G.M.L.; Withers, N.W. Science 1982, 217, 1034-1035.

31. The term aposymbiont refers to an invertebrate host disassociated from its algal symbiont. (source).

32. Rinehart, K.L., Jr. Results presented at the 3rd International IUPAC Symposium on Marine Natural Products, Brussels, September 1980.

33. Weinheimer, A.J.; Matson, J.A.; Karns, J.K.B.; Hossain, M.B.; Van der Helm, D.; In Food and Drugs from the Sea;

Kaul, P.M.; Sinderman, C.J. Eds,; University of Oklahoma, 1978; p 117.

34. Cheng, M.J.; Rinehart, K.L., Jr. J. Am. Chem. Soc. 1978, 100, 7409-7411.

35. Carter, G.T.; Rinehart, K.L., Jr. J. Am. Chem. Soc. 1978, 100, 4302-4304.

36. Carte, B.; Faulkner, D.J. Tetrahedron Lett. 1982, 23, 3863-3866.

37. Rinehart, K.L., Jr.; Harbour, G.C.; Graves, M.D.; Cheng, M.T. Tetrahedron Lett. 1983, 24, 1593-1596.

38. Kobayaski, J.; Nakamura, H.; Hirata, Y. Tetrahedron Lett. 1981, 22, 3001-3002.

39. Watanabe, K.; Matsunaga, S.; Konosu, S. Tetrahedron Lett. 1984, 25, 2003-2004.

40. Takemoto, T.; Daigo, K.; Takagi, N. Yakugaku Zasshi 1964, 84, 1176.

41. Swinehart, J.H.; Biggs, W.R.; Halks, D.J.; Schroeder, N.C. Biol. Bull. 1974, 146, 302.

42. Carlson, R.M.K. Proc. Natl. Acad. Sci. USA 1975, 72, 2216.

43. Heitz, S.; Durgeat, M.; Guyot, M.; Brassy, C.; Bachet, B. Tetrahedron Lett. 1980, 21, 1457-1458.

44. Hogan, I.T.; Sainsbury, M. Tetrahedron 1984, 40, 681-682.

45. Moquin, C.; Guyot, M. Tetrahedron Lett. 1984, 25, 5047-5048.

46. Rinehart, K.L., Jr.; Kobayashi, J.; Harbour, G.C.; Hughes, R.G., Jr; Mizsak, S.A.; Scahill, T.A. J. Am. Chem. Soc. 1984, 106, 1524-1526.

47. Kobayaski, J.; Harbour, G.C.; Gilmore, J.; Rinehart, K.C., Jr. J. Am. Chem. Soc. 1984, 106, 1526-1528.

48. Roll, D.M.; Ireland, C.M. Tetrahedron Lett. 1985, 26, 4303-4306.

49. Sesin, D.F.; Ireland, C.M. Tetrahedron Lett. 1984, 25, 403-404.

50. Ireland, C.M.; Durso, A.R., Jr. J. Nat. Prod. 1981, 44, 360-361.

51. Rinehart, K.L., Jr.; Gloer, J.B.; Hughes, R.G., Jr.; Renis, H.E.; McGovern, J.P.; Swynenberg, E.B.; Stringfellow, D.A.; Kuentzel, S.L.; Li, L.H. Science 1981, 212, 933-935.

52. Rinehart, K.L., Jr.; Gloer, J.B.; Cook, J.C., Jr.; Mizsak, S.A.; Scahill, T.A. J. Am. Chem. Soc. 1981, 103, 1857-1859.

53. Ireland, C.M., personal communication.

54. Ireland, C.M.; Scheuer, P.J. J. Am. Chem. Soc. 1980, 102, 5688-5691.

55. Ireland, C.M.; Durso, A.R., Jr.,; Newman, R.A.; Hacker, M.P. J. Org. Chem. 1982, 47, 1807-1811.

56. Wasylyk, J.M.; Biskupiak, J.E.; Costello, C.E.; Ireland, C.M. J. Org. Chem. 1983, 48, 4445-4449.

57. Hamamoto, Y.; Endo, M; Nakagawa, M.; Nakanishi, T.; Mizukawa, K. J. Chem. Soc. Chem. Comm. 1983, 323-324.

58. Biskupiak, J.E.; Ireland, C.M. J. Org. Chem. 1983, 48, 2302-2304.

59. Sesin, D.F.; Gaskell, S.J.; Ireland, C.M. Bull. Soc. Chim. Belges. 1986, 95, 853-868.

60. Hamada, Y.; Kato, S.; Shioiri, T. Tetrahedron Lett. 1985, 26, 3223-3226.

Hamada, Y.; Shibata, M,; Shioiri, T. Tetrahedron Lett. 1985,26, 5159-5162.

Hamada, Y.; Shibata, M.; Shioiri, T. Tetrahedron Lett. 1985, 26, 6501-6504.

61. Tam Ha, T.B.; Kokke, C.M.C.; Djerassi, C. Steroids 1982, 40, 433-453.

62. Guyot, M.; Durgeat, M. Tetrahedron Lett. 1981, 22, 1391-1392.

63. Guyot, M.; Davoust, D. Tetrahedron Lett. 1982, 23, 1905-1906.

64. Guyot, M.; Morel, E.; Belaud, C. J. Chem. Res. 1983, 188-189.

65. Ballantine, J.A.; Lavis, A.; Roberts, J.C.; Morris, R.J. J. Exp. Mar. Biol. Ecol. 1977, 30, 29-44.

66. Levine, E.P. Science 1961, 133, 1352.

67. Matsuno, T.; Ookubo, M. Tetrahedron Lett. 1981, 22, 4659-4660.

68. Matsuno, T.; Ookubo, M. Chem. Lett. 1982, 1605-1606.

69. Matsuno, T. Pure and Appl. Chem. 1985, 57, 659-666.

70. Ookubo, M.; Matsuno, T. Comp. Biochem. Physiol. 1985, 81B, 137-141.

71. Belaud, C.; Guyot, M. Tetrahedron Lett. 1984, 25, 3087-3090.

72. Wells, R.J., unpublished results.

73. Howard, B.M.; Clarkson, K.; Bernstein, R.L. Tetrahedron Lett. 1979, 46, 4449-4452.

74. Sesin, D.F.; Ireland, C.M., unpublished results.

75. Fenicall, W.H., personal communication.

76. Carter, G.Y.; Rinehart, K.L., Jr. J. Am. Chem. Soc. 1978, 100, 7441.

77. Mori, K.; Umemura, T. Tetrahedron Lett. 1981, 22, 3391-3394.

Mori, K.; Umemura, T. Tetrahedron Lett. 1981, 22, 4429-4432.

Mori, K.; Umemura, T. Tetrahedron Lett. 1981, 22, 4433-4436.

78. Gaill, F.; Momzikoff, A. Mar. Biol. 1975, 29, 315-319.

79. A representative sample of the ascidian was sent to Dr. Francois Monniot for taxonomical identification. The taxonomist was unable to identify the tunicate other than to say that the tunicate was a didemid species and also that it was devoid of all algal symbionts.

80. Budzikiewicz, H.; Djerassi, C.; Williams, D.H. Mass Spectrometry of Organic Compounds; Holden-Day, Inc.: San Francisco, 1967; p 239.

81. Gunsalus, I.C.; Smith, R.A., In Methods in Enzymology

III; Colowick, S.P.; Kaplan, N.O., Eds; Academic Press: New York 1957, p 963.

82. Kametani, T.; Suzuki, T.; Takahashi, K.; Fukamoto, K. Synthesis 1974, 131-132.

83. Woollett, G.H.; Johnson, W.W. Org. Syn. , 343-344.

84. Budzikiewicz, H.; Djerassi, C.; Williams, D.H. Mass Spectrometry of Organic Compounds; Holden-Day, Inc.: San Francisco, 1967; p 504.

85. Kupchan, S.M.; Britton, R.W.; Ziegler, M.F.; Sigel, C.W. J. Org. Chem. 1973, 38, 178-179.

86. House, H.O., Modern Synthetic Reactions; W.A. Benjamin, Inc.: London, 1972; p 542-543.

87. Noggle, J.H.; Schirmer, R.E., The Nuclear Overhauser Effect; Academic Press: New York, 1971.

88. Kobayashi, M.; Yasuzawa, T.; Yoshikara, M.; Akutsu, H.; Kyogoku, Y,; Kitagawa, I. Tetrahedron Lett. 1982, 23, 5331-5334.

89. Foye, W.O. Principles of Medicinal Chemistry; Lea and Febiger: Philadelphia, 1981; pp 580-585.

90. Kikuchi, H.; Tsukitani, Y.; Iguchi, K.; Yamada, Y. Tetrahedron Lett. 1983, 24, 1549-1552.

91. Baker, B.J.; Okuda, R.K,; Yu, P.T.K.; Scheuer, P.J. J. Am. Chem. Soc. 1985, 107, 2976-2977.

92. Kikuchi, H,; Tsukitani, Y. Tetrahedron Lett. 1982, 23, 5171-5174.

93. Weinheimer, A.J.; Spragrins, R.L. Tetrahedron Lett. 1969, 5785-5788.

94. Okuda, R.K.; Klein, D.; Kinnel, R.B.; Li, M.; Scheuer, P.J. Pure Appl. Chem. 1982, 54, 1907-1914.

95. Nagaoka, H.; Miyakoshi, T.; Yamada, Y. Tetrahedron Lett. 1984, 25, 3621- 3624.

96. Weinberger, M.A.; Greenhalgh, R. Can. J. Chem. 1963, 41, 1038-1041.

97. Bax, A.; Freeman, R. J. Magn. Reson. 1981, 44, 542.

98. Hull, W.E. Two Dimensional NMR: Bruker, 1982.

99. Benn, R.; Gunther, H. Angew. Chem. Int. Ed. Engl. 1983, 22, 350-380.

100. Barfield, M.; Al-Obeidi, F.A.; Hruby, V.J.; Walter, S.R. J. Amer. Chem. Soc. 1982, 104, 3302-3306.

101. Kessler, H.; Bermel, W.; Friedrich, A.; Krack, G.; Hull, W.E. J. Amer. Chem. Soc. 1982, 104, 6297-6304.

102. Jackman, L.M.; Sternhell, S. Applications of Nuclear Magnetic Resonance Spectroscopy in Organic Chemistry; Pergamon Press: Oxford, 1969; p 282.